

CANADIAN THESES ON MICROFICHE

I.S.B.N.

THESES CANADIENNES SUR MICROFICHE



National Library of Canada
Collections Development Branch

Canadian Theses on
Microfiche Service

Ottawa, Canada
K1A 0N4

Bibliothèque nationale du Canada
Direction du développement des collections

Service des thèses canadiennes
sur microfiche

NOTICE

The quality of this microfiche is heavily dependent upon the quality of the original thesis submitted for microfilming. Every effort has been made to ensure the highest quality of reproduction possible.

If pages are missing, contact the university which granted the degree.

Some pages may have indistinct print especially if the original pages were typed with a poor typewriter ribbon or if the university sent us a poor photocopy.

Previously copyrighted materials (journal articles, published tests, etc.) are not filmed.

Reproduction in full or in part of this film is governed by the Canadian Copyright Act, R.S.C. 1970, c. C-30. Please read the authorization forms which accompany this thesis.

THIS DISSERTATION
HAS BEEN MICROFILMED
EXACTLY AS RECEIVED

AVIS

La qualité de cette microfiche dépend grandement de la qualité de la thèse soumise au microfilmage. Nous avons tout fait pour assurer une qualité supérieure de reproduction.

S'il manque des pages, veuillez communiquer avec l'université qui a conféré le grade.

La qualité d'impression de certaines pages peut laisser à désirer, surtout si les pages originales ont été dactylographiées à l'aide d'un ruban usé ou si l'université nous a fait parvenir une photocopie de mauvaise qualité.

Les documents qui font déjà l'objet d'un droit d'auteur (articles de revue, examens publiés, etc.) ne sont pas microfilmés.

La reproduction, même partielle, de ce microfilm est soumise à la Loi canadienne sur le droit d'auteur, SRC 1970, c. C-30. Veuillez prendre connaissance des formules d'autorisation qui accompagnent cette thèse.

LA THÈSE A ÉTÉ
MICROFILMÉE TELLE QUE
NOUS L'AVONS REÇUE

Canada



National Library of Canada

Bibliothèque nationale du Canada

Canadian Theses Division

Division des thèses canadiennes

Ottawa, Canada
K1A 0N4

56905

PERMISSION TO MICROFILM — AUTORISATION DE MICROFILMER

• Please print or type — Écrire en lettres mouleées ou dactylographier

Full Name of Author — Nom complet de l'auteur
ISABELLE ~~TH~~ MAR GUERITE THOMAS

Date of Birth — Date de naissance: APRIL 26th, 1957
Country of Birth — Lieu de naissance: FRANCE

Permanent Address — Résidence fixe
Les Mandières - 38330 - Biviers - FRANCE

Title of Thesis — Titre de la thèse
OPTIMAL CONTROL OF A POLYMERIZATION REACTOR

University — Université
UNIVERSITY OF ALBERTA

Degree for which thesis was presented — Grade pour lequel cette thèse fut présentée
M. Sc.

Year this degree conferred — Année d'obtention de ce grade: SPRING 1982
Name of Supervisor — Nom du directeur de thèse: Costas KIPARISSIDES

Permission is hereby granted to the NATIONAL LIBRARY OF CANADA to microfilm this thesis and to lend or sell copies of the film

L'autorisation est, par la présente, accordée à la BIBLIOTHÈQUE NATIONALE DU CANADA de microfilmer cette thèse et de prêter ou de vendre des exemplaires du film.

The author reserves other publication rights, and neither the thesis nor extensive extracts from it may be printed or otherwise reproduced without the author's written permission.

L'auteur se réserve les autres droits de publication; ni la thèse ni de longs extraits de celle-ci ne doivent être imprimés ou autrement reproduits sans l'autorisation écrite de l'auteur.

Date: April 26th, 1982

Signature:

THE UNIVERSITY OF ALBERTA

OPTIMAL CONTROL OF A
POLYMERIZATION REACTOR

by

ISABELLE MARGUERITE THOMAS

A THESIS

SUBMITTED TO THE FACULTY OF GRADUATE STUDIES
AND RESEARCH IN PARTIAL FULFILLMENT OF THE
REQUIREMENTS FOR THE DEGREE OF MASTER OF SCIENCE
IN CHEMICAL ENGINEERING

DEPARTMENT OF CHEMICAL ENGINEERING

EDMONTON, ALBERTA

SPRING 1982

THE UNIVERSITY OF ALBERTA
FACULTY OF GRADUATE STUDIES AND RESEARCH

The undersigned certify that they have read,
and recommended to the Faculty of Graduate Studies
and Research, for acceptance, a thesis entitled
"OPTIMAL CONTROL OF A POLYMERIZATION REACTOR", sub-
mitted by ISABELLE MARGUERITE THOMAS in partial
fulfillment of the requirements for the degree of
Master of Science in Chemical Engineering.

..... *Chipanssiobez*

..... *Smith*

..... *V. Gourolankar*

..... *Decker*

.....

.....

Date . *April 26th* . . . 1982.

A mon grand-père Henry Thomas, décédé le dix
janvier mille neuf cent quatre-vingt un.

ABSTRACT

A mathematical model has been developed for the free radical bulk polymerization of methyl methacrylate initiated by 2-2' azobisisobutyronitrile. The dynamics of the system are described in terms of monomer conversion, zeroth and second moments of the molecular weight distribution. The kinetic parameters of the model are estimated using the experimental data of Balke (1972). The sensitivity of the output responses of the polymerization system relative to the kinetic parameters is investigated.

The terminal control problem of obtaining a polymer product with specified conversion, number average molecular weight M_n and weight average molecular weight M_w is solved by considering the polymerization temperature, and/or the initiator feed rate as control variables. The optimal profiles are calculated via the application of the Pontryagin Maximum Principle to the developed mathematical model. Two algorithms (discrete control method and shooting method) are implemented to solve the resulting two-point boundary value problem. A variety of products with desired molecular weight distributions are produced by applying the optimal control policies to the polymerization reactor. Furthermore, it is shown that it is possible to reduce the polymerization batch time by successive minimization of the objective function while keeping the same polymer quality. The extensive simulation results presented in this thesis clearly demonstrate the benefits that can be gained from the application of the optimal control theory to the industrial polymerization reactors.

ACKNOWLEDGEMENTS

The author wishes to express her appreciation of the criticism, encouragement and academic guidance given by Dr. C. Kiparissides in the successful completion of this thesis.

The author acknowledges the University of Alberta, whose financial assistance made possible this project.

Thanks also go to the staff of the DACS Centre in the Department of Chemical Engineering, and particularly to Henry Sit, who aided in the use of computing facilities, and to the graduate students for their advice and help.

The author is also grateful to Mrs. Elizabeth Broden of the Department for the conscientious and interested efforts she made in typing the manuscript.

Finally the author wishes to thank very much her family for their moral support, and Mr. and Mrs. Ruiter for their profiterolles.

TABLE OF CONTENTS

I.	INTRODUCTION	1
	I.1 Objectives	1
	I.2 Literature Survey: Kinetics of the Polymerization of MMA	4
	I.3 Literature Survey: Optimal Control	7
II.	DEVELOPMENT OF POLYMERIZATION KINETICS FOR MMA	13
	II.1 Description of the Reaction Mechanism	13
	II.2 Derivation of the Kinetic Equations	15
	II.3 Parameter Estimation and Parameter Sensitivity	19
III.	APPLICATION OF THE OPTIMAL CONTROL THEORY TO THE POLYMERIZATION REACTOR	37
	III.1 Formulation of the Optimal Control Problem	37
	III.2 Application of the Minimum Principle to the Polymerization of MMA	40
IV.	SOLUTION OF THE TPBV PROBLEM	47
	IV. 1 Introduction	47
	IV. 2 Discrete Control Method Algorithm	47
	IV. 3 Shooting Method Algorithm	60
	IV. 4 Comparison of DCM and SM Algorithms	67
V.	OPTIMAL TEMPERATURE POLICIES	72
	V.1 Reduction of the Batch Polymerization Time	72
	V.2 Quality Improvement of the Polymer Product	74
VI.	OPTIMAL CATALYST FEED RATE POLICIES	95
	VI.1 Problem Formulation	95

VI.2 The Optimal Initiator Policy	99
VI.3 The Optimal Temperature and Initiator Policies	101
VI.4 Controllability of the System	103
VII. CONCLUSION	109
REFERENCES	112
APPENDIX A: Derivation of Kinetic Equations	115
APPENDIX B: Derivation of the Sensitivity Equations	125
APPENDIX C: Derivation of Necessary Conditions for Optimality	136
APPENDIX D: DCM and SM Algorithms Computer Programs	142
APPENDIX E: Experimental Equipment	152

LIST OF TABLES

Table	Description	
II.1	Numerical Values of the Parameters in $g(X,T)$	22
IV.1	Desired Properties of the Polymer Product	67
IV.2	Comparison of the Results of the two Algorithms	68
V.1	Final MWD for the Isothermal Polymerization of MMA at 50°C	72
V.2	Final MWD for the Isothermal Polymerization of MMA at 70°C	73
V.3	Desired and Attained MWDs: Fixed, M_n , Varying M_w	75
V.4	Desired and Attained MWDs: Varying M_n , Fixed M_w	76
V.5	Effect of Parameter Perturbations on the Minimum Time	78
VI.1	Desired and Attained MWDs - Optimization of [I] only	100
VI.2	Desired and Attained MWDs - Simultaneous Optimization of [I] and T	100
VI.3	Effect of Tolerance limits on the Convergence	104
A.1	Justification of Approximations	124

LIST OF FIGURES

Figure	Description	
II.1	Conversion vs Time - Isothermal Run at 50°C	26
II.2	Conversion vs Time - Isothermal Run at 70°C	27
II.3	Conversion vs Time - Isothermal Run at 90°C	28
II.4	Number Average Molecular Weight and Weight Average Molecular Weight vs Time - Isothermal Run at 50°C	29
II.5	Number Average Molecular Weight and Weight Average Molecular Weight vs Time - Isothermal Run at 70°C	30
II.6	Number Average Molecular Weight and Weight Average Molecular Weight vs Time - Isothermal Run at 90°C	31
II.7	Gel Effect Function $g(X,T)$	32
II.8	Effect of the Perturbations of the Parameters on the Conversion	33
II.9	Effect of the Perturbations of the Parameters on the Second Moment of the MWD	34
II.10	Sensitivity Coefficients of the Output Variables relative to the Temperature	35
II.11	Sensitivity Coefficients of the Output Variables relative to the Initial Initiator Concentration	36
IV.1	Discrete Control Method Algorithm	52
IV.2	Effect of the Subinterval $[t_{k-1}, t_k]$ Length on the Optimal Temperature Profile (Optimal Time = 275 min)	55
IV.3	Effect of the Subinterval $[t_{k-1}, t_k]$ Length on the Optimal Temperature Profile (Optimal Time = 67 min)	56
IV.4	Effect of the Numerical Value of α on the Convergence of the DCM Algorithm	58

Figure	Description	
IV.5	Effect of the Number of Iterations on the Optimal Temperature Profile	59
IV.6	Shooting Method Algorithm	66
IV.7	Comparison of DCM and SM Algorithms	69
V.1	Optimal Temperature Profile (Optimal Time = 275 min)	80
V.2	Optimal Temperature Profile (Optimal Time = 67 min)	81
V.3	Conversion and Rate of Polymerization for Optimal Run (Optimal Time = 275 min)	82
V.4	Conversion and Rate of Polymerization for Isothermal Run at 50°C	83
V.5	Conversion and Rate of Polymerization for Optimal Run (Optimal Time = 67 min)	84
V.6	Conversion and Rate of Polymerization for Isothermal Run at 70°C	85
V.7	Optimal Temperature Profiles (Desired MWDs are given in Table V.3)	86
V.8	Rate of Polymerization for the Optimal Runs (Desired MWDs are given in Table V.3)	87
V.9	Number and Weight Average Molecular Weights for Optimal Runs (Desired MWDs are given in Table V.3)	88
V.10	Polydispersities for Optimal Runs (Desired MWDs are given in Table V.3)	89
V.11	Optimal Temperature Profiles (Desired MWDs are given in Table V.4)	90
V.12	Conversion and Rate of Polymerization for Optimal Runs (The desired MWDs are given in Table V.4)	91
V.13	Number and Weight Average Molecular Weights for Optimal Runs (The desired MWDs are given in Table V.4)	92
V.14	Polydispersities for Optimal Runs (The desired MWDs are given in Table V.4)	93
V.15	The Effect of Perturbations in the Kinetic Parameters on the Optimal Temperature Profile	94

Figure	Description	
VI.1	Initiator Concentration Profiles for Optimal Runs ($PD_d = 2.5$)	105
VI.2	Initiator Concentration Profiles for Optimal Runs ($PD_d = 4.1$)	106
VI.3	Temperature Profiles for Optimal Runs ($PD_d = 2.5$)	107
VI.4	Temperature Profiles for Optimal Runs ($PD_d = 4.1$)	108
E.1	Experimental Apparatus	155

NOMENCLATURE

- $A_1(^{\circ}K^{-1})$, $B_1(^{\circ}K^{-1})$, $C_1(^{\circ}K^{-1})$, A_2 , B_2 , C_2 : Kinetic parameters in the expression of the gel effect function $g(x, T)$.
- E_d, E_2 : Activation energies in k_d and K_2 (cal. mole⁻¹)
- f : Catalyst efficiency factor.
- \underline{f} : Vector function describing the derivative of the state vector.
- F_c : Catalyst feed rate (gmole.s⁻¹)
- F_{cmax} : Maximum allowed catalyst feed rate (gmole.s⁻¹)
- F_N : Inhibitor feed rate (gmole.s⁻¹)
- $g(x, T)$: Gel effect function, $g(x, T) = K_2/K_{20}$.
- G : Scalar functional in the expression of J .
- H : Hamiltonian.
- $[I]$: Initiator concentration (gmole.l⁻¹).
- $[I_0]$: Initiator concentration at time $t=0$ (gmole.l⁻¹).
- J : Objective functional.
- k_d : Rate constant for dissociation of initiator (s⁻¹).
- k_f : Rate constant for transfer to monomer (l.gmol⁻¹.s⁻¹).
- k_i : Initiation rate constant (l.gmole⁻¹.s⁻¹).
- k_N : Rate constant for consumption of initiator due to an inhibitor (l.gmole⁻¹.s⁻¹)
- k_p : Propagation rate constant (l.gmol⁻¹.s⁻¹).
- k_t : Termination rate constant, $k_t = k_{tc} + k_{td}$ (l.gmole⁻¹.s⁻¹).

k_{tc} :	Rate constant for termination by combination ($\ell \cdot \text{gmole}^{-1} \cdot \text{s}^{-1}$).
k_{td} :	Rate constant for termination by disproportionation ($\ell \cdot \text{gmol}^{-1} \cdot \text{s}^{-1}$).
K_2 :	$K_2 = k_p^2 / k_t$ ($\ell \cdot \text{gmole}^{-1} \cdot \text{s}^{-1}$).
K_{20} :	K_2 at conversion $x = 0$ ($\ell \cdot \text{gmole}^{-1} \cdot \text{s}^{-1}$).
$[M]$:	Monomer concentration ($\text{gmole} \cdot \ell^{-1}$).
$[M_0]$:	Monomer concentration at time $t=0$ ($\text{gmole} \cdot \ell^{-1}$).
M_n :	Number average molecular weight.
$[N]$:	Inhibitor concentration ($\text{gmole} \cdot \ell^{-1}$).
P :	Parameter vector.
\underline{P} :	Costate vector.
PD :	Polydispersity.
PD_d :	Desired polydispersity.
$[P_x]$:	Concentration of dead polymer of chain length x ($\text{gmole} \cdot \ell^{-1}$).
$[R_x^*]$:	Concentration of live radical of chain length x ($\text{gmole} \cdot \ell^{-1}$).
t :	Time (s).
t_0 :	Initial time (s).
t_f :	Final time (s).
T :	Polymerization temperature ($^{\circ}\text{K}$).
\underline{u} :	Control vector
V :	Volume of the reactor (ℓ).
w_t :	Weighting factor in the expression of J .
X :	Monomer conversion

X_d : Desired monomer conversion.

x, y : Chain length of polymer

\underline{Y} : Dimensionless state vector, $\underline{Y} = \left(\begin{array}{c} [I] \\ [I_0] \end{array}, \frac{x}{X_d}, \frac{\mu_0}{\mu_{0d}}, \frac{\mu_2}{\mu_{2d}} \right)^T$

\underline{Z} : Polymerization system output.

$$Z = ([I], x, \mu_0, \mu_2)^T$$

Greek Symbols

α, α_1 : Weighting factor in updating control T.

α_2 : Weighting factor in updating control [I].

δ_{ij} : Kronecker symbol.

ϵ_{ij} : Sensitivity coefficient.

η_{ij} : Normalized sensitivity coefficient.

λ_k : k^{th} moment of live radical distribution ($\text{gmole} \cdot \ell^{-1}$).

μ_k : k^{th} moment of the dead polymer distribution ($\text{gmole} \cdot \ell^{-1}$).

μ_{0d} : desired zeroth moment of the dead polymer distribution ($\text{gmole} \cdot \ell^{-1}$).

μ_{2d} : desired second moment of the dead polymer distribution ($\text{gmole} \cdot \ell^{-1}$).

CHAPTER I

INTRODUCTION

I.1 Objectives

The manufacturing of polymers occupies a significant portion of the chemical industry today. The polymer industry has grown tremendously in the past four decades as the uses of polymers have multiplied. Nevertheless, the production of a great number of polymeric products is even today an art. The basic reasons for this are:

- (i) The difficulty to characterize and especially measure on-line the physical properties (e.g. molecular weight distribution) of the polymer product
- (ii) The lack of good mathematical models for industrial polymerization reactors, which makes the application of optimization techniques to these systems questionable.

The present work was undertaken and motivated by a need to (a) develop a suitable mathematical model for the bulk polymerization of methylmethacrylate (MMA) and (b) show the feasible application of optimal control to polymerization reactors. Based on the above needs the goals of this work were defined as follows:

- (i) Obtain a mathematical model for the free radical batch polymerization of methylmethacrylate.

(ii) Estimate the unknown kinetic parameters of the model from available experimental data.

(iii) Apply the Pontryagin Minimum Principle to the reactor model and establish a systematic procedure for the time optimal control of the batch process.

(iv) Study the sensitivity of the optimal policies with respect to the model parameters.

The system chosen for this study was the free radical bulk polymerization of MMA initiated by a 2 - 2' azobisisobutyronitrile (AIBN) catalyst. This polymerization was selected because of its commercial importance and the extensive experimental data available in the literature on the physical properties and kinetic characteristics of the system.

This thesis is organized into seven chapters. The first chapter states the objectives of this work and presents a literature survey on the kinetics of the polymerization of MMA, and on the application of optimal control theories to the optimization of polymerization systems.

The second chapter deals with the modelling of the bulk polymerization of MMA in a batch reactor. Using the general population balance equations, a mathematical model is developed that describes the dynamic behaviour of the system. The model consists of four non-linear differential equations and can predict monomer conversion and the first three moments of the molecular weight distribution as a function of the polymerization temperature

and initiator concentration. The kinetic parameters of the model are estimated from experimental data. The accuracy and sensitivity of the model responses relative to the numerical values of the kinetic parameters is also studied.

The third chapter discusses the application of the Pontryagin Minimum Principle to polymerization reactors.

In the fourth chapter, two algorithms are developed to solve the minimum time problem. It is shown that it is possible to produce a polymer product with prespecified desired properties (conversion, number average molecular weight, weight average molecular weight) by controlling the polymerization temperature in the reactor.

The fifth chapter presents the optimal temperature profiles computed for different desired molecular weight distributions. The sensitivity of the optimal temperature policy with respect to kinetic parameters is also investigated.

In the sixth chapter, both the catalyst feed rate into the reactor and the polymerization temperature are considered simultaneously as control variables. An algorithm is developed to solve the minimum time problem and get desired physical properties for the polymer. Optimal temperature and catalyst concentration profiles are presented.

The seventh chapter discusses the significance of this work and its possible extensions.

I.2 Literature Survey: Kinetics of the Polymerization of MMA

The single most important property of a polymer that determines its quality and final use is its molecular weight distribution (MWD). MWD of a polymer and monomer conversion in a reactor are the results of a number of elementary reactions occurring in polymerization and of their respective rates. In bulk free radical vinyl polymerization, much work has been done to establish the reaction mechanism at low conversions (less than 10% conversion). Beyond this range, diffusion control of some reactions (e.g. termination reaction) coupled with experimental difficulties has severely hindered progress in kinetic modelling.

Matheson and co-workers (1949) measured as a function of temperature the average lifetime of polymethylmethacrylate radicals in the photosensitized polymerization of the liquid monomer. By combining their experimental results with those of Schulz and Blaschke (1942), and Schulz and Harborth (1947), they obtained the rate constants for propagation, termination, and transfer to monomer for conversion up to 10%. They asserted that the accelerated polymerization rate occurring in the later stages was due to a decrease in the termination rate constant.

Nandi (1957), Ferington and Tobolsky (1957) presented results on the bulk polymerization of MMA. The reported experimental results were obtained with a wide

variety of initiators and under different isothermal conditions. From this data, they calculated the rate constant for chain transfer to monomer and the ratio $(k_t^{1/2}/k_p)$, where k_p and k_t are the rate constants for propagation and termination reactions respectively. Their results were in good agreement with the results of Matheson et al. (1949).

Hayden and Melville (1960), Tonoyan et al. (1973) measured the increase in temperature in an adiabatic polymerization reactor as a function of time. They reported that after 10% conversion, the polymerization rate and lifetime of the polymer chains increased due to the increase of the viscosity of the reaction mixture resulting, thus, in a decrease of the collision rate of the growing radicals. They found out that, beyond 40% conversion, the activation energy for the propagation reaction increased while the corresponding velocity coefficient decreased, due to the monomer addition step becoming diffusion controlled.

Paul et al. (1973) observed a similar decrease in the propagation rate constant and studied also the influence of the stoichiometry of the initiator system (benzoyl peroxyde, lauroyl peroxyde, N-N-dimethyl-p-toluidine) on the rate of polymerization.

Pavlinets and Lazar (1973) investigated the polymerization of MMA initiated by hydroperoxydes-SO₂ organo-complex systems to high degrees of conversion at 10-45°C. They showed that the initiating systems used ensured high

polymerization rates even at room temperature with an activation energy of 6.8 kcal/mole.

Yokota and co-workers (1968) carried out rotating sector determinations of radicals lifetime for ten methacrylates undergoing radical polymerization at 30°C. The rate constant of propagation k_p and the rate constant of termination k_t have been computed from these experimental results. However, there appears to exist a discrepancy between their values and those calculated by other investigators.

Balke (1972) investigated the bulk free radical polymerization of MMA to high conversions. The experimental conditions of Balke were similar to those used in industrial reactors (high initiator concentration and high temperature). Using gel permeation chromatography (GPC) and a novel technique for the interpretation of the chromatograms, he was able to follow the changes in the MWD as polymerization proceeded. He found that the rate of polymerization was proportional to the monomer concentration at low conversion (less than 20%), and followed a second order expression in monomer concentration after the onset of the gel effect. Using Sawada's (1963) equation to account for the gel effect, Balke predicted the change of conversion with time. It should be noted that his model included two different expressions for the rate of polymerization, a first order expression with respect to monomer concentration before the onset of the gel effect, and

a second order expression after the onset of the gel effect. This introduced a discontinuity in the conversion profile plotted as a function of time. Apparently this model cannot be used for optimization studies.

Mahabadi and Meyerhoff (1979) proposed a new model for estimation of the characteristic rate constant for primary radical termination, using the radical lifetime rate of polymerization and rate of initiation. By applying this model to high conversion polymerization experimental data, they showed the conversion dependence of the termination rate constant and the conversion dependence of the initiation rate.

In the present work, a mathematical model for the free radical bulk polymerization of methylmethacrylate has been developed that accounts for the diffusion controlled termination and propagation reactions. The kinetic parameters of the proposed model have been determined by fitting the experimental data of Balke (1972). Continuous differential equations which describe conversion, number average molecular weight, and weight average molecular weight are developed and solved numerically.

1.3 Literature Survey: Optimal Control

The Principle was first hypothesized by the Russian mathematician Pontryagin in 1956. In 1958, it was fully proved by Boltyanskii and co-workers that the maximum principle was a necessary condition for optimality. Relatively little work has been done with respect to the optimal control of polymerization systems.

Ray (1967) drew conclusions on optimum settings of temperature and catalyst concentration which minimize a

performance index described at final time only by conversion and polydispersity, in a series of tank reactors in which polymerization of styrene was taking place. He applied a peak-seeking method to compute the best temperature and the best catalyst concentration in each tank. Appropriate weighting factors were applied to each term of the objective function in order to emphasize the importance of one variable over another. Hicks and co-workers (1969) formulated a similar objective function, and tried to optimize the performance of a polymerization reactor: (a) by controlling the polymerization temperature while keeping a constant initiator concentration, (b) by using both temperature and initiator concentration as control variables. The latter attempt proved unsuccessful due to computational problems. In both situations, the minimum time problem was not addressed.

Osakada and Fan (1970) calculated sub-optimal temperature and catalyst feed rate policies in an attempt to obtain a desired molecular weight distribution. These near-optimal policies were represented by two time varying polynomials, the coefficients of which were estimated by a pattern search technique, coupled with a non-linear search technique. They found that the suboptimal temperature and catalyst feed rate policies were oscillatory.

Crescitelli and Nicoletti (1973) derived a modified form of the discrete maximum principle for systems with finite memory and presented a computational procedure to

find near-optimal policies in practical applications. They gave a numerical example relative to the computation of the optimal temperature profile in a batch reactor where two consecutive irreversible reactions were taking place.

Sacks and co-workers (1972) applied the continuous maximum principle to minimize the reaction time for chain addition polymerization in batch reactors, while the number average molecular weight at the end of the reaction was fixed. The optimal policy was found to be a rising temperature profile for a given constant initiator concentration.

Shatkan and Gilman (1966) applied the method of variational calculus to search for an optimal temperature policy for batchwise thermally initiated bulk polymerization of styrene. In the searching process, they first set the final conversion at 95% and predetermined the number average molecular weight at some specific value. The optimal temperature so obtained increased with monomer conversion and reached an extremely high level (far above 200°C). Then they applied this temperature policy to the case where monomer conversion was nearly complete (99%) by following the optimal temperature trajectory until a predetermined upper limit of temperature was reached, then held the temperature at this limit till the end of the reaction. Obviously the temperature policy for the entire reaction was not optimal.

Show-An Chen and W.F. Jeng (1978) studied the minimum-

time problem for the polymerization of styrene in a batch reactor by considering the polymerization temperature $T(t)$ and the initial initiator concentration $[I_0]$ as two control variables. Their kinetic model included the gel effect. Calculations showed that the optimal temperature policy was significantly better than the best isothermal policy. Experimental verification of their theoretical findings revealed that there was a good agreement between experimental and calculated final conversion values. However, an appreciable deviation existed between experimental and calculated number average chain length. In 1980, Chen and Lin considered a two-stage polymerization process. The first stage of the process, initiated by a chemical initiator, was operated along the best isothermal policy computed to obtain predetermined number average molecular weight and monomer conversion at the end of the stage. The second stage was operated at a higher temperature at which thermal initiation was important. They used the Minimum Principle to find the optimal temperature profile during the second stage, in order to minimize a performance index described by final time, conversion and number average molecular weight at the end of the second stage. Calculations showed that the optimal two-stage process was significantly better (in terms of final time for a predetermined quality of polystyrene) than the best isothermal one-stage process.

Masterson (1977) and Clough et al. (1978) applied the maximum principle to solve the minimum time problem for batch

polymerization of styrene. They obtained a product with desired conversion, desired number average molecular weight and desired weight average molecular weight by controlling temperature and initiator feed rate. The numerical solution has proven challenging. The search was successful only when carried out first by a gradient approach, then by a novel vertex technique. They found one temperature profile which conformed to industrial applied temperature profiles. They reported that a similar study would entail a cost of \$2000 in CPU time.

Wu et al. (1980) gave a shrewd graphical solution to the minimum time problem of styrene polymerization. Their performance index depended only on conversion and number average molecular weight at the end of the reaction. Thus, by applying the maximum principle, they were able to obtain analytical expressions for the costate variables and derived a differential equation describing the optimal variation of temperature with time. Their theoretical predictions were in agreement with experimental measurements of conversion and number average molecular weight.

In this work a general algorithm which solves the minimum time problem for obtaining a polymer with desired final conversion, final number average molecular weight and weight average molecular weight, is developed. Optimal temperature policies and initiator feed rate programs are computed for obtaining a polymer with desired molecular weight distribution. A pilot scale batch polymerization

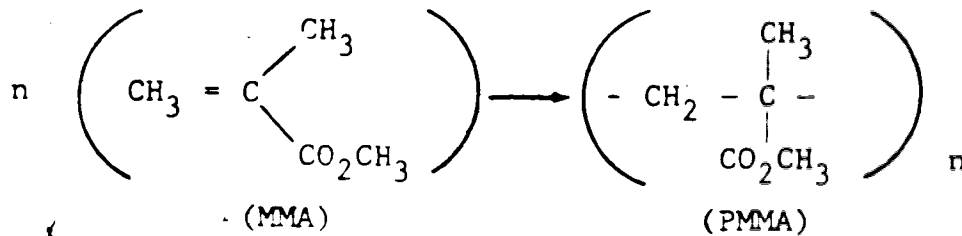
reactor has been built by the author to verify the optimal policies as part of another project. In this equipment, the temperature of the polymerization reactor is adjusted as per predetermined optimal policies by supervisory computer control of the temperature loop under analogue PID control. Conversion, number average molecular weight and weight average molecular weight can be measured on and off-line and checked against simulation results. A detailed description of the experimental apparatus is shown in Appendix E.

CHAPTER II

DEVELOPMENT OF POLYMERIZATION KINETICS FOR MMA

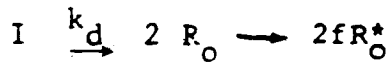
II.1 Description of the Reaction Mechanism

Polymethylmethacrylate (PMMA) can be obtained via the free radical polymerization of MMA monomer.



A general description of the reactions which are taking place during the free radical polymerization of vinyl monomers initiated by a free radical catalyst is as follows:

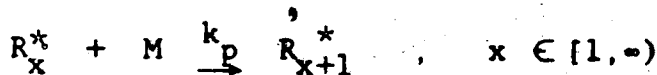
Catalyst decomposition



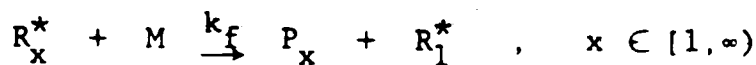
Initiation



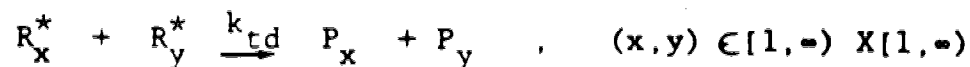
Propagation



Transfer to monomer



Termination by disproportionation



Termination by combination



where I denotes the initiator molecules, R_0 , the initiator radicals and R_0^* , the activated initiator radicals. M denotes the monomer, R_x^* represents the live radicals of chain length x. f is the initiator efficiency factor. k_d , k_i , k_p , k_f , k_d , and k_{tc} are the rate constants for initiator dissociation, initiation, propagation, transfer to monomer, termination by disproportionation and termination by combination reactions respectively.

The initiator used in this study is 2 - 2' azobisisobutyronitrile (AIBN), which is very common in industrial reactors; its decomposition rate follows first-order kinetics.

Using the above proposed kinetic scheme, equations describing the conversion of monomer, the concentration of initiator, and the molecular weight distribution (MWD) in a batch reactor are derived. To simplify the mathematical description of the system, the following assumptions are made:

- (i) All reactions are irreversible.
- (ii) Reaction rate constants are independent of chain length.

- (iii) Transfer to monomer is negligible.
- (iv) Termination reaction is by disproportionation only.
- (v) Reactor contents are perfectly mixed and there are no temperature gradients in the reactor.

These assumptions are common and well documented in the modelling of the free radical polymerization of MMA.

II.2 Derivation of the Kinetic Equations

The catalyst decomposition reaction follows first-order kinetics. The rate of disappearance of catalyst is described by the following differential equation:

$$\frac{d[I]}{dt} = -k_d [I] + \frac{F_c}{V} \quad (\text{II.1})$$

where $[I]$ is the initiator concentration, t is the time, k_d is the rate constant of catalyst decomposition, F_c the catalyst feed rate in the reactor during the polymerization and V is the volume of the reactor. Any variation of the volume of the reacting mixture due to density changes and/or initiator addition is assumed to be negligible.

Pertinent steps in the derivation of the equation describing the rate of disappearance of monomer are outlined in Appendix A. The monomer conversion X is defined as:

$$X = \frac{[M] - [M_o]}{[M_o]} \quad (\text{II.2})$$

where $[M]$ is the monomer concentration in the reactor during

the polymerization, and $[M_0]$ is the monomer concentration in the reactor at time $t = 0$. The change of the monomer conversion is described by the following differential equation:

$$\frac{dX}{dt} = \sqrt{\frac{2 f k_d [I]}{k_t}} k_p (1-X) \quad (\text{II.3})$$

where f is the initiator efficiency, k_p is the propagation rate constant and k_t is the termination rate constant.

The MWD of polymers can be expressed in terms of its moments when the MWD is unimodal, as it is the case for the polymerization of MMA in the range of interest (Balke, 1972). The moments of the live and dead polymer distributions are defined as follows:

$$\lambda_k = \sum_{x=1}^{\infty} x^k [R_x^*] \quad (\text{II.4})$$

where λ_k is the k^{th} moment of the live polymer distribution and $[R_x^*]$ is the concentration of live radicals of chain length x in the reactor.

$$\nu_k = \sum_{x=2}^{\infty} x^k [P_x] \quad (\text{II.5})$$

where ν_k is the k^{th} moment of the dead polymer distribution, and $[P_x]$ is the concentration of dead polymer of chain length x in the reactor. The zeroth moment of the live

polymer distribution, λ_0 , represents the total concentration of live polymer in the reactor. The zeroth moment of the dead polymer distribution, ν_0 , represents the total concentration of dead polymer in the reactor. The sum ($\nu_1 + \lambda_1$) represents the portion of monomer which has reacted and is equal to:

$$\nu_1 + \lambda_1 = [M_0] - [M] = [M_0] X \quad (\text{II.6})$$

The differential equations describing the variation of the moments of the dead polymer distribution are derived in Appendix A. The rate of change of the zeroth and second moment of the dead polymer distribution can be expressed as:

$$\frac{d \nu_0}{dt} = 2 f k_d [I] \quad (\text{II.7})$$

$$\frac{d \nu_2}{dt} = 2 \frac{k_p^2}{k_t} [M]^2 \quad (\text{II.8})$$

Physical properties of a polymer (such as melt viscosity, chemical resistance, flexibility, strength ...) do depend upon the number average molecular weight, M_n , and the weight average molecular weight M_w of a polymer. M_n and M_w are directly related to the moments of the MWD.

$$M_n = MW \cdot \frac{\nu_1 + \lambda_1}{\nu_0 + \lambda_0} \quad (\text{II.9})$$

$$M_w = MW \cdot \frac{\nu_2 + \lambda_2}{\nu_1 + \lambda_1} \quad (\text{II.10})$$

where MW is the molecular weight of methylmethacrylate monomer. Since λ_k is negligible compared to ν_k ($\lambda_k \ll \nu_k$), equations (II.9) and (II.10) can be simplified by neglecting the contribution of λ_0 , λ_1 , and λ_2 moments to the calculation of M_n and M_w . Therefore,

$$M_n = MW \cdot \frac{\nu_1}{\nu_0} = MW \cdot \frac{X [M_0]}{\nu_0} \quad (\text{II.11})$$

$$M_w = MW \cdot \frac{\nu_2}{\nu_1} = MW \cdot \frac{\nu_2}{X [M_0]} \quad (\text{II.12})$$

The polydispersity of a polymer (PD) is defined as the ratio (M_w/M_n), and is an indication of the breadth of the MWD

$$PD = \frac{M_w}{M_n} = \frac{\nu_2 \nu_0}{X^2 [M_0]^2} \quad (\text{II.13})$$

In bulk polymerization of methylmethacrylate, dramatic physical changes take place during the course of the reaction. As polymer concentration increases, a point is reached where appreciable chain entanglements occur, and eventually a glassy state may result. These physical changes often have a significant effect on both rate of polymerization and molecular weight development, and any attempt of modeling such reactions must properly account for these phenomena.

Experimental data show evidence of an autoacceleration

of the rate of polymerization at conversions above 10 - 20%. Because of the increasing viscosity of the mixture, the rate of termination becomes diffusion controlled. Polymer chains begin to entangle causing a dramatic reduction in radical chain mobility, giving a drop in k_t . Because of the higher concentration of free radicals in the reactor, the rate of polymerization increases. It is interesting to note that even relatively slow propagation reactions involving the small monomer molecules become diffusion controlled. The propagation rate constant k_p drops dramatically. That means that no more reactions are taking place in the reactor, therefore a limiting conversion below 100% may be observed.

II.3 Parameter Estimation and Parameter Sensitivity

The parameters which appear in the kinetic equations (II.1, II.3, II.7, II.8) are the initiator efficiency, f , the rate constant of catalyst dissociation, k_d , and the ratio of the square of the propagation rate constant over the termination rate constant $K_2 = (k_p^2 / k_t)$.

The initiator efficiency, f , represents the fraction of the total number of initiator radicals that are actually used in the formation of polymer chains. f is an empirical factor with values in the range 0.5 - 1.0. The efficiency factor usually falls with increasing reaction temperatures and with conversions of monomer to polymer. The changes however are relatively small and it is reasonable to assume

that f is independent of temperature and monomer conversion for practical calculations. In this work, the value of f has been chosen as 0.6, figure commonly used in literature.

The decomposition rate constant of AIBN, k_d , has been determined by many workers. Data after Balke (1972), O'Driscoll and Dickson (1968), and Ito (1969), were correlated with an Arrhenius type plot giving the following equation which was used in this work:

$$k_d = 1.35 \times 10^6 \times \text{EXP} (-16298.0/T), (\text{s}^{-1}) \quad (\text{II.14})$$

where T is the absolute temperature in the reactor ($^{\circ}\text{K}$).

As explained above, the termination rate constant, k_t , and the propagation rate constant, k_p , change with conversion. As a result of this the ratio ($K_2 = k_p^2/k_t$) will also vary with conversion. To express this variation quantitatively the following equation is used

$$K_2 = K_{20} (T) \cdot g(X, T) \quad (\text{II.15})$$

where K_{20} is the value of K_2 at conversion $X = 0$. $g(X, T)$ may be called the gel effect function, because it accounts for the conversion dependence of k_t and k_p due to the diffusion control of termination and propagation reactions.

K_{20} can be determined by measuring the rate of polymerization at low conversions. Data were correlated in an Arrhenius type plot by Balke (1972), which gave the follow-

ing expression for K_{20} :

$$K_{20} = 100.4 \times \text{EXP} (-2960/T), \text{ (l.mole}^{-1}\text{s}^{-1}\text{)} \quad (\text{II.16})$$

Because of the gel effect the termination rate constant decreases. This results in an increase of the rate of polymerization in the conversion range of 20 - 80%. Beyond this conversion range, even the propagation reaction could become diffusion controlled, which in turn could cause a dramatic decrease of the polymerization rate. To describe this unusual behavior of the polymerization rate over the whole monomer conversion range, the gel effect function, $g(X,T)$, must first monotonically increase up to some monomer conversion value (60 - 80%, depending on the polymerization temperature), then decrease up to the final limiting conversion value. To account for this type of behavior, an exponential relationship of g on X and T was assumed. Friis and Hamielec (1975) have used a similar expression.

$$g(X,T) = \text{EXP} (AX^3 + BX^2 + C) \quad (\text{II.17})$$

with

$$A = A_1/T + A_2$$

$$B = B_1/T + B_2$$

$$C = C_1/T + C_2$$

(II.18)

$A_1, B_1, C_1, A_2, B_2, C_2$, are unknown parameters estimated by

fitting our model to the experimental data (conversion, M_n , M_w) of Balke obtained at different temperatures. To obtain estimates of these parameters (Table II.1), a finite difference Levenberg Marquardt routine from the IMSL Library was used.

Table II.1

Numerical values of the parameters in $g(X,T)$

A_1	A_2	B_1	B_2	C_1	C_2
$-96500 \pm 50.$	$250. \pm 0.5$	$75000 \pm 50.$	$-185. \pm 0.5$	$-25. \pm 0.5$	-0.25 ± 0.005

Much care has to be taken in the estimation of A, B, C parameters and especially in the choice of the initial guesses of A_1 , B_1 , C_1 , A_2 , B_2 , C_2 , because the system responses are sensitive to the numerical values of these parameters. This is discussed later in this section.

The results of the parameter estimation are shown in Figures II.1 to II.6. In these Figures, calculated results for monomer conversion, M_n and M_w , are compared with the experimental values of Balke obtained at three different polymerization temperatures. The solid lines represent the calculated model response and the small squares represent the experimental points of Balke (1972). It can be seen that the model is describing accurately the variations of conversion with time. The slight discrepancy observed in fitting the molecular weight distribution (M_n , M_w) could be due to possible errors in experimental measurements.

Figure II.7 shows the variation of the function $g(X,T)$ with conversion at two different temperatures (50°C and 90°C).

Although the mathematical model chosen in this work can describe satisfactorily the polymerization of methylmethacrylate, yet our knowledge of the kinetic parameters of this model may be imperfect. This gives rise to the important problem of parameter sensitivity, which is defined as the effect of uncertainties in the rate coefficients on the calculated output responses, namely, the effect of parameter uncertainties in k_d , f , K_2 , on the calculated $[I]$, X , u_0 , u_2 . In addition to the sensitivity of the system responses to the above parameters, we are also interested in knowing the effects of the initial catalyst concentration $[I_0]$ and polymerization temperature T on the output variables.

The sensitivity coefficient for the parameter, p_j , and the output, Z_i , is defined as the first partial derivative of Z_i with respect to p_j

$$\phi_{ij} = \frac{\partial Z_i}{\partial p_j} \quad (\text{II.19})$$

Sensitivity coefficients indicate the magnitude and the direction of change of the response Z due to perturbations in the values of the parameters. Since the model is a set of non-linear ordinary differential equations, the sensitivity coefficients cannot be written explicitly. Application of the well documented sensitivity analysis to the

model equations (Atherton et al., 1975; Beck and Arnold, 1977), yields a system of differential equations for the sensitivity coefficients, called sensitivity equation (see Appendix B for further details). The variation of the sensitivity coefficients with respect to time is obtained by integrating numerically the sensitivity equations. The results of the integration of the sensitivity equations for k_d , f , K_{20} , A_1 , B_1 , C_1 , A_2 , B_2 , C_2 are summarized in Figures II.8 and II.9. In order to show the relative influence of the parameters on the output variables, normalized sensitivity coefficients, as defined by equation (II.20) have been plotted.

$$\psi_{ij} = \epsilon_{ij} \left(\frac{P_j}{Z_i} \right) \quad (\text{II.20})$$

A positive sensitive coefficient indicates that a positive variation of the corresponding parameter causes an increase in the output variable. A negative sensitivity coefficient indicates that a positive variation of the parameter results in a decrease in the output variables. It is seen that the output variables are most sensitive to A_1 , B_1 , A_2 , B_2 parameters.

An increase in k_d or in f does not cause any significant perturbation on the initiator concentration and on the zeroth moment, however it causes a slight increase in monomer conversion, and a slight decrease in second moment at the end of the reaction (Figures II.8 and II.9).

The effect of perturbations in the reaction temperature is shown in Figure II.10. An increase in temperature results in an increase in monomer conversion and zeroth moment, a small decrease in initiator concentration, and a decrease in second moment at the end of reaction.

The effect of perturbations in the initial concentration of catalyst $[I_0]$ is shown in Figure II.11. The output variables are much less sensitive to $[I_0]$ than to T . However, the profiles of respective sensitivity coefficients have the same shape. An increase in $[I_0]$ causes an increase in monomer conversion and zeroth moment, and a decrease in the second moment at the end of the reaction.

The quantitative interpretation of figures II.8 to II.11 shows how accurate the estimation of the kinetic parameters should be. As an example, consider the effect of a perturbation in B_1 on the conversion X . In figure II.8, it is seen that the dimensionless sensitivity coefficient ψ_{26} can be equal up to 25,

$$\psi_{26} = 25 = \left(\frac{X}{B_1}\right)^{-1} \frac{\partial X}{\partial B_1}$$

For a small perturbation of B_1 (as 1%), $\frac{\partial X}{\partial B_1}$ can be approximated by $\frac{\Delta X}{\Delta B_1}$.

Therefore,

$$\frac{\Delta X}{X} = \frac{\Delta B_1}{B_1} \quad \psi = \frac{1}{100} \times 25 = 25\%$$

A 1% perturbation in B_1 involves a 25% variation in X !

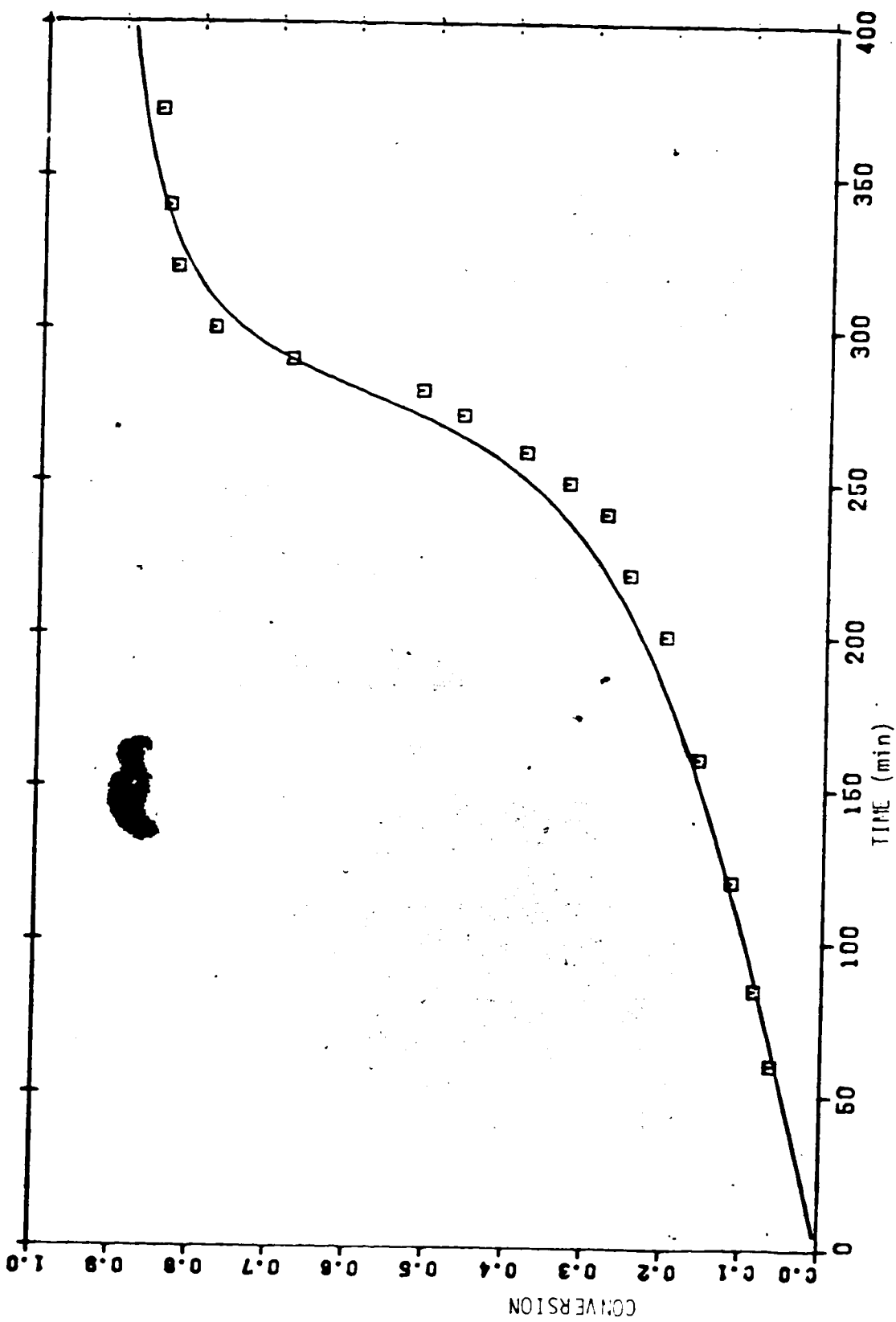


Figure II.1: Conversion versus Time, Isothermal Run at 50°C.,
($I_0 = 0.01699 \text{ gmole.l}^{-1}$)

— Mathematical Model

□ Experimental Points (Balke - 1972).

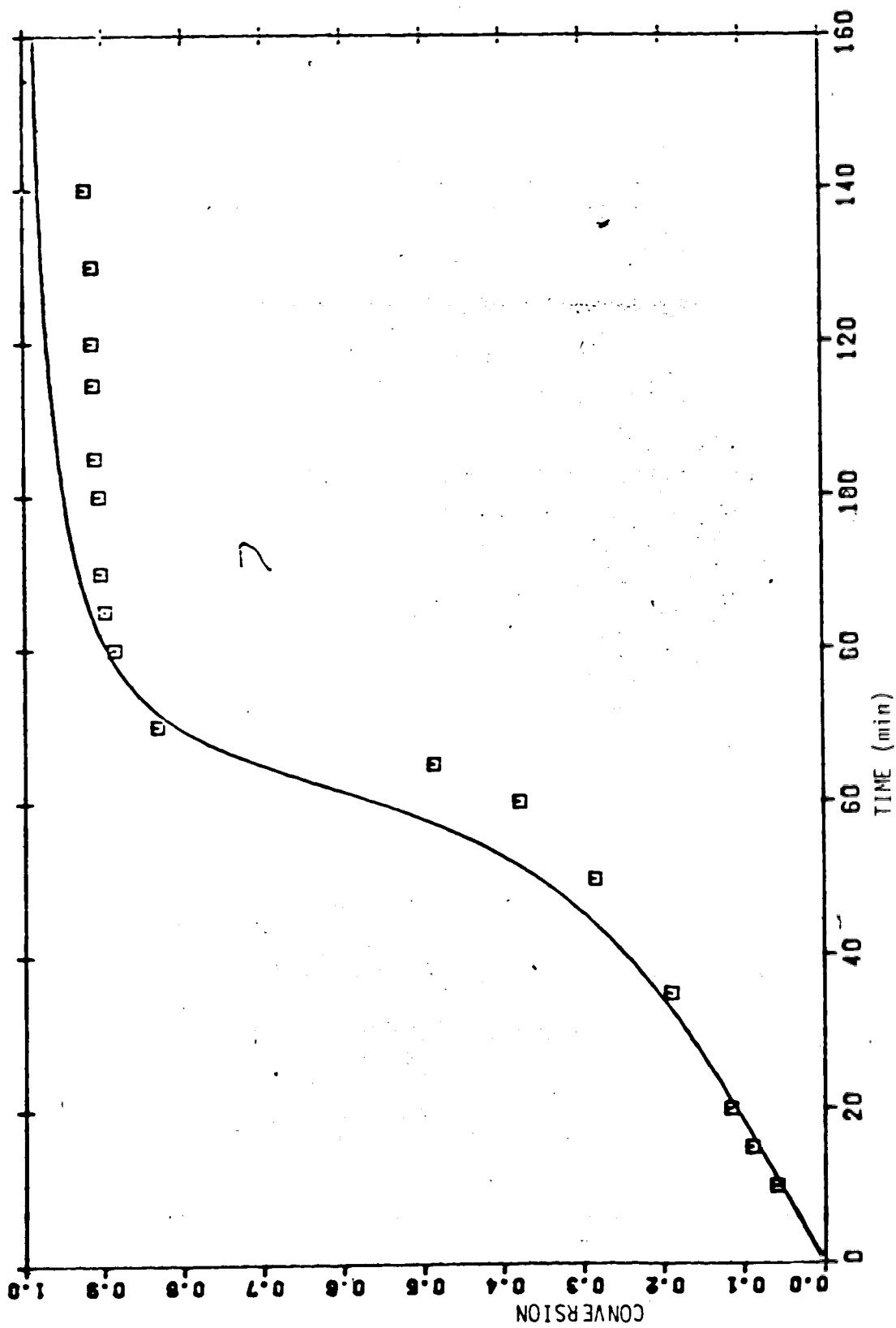


Figure II-2: Conversion versus Time. Isothermal Run at 70°C. ($I_0 = 0.01699 \text{ gmole.l}^{-1}$)

— Mathematical Model
 □ Experimental Points (Balke - 1972).

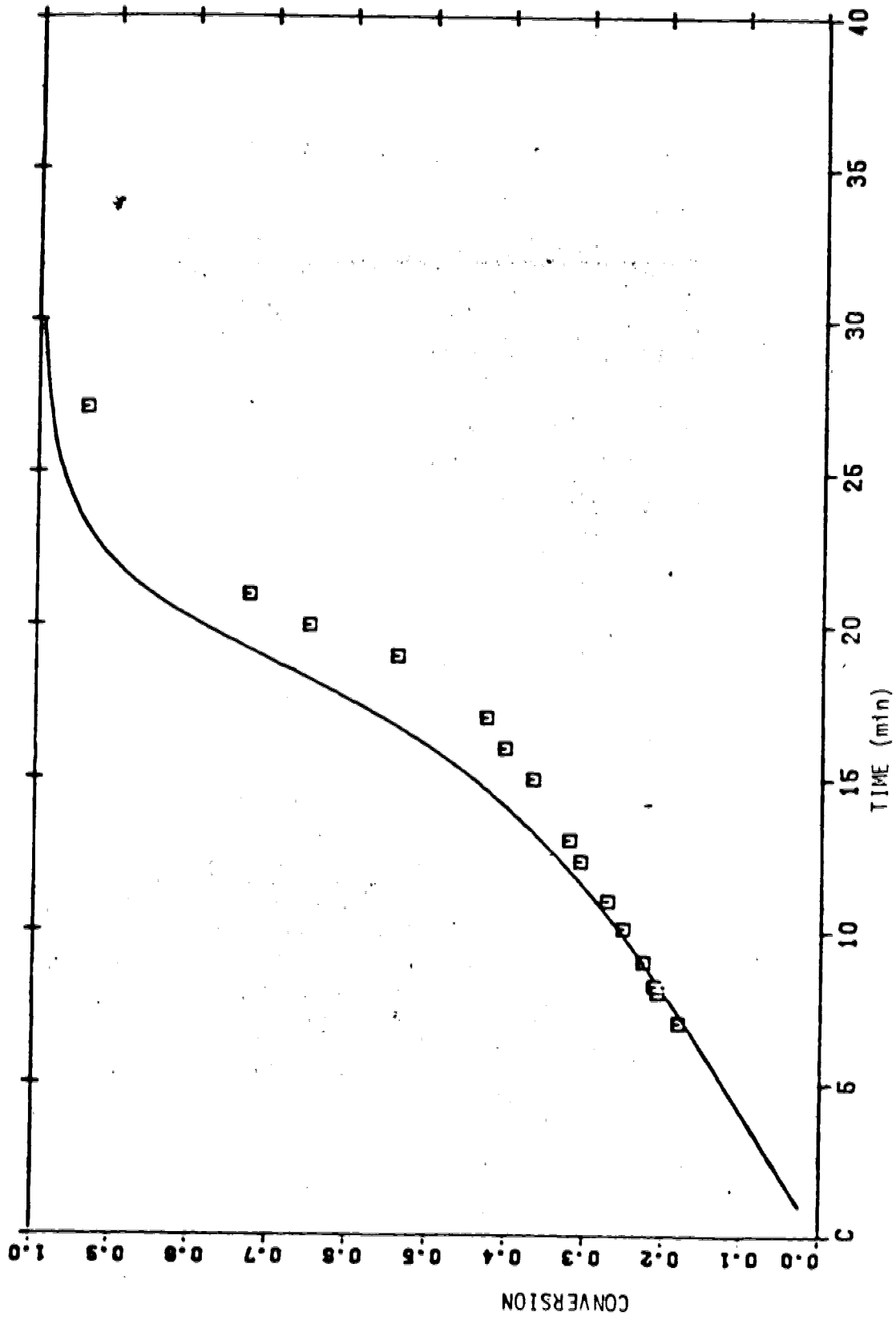


Figure II.3: Conversion versus Time. Isothermal run at 90°C. ($I_0 = 0.01699 \text{ mole.l}^{-1}$)
 — Mathematical Model
 □ Experimental Points (Balke - 1972).

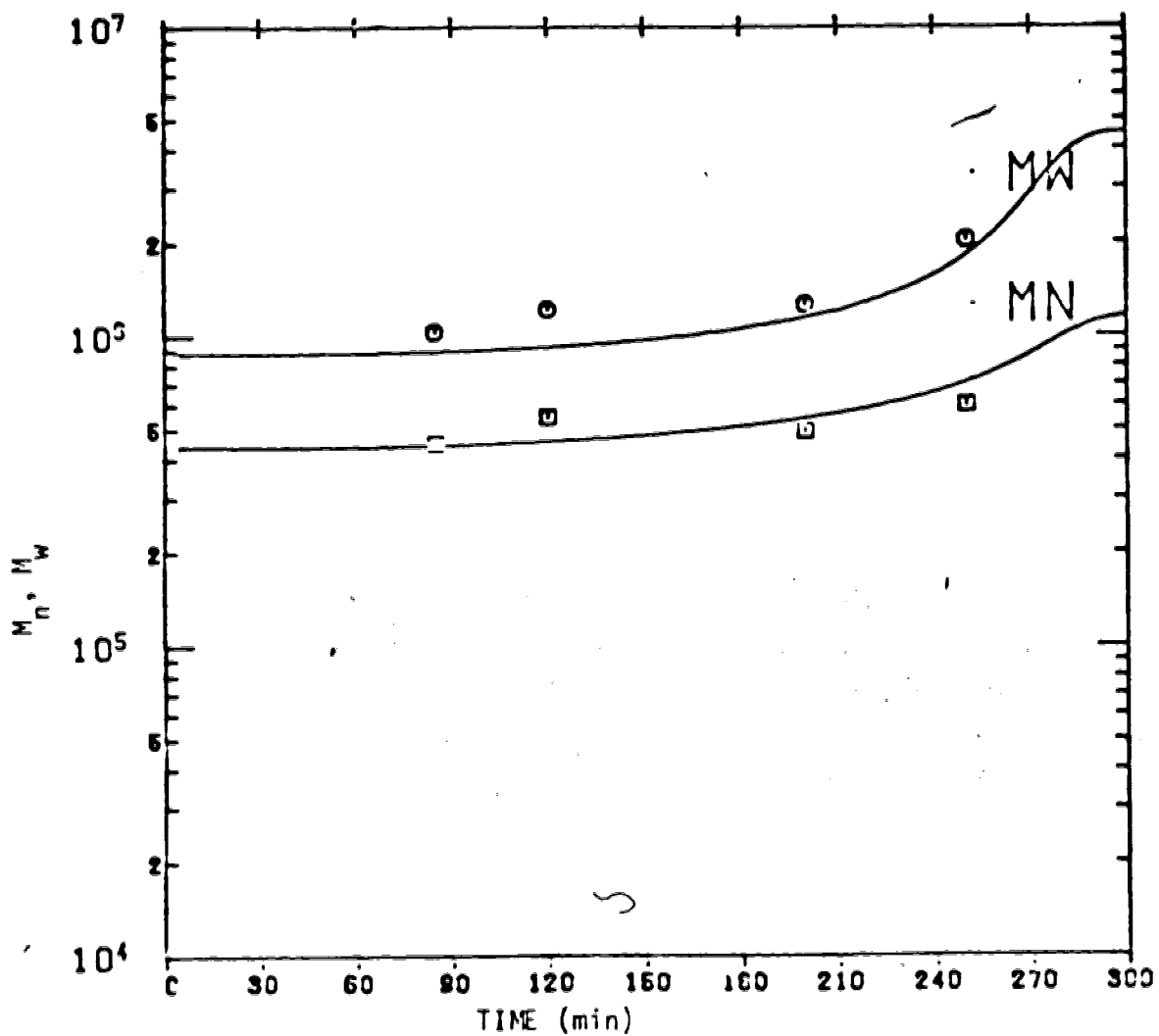


Figure II.4. Number Average Molecular Weight and Weight Average Molecular Weight versus Time. Isothermal Run at 50°C . ($I_0 = 0.01699 \text{ gmole.l}^{-1}$)
 — Mathematical Model
 □ □ Experimental Points (Balke - 1972).

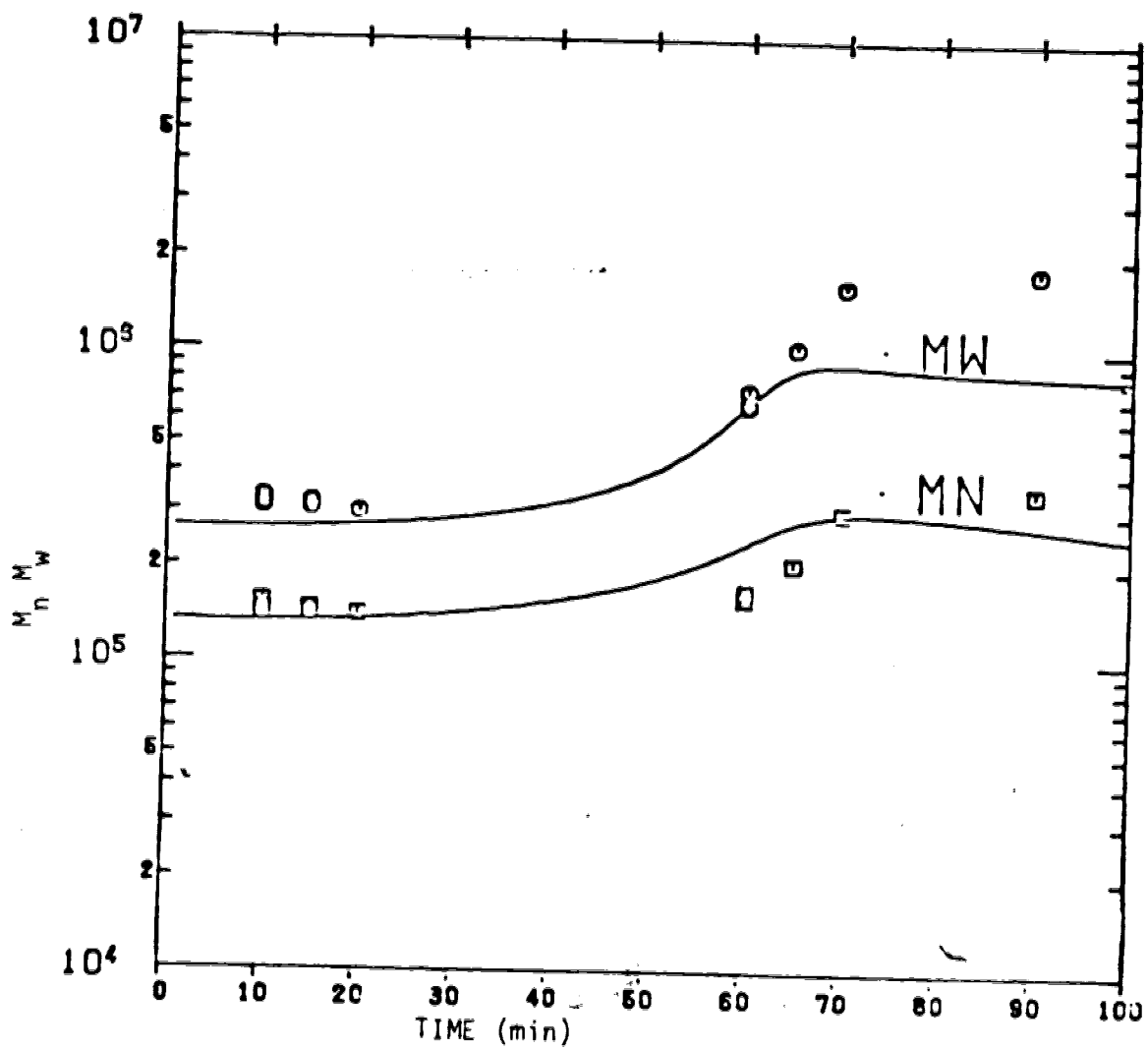


Figure II.5: Number Average Molecular Weight and Weight Average Molecular Weight versus Time, Isothermal Run at 70°C . ($I_0 = 0.01699 \text{ gmole.l}^{-1}$)
 — Mathematical Model
 □ □ Experimental Points (Balke - 1972).

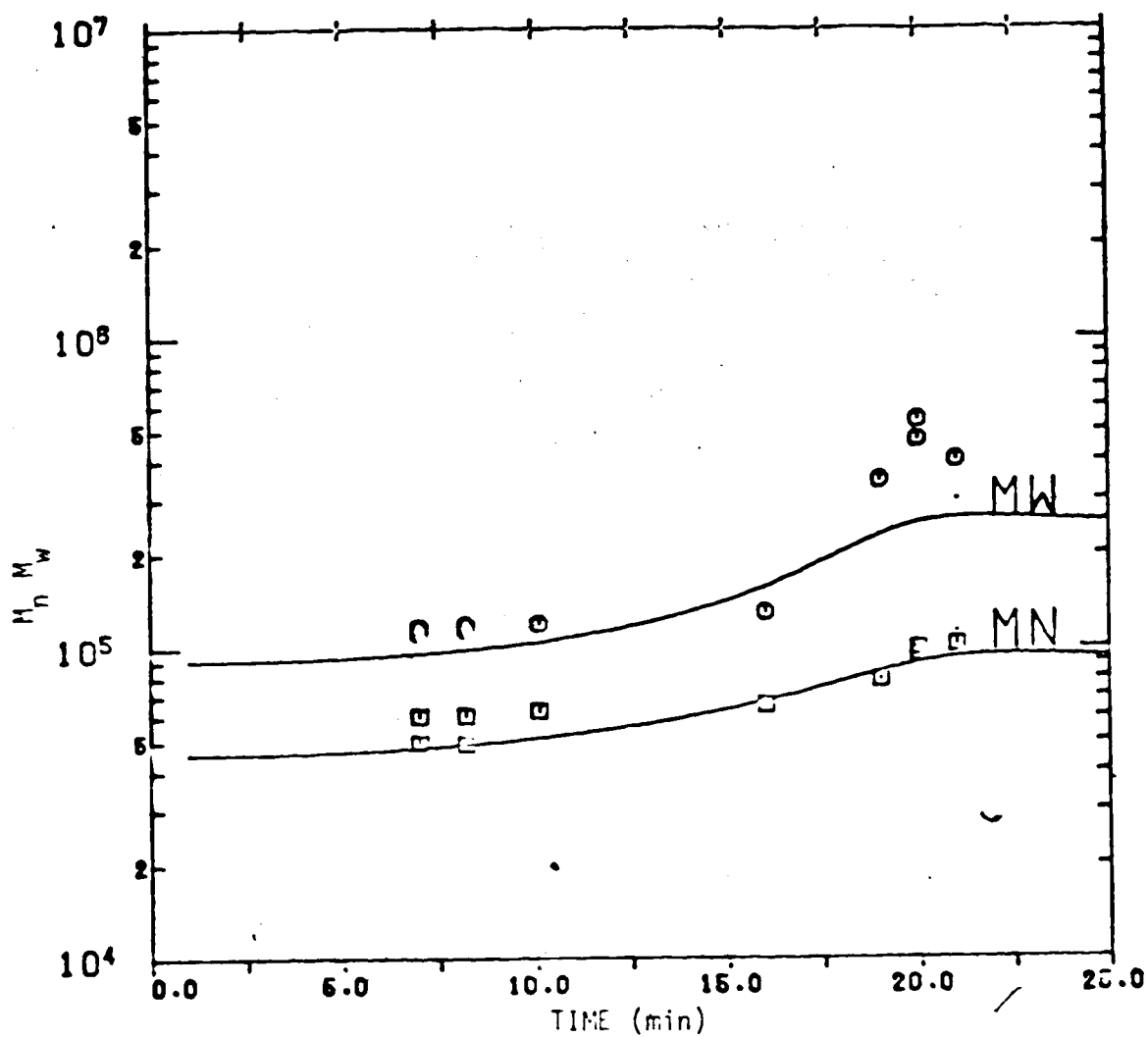


Figure II.6: Number Average Molecular Weight and Weight Average Molecular Weight versus Time. Isothermal Run at 90°C . ($I_0 = 0.01699 \text{ mole.l}^{-1}$)
 — Mathematical Model
 □ ⊙ Experimental Points (Balke - 1972).

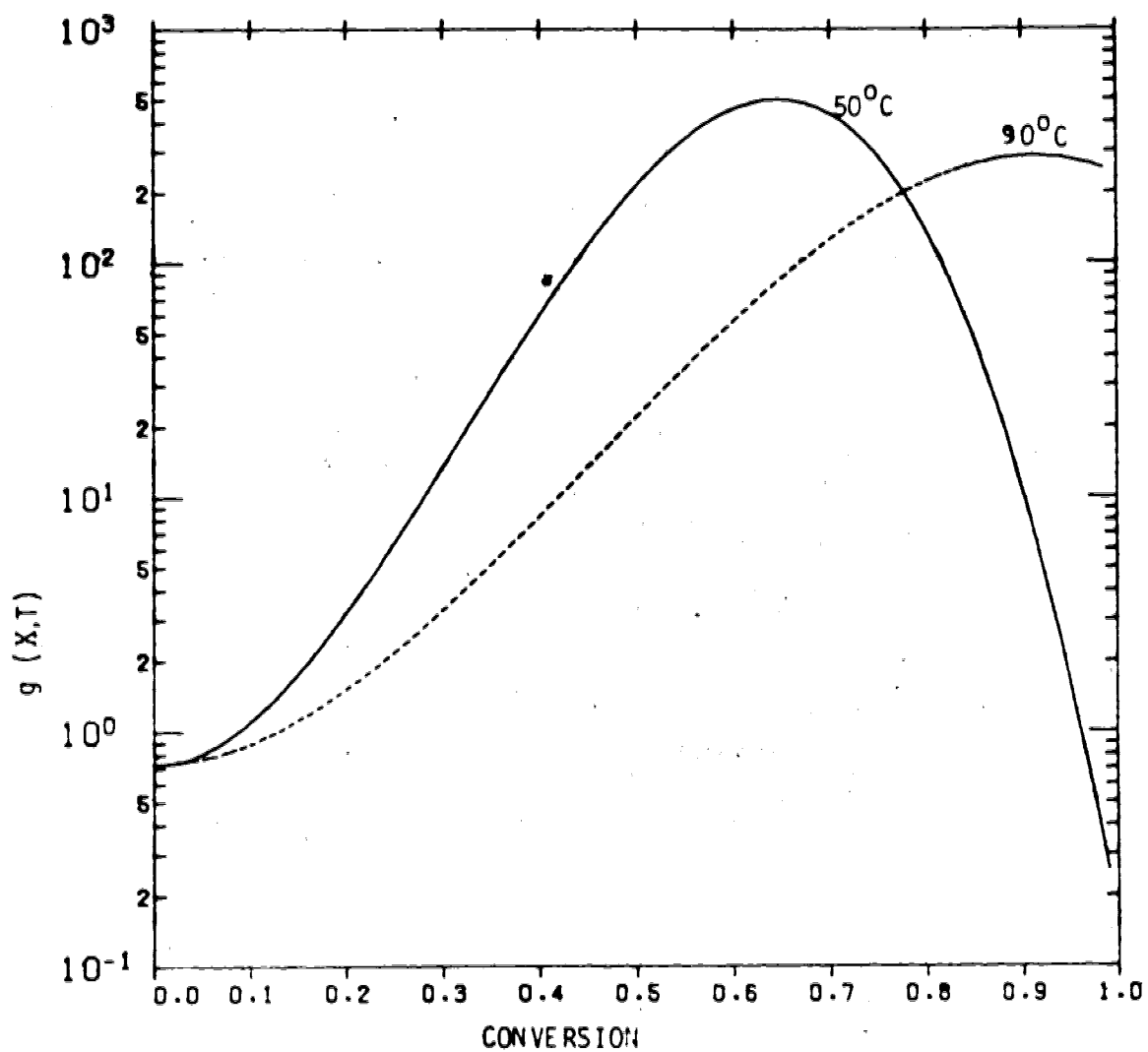


FIGURE II. 7: Gel Effect Function $g(X,T)$.

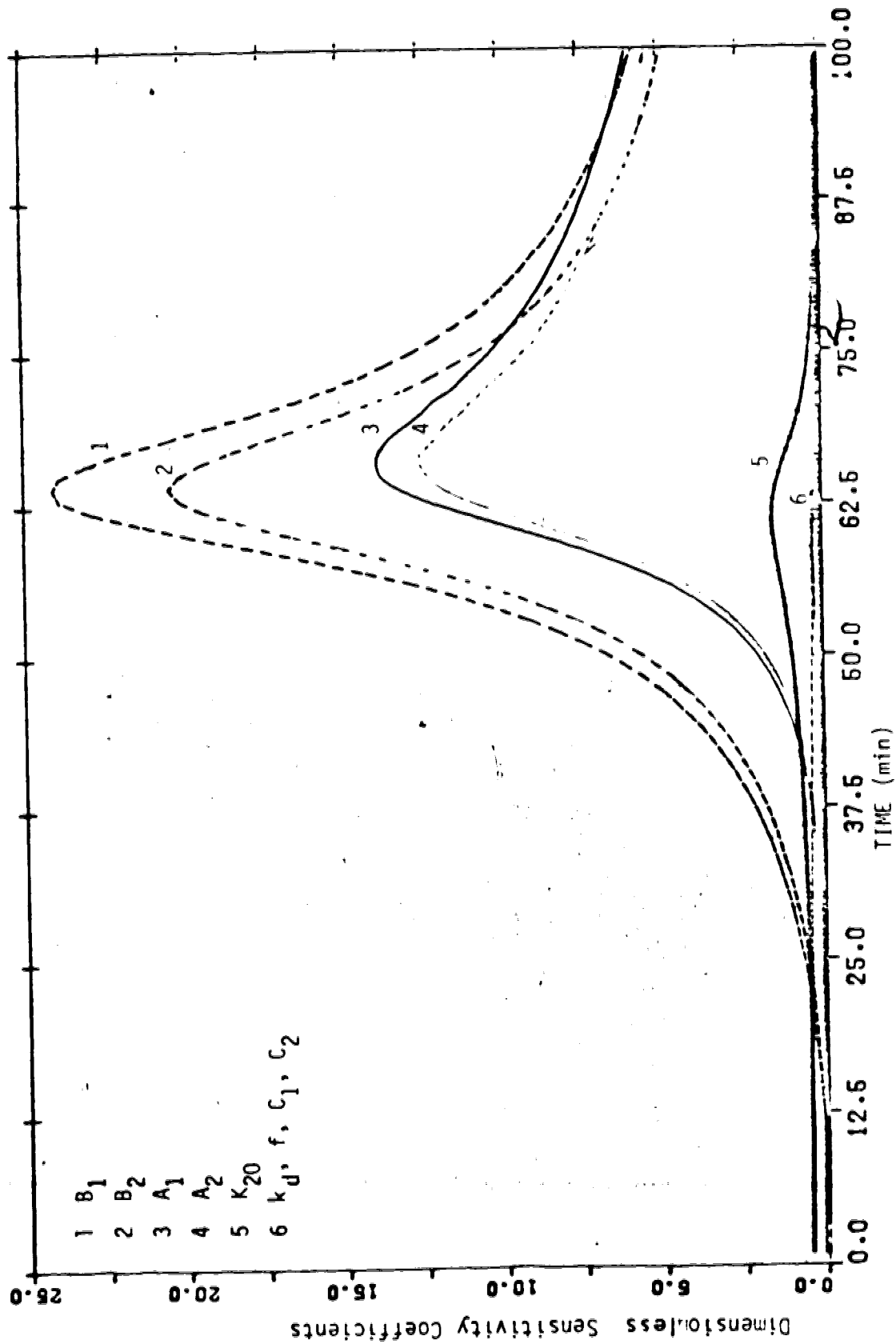


Figure II.8: Effect of the Perturbations of the Parameters on the Conversion.
 ($I_0 = 0.01699 \text{ gmole.l}^{-1}$, $T = 70^\circ \text{C}$)

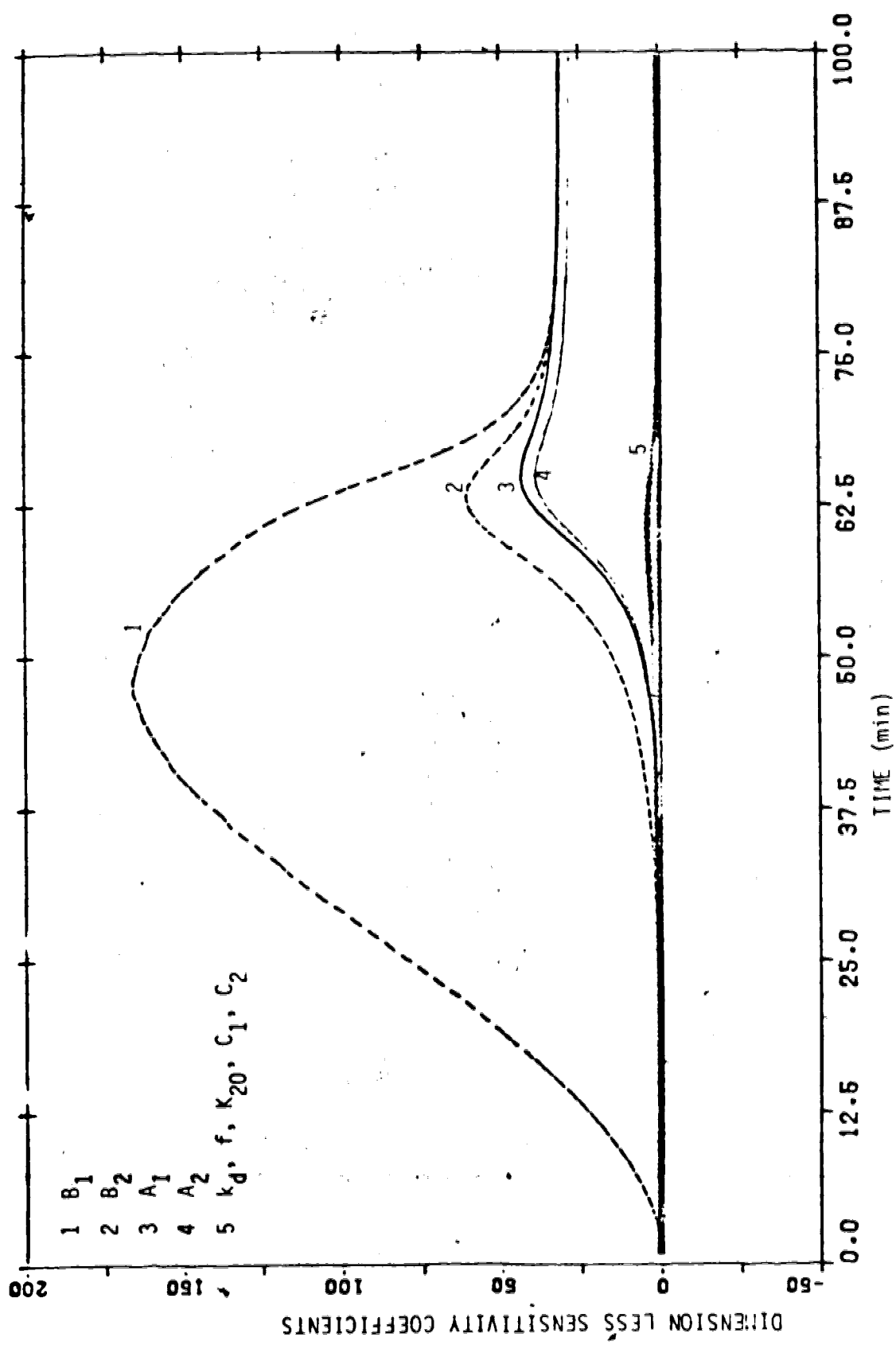


Figure II.9: Effect of the Perturbations of the Parameters on the 2nd Moment of the MMU
(I₀ = 0.01699 gmole.l⁻¹, T = 70°C).

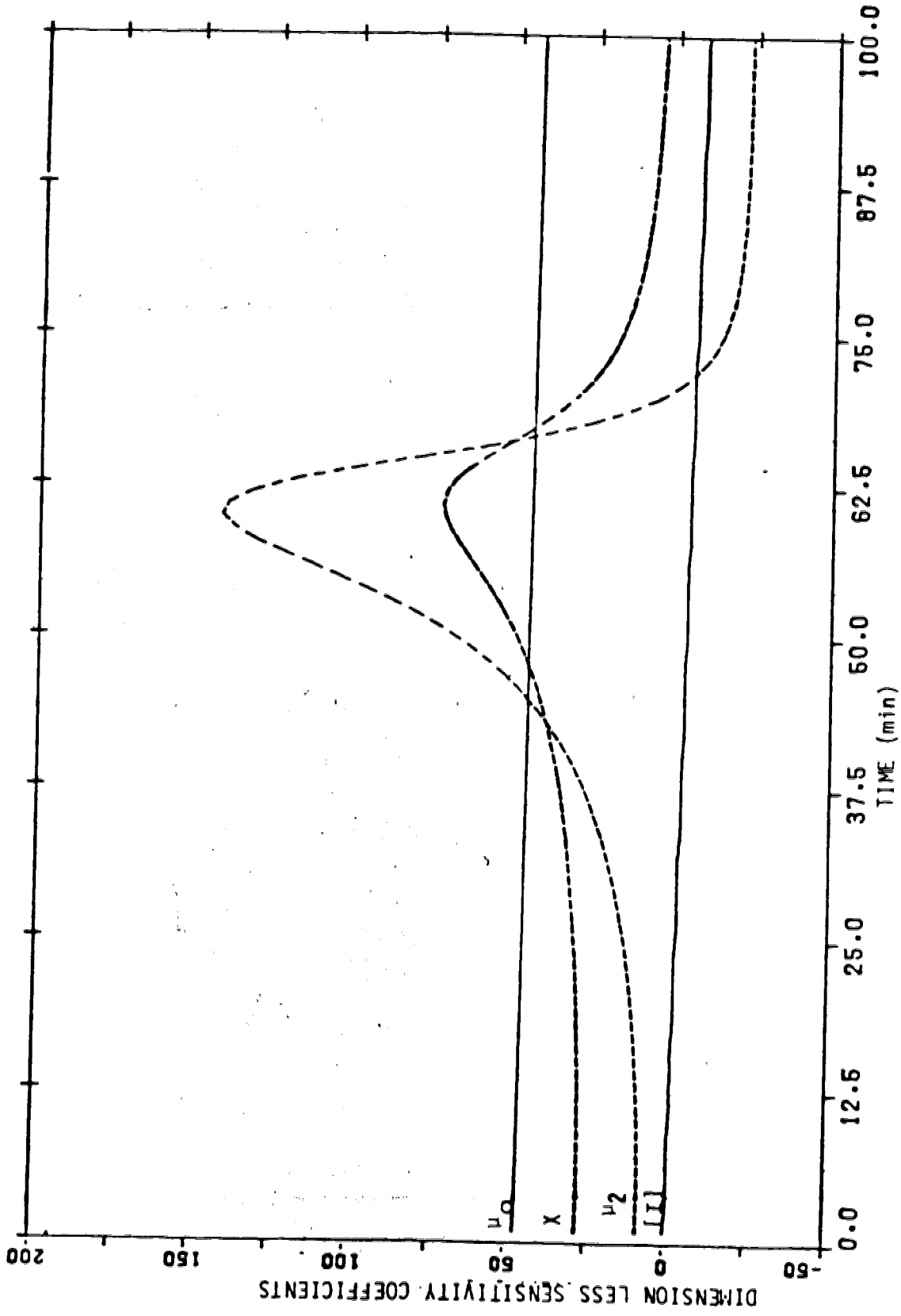


Figure II.10: Sensitivity Coefficients of the Output Variables relative to the Temperature. ($I_0 = 0.01699 \text{ gmole. l}^{-1}$)

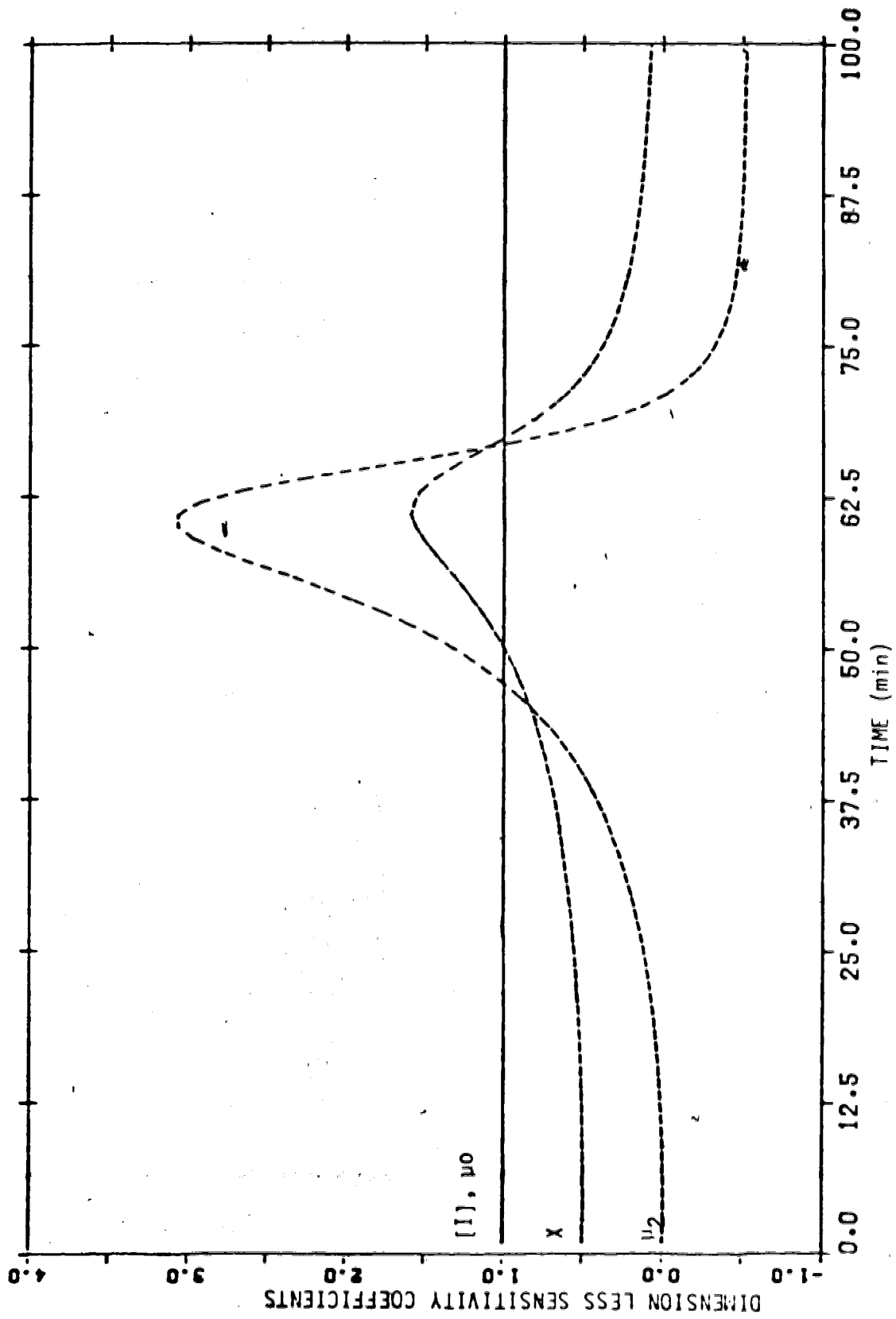


Figure II.11: Sensitivity Coefficients of the Output Variables relatively to the Initial Initiator Concentration $[I_0]$. ($T = 70^\circ\text{C}$).

CHAPTER III
APPLICATION OF THE OPTIMAL CONTROL THEORY
• TO THE POLYMERIZATION REACTOR

III. 1 Formulation of the Optimal Control Problem

The theory of time optimal control has arisen from the need to improve the performance of dynamic systems. More specifically, given a process described by a mathematical model, it is required to find the admissible inputs (or control variables) which generate the desired output and which, in so doing, minimize a chosen cost functional. Stated mathematically, problems such as these belong to the calculus of variations. However, classical variational theory can not readily handle the hard physical constraints usually imposed on state variables and control variables. This difficulty led Pontryagin (1956) to first conjuncture his celebrated "Minimum Principle", and then together with Boltyanskii and Gämkelidze (1962) to provide proof of it. The Minimum Principle gives a solution to optimal control problems which cannot be solved by the classical variational theory.

Consider any controlled process which can be described by a system of ordinary differential equations:

$$\frac{d\underline{Y}}{dt} = \underline{f}(\underline{Y}, t, \underline{u}) \quad (\text{III.1})$$

$$\underline{Y}(t_0) = \underline{Y}_0 \quad (\text{III.2})$$

where \underline{Y} is the state vector of dimension n

\underline{Y}_0 is the initial value of the state vector at time t_0

t is the time

\underline{u} is the control vector of dimension m

Given the initial value for \underline{Y} , equation (III.2), the solution for equation (III.1) is uniquely defined, once the control vector \underline{u} is chosen.

Consider the performance functional J :

$$J = G(\underline{Y}(t_f), t_f) + \int_{t_0}^{t_f} L(\underline{Y}(t), t, \underline{u}(t)) dt \quad (\text{III.3})$$

where t_0 and t_f denote the initial and final time, G and L are scalar functionals. It is required to find an admissible control $\underline{u}^*(t)$ which causes the general non-linear system (III.1) with initial condition (III.2) to follow an admissible trajectory $\underline{Y}^*(t)$ that minimizes the performance functional J . Then such a control $\underline{u}^*(t)$ is called the optimal control and $\underline{Y}^*(t)$ the optimal trajectory.

The classical calculus of variations leads to the following solution.

Define the Hamiltonian H (scalar functional) as:

$$H(\underline{Y}(t), \underline{u}(t), \underline{P}(t), t) = L(\underline{Y}(t), t, \underline{u}(t)) + \underline{P}(t) \cdot \underline{f}(\underline{Y}(t), t, \underline{u}(t)) \quad (\text{III.4})$$

where $\underline{P}(t)$ is called the costate vector or adjoint variable. It is a vector of dimension n . The costate variables must satisfy the canonical equations,

$$\dot{\underline{p}} = - \frac{\partial H}{\partial \underline{Y}} \quad (\text{III.5})$$

The final boundary values for costate vector \underline{p} depend upon the particular form of $G(\underline{Y}(t_f), t_f)$ and upon the final conditions for the state vector $\underline{Y}(t_f)$. That is,

(i) if the costate vector $\underline{Y}(t_f)$ is free, then $\underline{p}(t_f)$ must satisfy the following equation,

$$\underline{p}(t_f) = \frac{\partial G(\underline{Y}(t_f), t_f)}{\partial \underline{Y}(t_f)} \quad (\text{III.6})$$

(ii) If some of the components of $\underline{Y}(t_f)$ are specified at the final time, i.e.,

$$Y_i(t_f) = Y_{if} \quad i = 1, 2, \dots, r \quad (\text{III.7})$$

$$Y_j(t_f) \text{ is free for } j = r+1, \dots, n$$

then $\underline{p}(t_f)$ must satisfy the following conditions:

$$\left\{ \begin{array}{ll} P_i(t_f) \text{ is free} & i = 1, 2, \dots, r \\ P_j(t_f) = \frac{\partial G(\underline{Y}(t_f), t_f)}{\partial Y_j(t_f)} & j = r+1, \dots, n \end{array} \right. \quad (\text{III.8})$$

A necessary condition for optimality, derived from the classical calculus of variations is that the gradient of the Hamiltonian H relative to the control vector \underline{u} must be zero along the optimal trajectory.

$$\frac{\partial H}{\partial \underline{u}} = 0 \quad \text{III.9}$$

A heuristic proof of conditions (III.6), (III.8) and (III.9) is given in Appendix C. Equation (III.9) is valid only if the control \underline{u} is not constrained. However, in most control problems, restrictions have to be imposed on the control \underline{u} (e.g. $|u_j(t)| \leq M_j, j = 1, 2 \dots m$), because of economical and physical constraints. Then the above relationship (III.9) cannot be used because it breaks down on the boundary. This relationship is replaced by the following inequality:

$$H(\underline{Y}^*, \underline{u}^*, \underline{P}^*, t) \leq H(\underline{Y}^*, \underline{u}, \underline{P}^*, t) \quad (\text{III.10})$$

for all admissible controls $\underline{u}(t)$, and all $t \in [t_0, t_f]$, where $\underline{Y}^*, \underline{u}^*, \underline{P}^*$ represent the optimal trajectories for $\underline{Y}, \underline{u}, \underline{P}$. H is minimized by selecting the admissible controls which give the smallest value for the Hamiltonian Equation (III.10) and which is the basic statement of the Pontryagin Minimum Principle. Solution to the optimal control problem can be obtained by solving a two-point boundary value problem (TPBV) for the differential equations (III.1) and III.5), with n initial values for $\underline{Y}(t_0)$, r final values for $\underline{Y}(t_f)$, and $(n-r)$ final values for $\underline{P}(t_f)$, while minimizing the Hamiltonian H . It must be noted that (a) it may not be known in advance that an optimal control exists and (b) even if an optimal control exists, it may not be unique. (Pontryagin(1962)).

III.2 Application of the Minimum Principle to the Polymerization of MMA.

The bulk free radical polymerization of MMA in a batch

reactor can be described by a knowledge of initiator concentration $[I]$, monomer conversion X , zeroth moment of the MWD μ_0 , and second moment of the MWD μ_2 . These state variables obey the differential equations (II.1), (II.3), (II.7), (II.8) derived in Chapter II. Because the state variables $[I]$, X , μ_0 , μ_2 are of a different order of magnitude ($[I] \approx 10^{-2}$, $X \approx 1$, $\mu_0 \approx 10^{-3}$, $\mu_2 \approx 10^4$), the numerical integration of the differential equations has been proved challenging and was eased by the introduction of the following state variables:

$$\text{Dimensionless catalyst concentration: } Y_1 = \frac{[I]}{[I_0]}$$

$$\text{Dimensionless monomer conversion: } Y_2 = \frac{X}{X_d}$$

$$\text{Dimensionless zero}^{\text{th}} \text{ moment: } Y_3 = \frac{\mu_0}{\mu_{0d}}$$

$$\text{Dimensionless second moment: } Y_4 = \frac{\mu_2}{\mu_{2d}}$$

where X_d , μ_{0d} , μ_{2d} are the desired values of X , μ_0 and μ_2 at final time t_f . In terms of the dimensionless state variables equations (II.1), (II.3), (II.7) and (II.8) can be rewritten as

$$\frac{dY_1}{dt} = -k_d Y_1 + \frac{F_c}{V[I_0]}$$

$$\frac{dY_2}{dt} = \sqrt{2 f k_d [I_0] Y_1 K_2} \frac{(1 - Y_2 X_d)}{X_d} \quad (\text{III.11})$$

$$\frac{dY_3}{dt} = \frac{1}{\nu_{0d}} 2 f k_d [I_0] Y_1$$

$$\frac{dY_4}{dt} = \frac{1}{\nu_{2d}} 2 K_2 [M_0]^2 (1 - Y_2 X_d)^2$$

The initial values for the dimensionless state variables are given as

$$\underline{Y}(0) = (1., 0., 0., 0.)^T \quad (\text{III.12})$$

The choice of a mathematical performance functional is a highly subjective matter, as the choice of one engineer needs not be the choice of another. The objective functional is based on product quality and economical needs. In this particular problem of polymerization it is desired to produce the "best polymer" in the minimum batch time. The mathematical definition of the term "best polymer" depends on the final application of the polymeric product, hence it can widely vary. The useful mechanical and physical properties of a polymer are strongly related to its MWD. In most cases, there is a molecular weight range in which a polymeric product will have desired physical and

mechanical characteristics. Thus the term "best polymer" will mean a polymer with specified M_n and M_w , and consequently will possess certain desired physical and mechanical properties. Prespecified conversion, number average molecular weight and weight average molecular weight for the final product determine uniquely the zero, first and second moments of the MWD at the end of the reaction. Accordingly the objective function to be minimized may be expressed as:

$$J = (Y_2(t_f) - 1)^2 + (Y_3(t_f) - 1)^2 + (Y_4(t_f) - 1)^2 \quad (\text{III.13})$$

This is a Mayer problem.

The final time t_f is fixed in the above objective function. By successively minimizing this objective function for smaller values for t_f , the minimal batch time problem can be solved. Comparing equations (III.3) and (III.13), we obtain the following expressions for L and G:

$$G(\underline{Y}(t_f), t_f) = (Y_2(t_f) - 1)^2 + (Y_3(t_f) - 1)^2 + (Y_4(t_f) - 1)^2 \quad (\text{III.14})$$

$$L(\underline{Y}(t), t, \underline{u}(t)) = 0.$$

Because the final conditions on \underline{Y} have been included in equation (III.14), $\underline{Y}(t_f)$ will be free, and therefore $\underline{P}(t_f)$ will be given by equation (III.6).

J is to be minimized by finding the optimal policy for the

control $\underline{u}(t)$. In this study the two control variables are the reaction temperature T and the catalyst feed rate F_c . It is assumed that F_c and T can be manipulated and fixed at our convenience, although they could be bound by physical constraints.

The expression for the Hamiltonian can be derived from equations (III.4) and (III.11):

$$\begin{aligned}
 H = 0. & + \left(-k_d Y_1 + \frac{F_c}{V[I_0]} \right) P_1 \\
 & + \left(\sqrt{2 f \cdot k_d [I_0] Y_1 K_2} \left(\frac{1 - Y_2 X_d}{X_d} \right) \right) P_2 \\
 & + \frac{2 f k_d [I_0] Y_1}{v_{0d}} P_3 \\
 & + \frac{2 K_2 [M_0]^2 (1 - Y_2 X_d)^2}{v_{2d}} P_4 \quad \text{(III.16)}
 \end{aligned}$$

H is not an explicit function of time. Therefore, as is proven in Appendix C, H must remain constant along the optimal trajectory if the equation (III.9) is to be satisfied.

The costate differential equations are derived from equations (III.5) and (III.16),

$$\frac{d P_1}{dt} = k_d P_1 - \sqrt{\frac{f k_d [I_0] K_2}{2 Y_1}} \frac{(1 - Y_2 X_d)}{X_d} P_2 - \frac{2 f k_d [I_0]}{v_{0d}} P_3$$

$$\begin{aligned} \frac{d P_2}{dt} = & \left[1 - \frac{1}{2} \left(3 A Y_2^2 X_d^3 + 2 B Y_2 X_d^2 \right) \left(\frac{1 - Y_2 X_d}{X_d} \right) \right] \\ & \sqrt{2 f k_d [I_0] Y_1 K_2} P_2 \\ & + \left[4 X_d - 2 \left(3 A Y_2^2 X_d^3 + 2 B Y_2 X_d^2 \right) (1 - Y_2 X_d) \right] \\ & \frac{K_2 [M_0]^2 (1 - Y_2 X_d)}{v_{2d}} P_4 \end{aligned}$$

(III.17)

$$\frac{d P_3}{dt} = 0$$

$$\frac{d P_4}{dt} = 0$$

Using equations (III.6) and (III.14), final values of \underline{P} can be calculated:

$$P_1(t_f) = 0$$

$$P_2(t_f) = 2(Y_2(t_f) - 1)$$

$$P_3(t_f) = 2(Y_3(t_f) - 1) \quad (\text{III.18})$$

$$P_4(t_f) = 2(Y_4(t_f) - 1)$$

The systems of differential equations (III.11) and (III.17) have to be integrated simultaneously with the initial and final conditions (III.12) and (III.18). Therefore, a two-point boundary value problem has to be solved, along with the minimization of the Hamiltonian H to obtain the optimal control policies.

In this work three separate problems are considered:

(i) Obtain a polymer with desired X , M_n , M_w in the minimum batch time by calculating the optimal temperature policy in the reactor.

(ii) Obtain a polymer with desired X , M_n , M_w in the minimum batch time by calculating the optimal policy for catalyst feed rate.

(iii) Obtain a polymer with desired X , M_n , M_w in the minimum batch time by calculating the optimal policies for polymerization temperature and catalyst feed rate.

Solution for problem (i) is developed in Chapters IV and V. Solutions for problems (ii) and (iii) are developed in Chapter VI.

CHAPTER IV

SOLUTION OF THE TPBV PROBLEM

IV.1 Introduction

In this chapter, we solve the TPBV optimal control problem by assuming only one control variable, the polymerization temperature T in the reactor. No catalyst is added to the reactor during the polymerization, and the initial concentration of catalyst $[I_0]$ is fixed to a value of 0.5% in weight. Two algorithms that compute the optimal temperature profile in the batch reactor are developed and their results are compared. The first one is based on the discretization of the total polymerization time in N equal intervals. The control variable (temperature) remains constant in each time interval, and the Hamiltonian is minimized by a first-order gradient method. For the sake of brevity, this algorithm will be referred to as the discrete control method (DCM) algorithm. The second algorithm, which solves the two-point boundary value problem by a shooting method will be referred to as shooting method (SM) algorithm.

IV.2 Discrete Control Method Algorithm

The polymerization of MMA in a batch reactor can be described by the following set of differential equations:

$$\frac{dY}{dt} = \underline{f}(Y, t, T) \quad (\text{IV.1})$$

with the initial conditions:

$$\underline{Y}(t_0) = \underline{Y}_0 \quad (IV.2)$$

The objective function to be minimized is defined as:

$$J = (Y_2(t_f) - 1)^2 + (Y_3(t_f) - 1)^2 + (Y_4(t_f) - 1)^2 + \int_{t_0}^{t_f} w_t dt \quad (IV.3)$$

According to the previous analysis in Chapter III, the necessary conditions for the optimality of the costate trajectory can be expressed as:

$$\frac{d \underline{P}}{dt} = - \frac{\partial H}{\partial \underline{Y}} \quad (IV.4)$$

$$\underline{P}(t_f) = \frac{\partial G(\underline{Y}(t_f), t_f)}{\partial \underline{Y}} \quad (IV.5)$$

Suppose that a temperature history $T^i(t)$, $t \in [t_0, t_f]$ is known and used to solve the differential equations (IV.1) and (IV.4), so that the state-costate trajectories $\underline{Y}^i(t)$ and $\underline{P}^i(t)$ satisfy the boundary conditions (IV.2) and (IV.5). If this temperature history $T^i(t)$ also satisfies equation (IV.6):

$$\frac{\partial H}{\partial T} (\underline{Y}^i, \underline{P}^i, T^i, t) = 0 \quad (IV.6)$$

for all $t \in [t_0, t_f]$, then $T^i(t)$ satisfies all necessary conditions for being an optimal control.

However, suppose that equation (IV.6) is not satisfied, then for a change $\delta T^i(t)$ around the control $T^i(t)$,

$$\delta T^i(t) = T^{i+1}(t) - T^i(t), \quad (\text{IV.7})$$

the first variation of the functional J may be expressed as:
(See equation C.12, Appendix C)

$$\delta J = \int_{t_0}^{t_f} \left(\frac{\partial H}{\partial T} \right)^i \delta T^i dt \quad (\text{IV.8})$$

Hence, if the change in T^i is selected using a steepest gradient method

$$\delta T^i(t) = -\alpha^i \left(\frac{\partial H}{\partial T} \right)^i \quad \text{with } \alpha^i > 0 \quad (\text{IV.9})$$

Then

$$\delta J = -\alpha^i \int_{t_0}^{t_f} \left(\frac{\partial H}{\partial T} \right)^i \left(\frac{\partial H}{\partial T} \right)^i dt \quad (\text{IV.10})$$

Because the integrand is positive for all $t \in [t_0, t_f]$, $\delta J \leq 0$. For a sufficiently small δJ (i.e., a sufficiently small α^i), this implies that $J(T^{i+1}(t)) \leq J(T^i(t))$, since the increment in J is governed essentially by the first variation δJ . Hence, if the control $T^i(t)$ is updated according to equation (IV.9), $T^i(t)$ will eventually converge

to the optimal control $T^*(t)$, if the optimal control exists.

We shall now outline the steps required to determine the optimal control $T^*(t)$ using the discrete control method algorithm (V. Gourishankar, 1980).

Step 1: Select a discrete approximation to the temperature history $T^i(t)$, $t_0 \leq t \leq t_f$, by subdividing the interval $[t_0, t_f]$ into N suitably chosen subintervals of equal duration. Consider the control T^i as being piecewise constant during each of these subintervals, that is:

$$T^i(t) = T^i(t_k), \quad t \in [t_{k-1}, t_k], \quad k=1, 2, \dots, N \quad (\text{IV.11})$$

and store the value of $T^i(t_k)$.

Step 2: Using $T^i(t)$, integrate the state equation (IV.1) from t_0 to t_f with the initial condition (IV.2) and store the resulting state trajectory $\underline{Y}^i(t)$.

Step 3: Obtain $\underline{P}^i(t_f)$ by substituting $\underline{Y}^i(t_f)$ in equation (IV.5). Using this value of $\underline{P}^i(t_f)$, the computed values of the state trajectory $\underline{Y}^i(t)$, and the control history $T^i(t)$, integrate backward equation (IV.4) from t_f to t_0 ; compute

$$g^i(t_k) = \left(\frac{\partial H}{\partial T} \right)^i \Big|_{t_k}$$

in each interval $[t_{k-1}, t_k]$ and save this value.

Step 4: If the stopping criterion is satisfied, terminate the iterative procedure; in this case $T^i(t)$ is the required

optimal control. Otherwise generate a new piecewise constant control history

$$T^{i+1}(t_k) = T^i(t_k) - \alpha^i g^i(t_k) \quad k=1,2, \dots, N \quad (\text{IV.12})$$

and restart the procedure from Step 2.

This algorithm is summarized in Figure IV.1.

In the above algorithm, the final time is fixed. The minimum time is found by solving the same problem for different final times and selecting the smallest final time for which convergence is possible.

In the DCM algorithm, $T^i(t)$ is not constrained, therefore, the necessary condition for optimality relative to the minimization of H is

$$g^i(t) = \left. \frac{\partial H}{\partial T} \right|_t = 0 \quad \text{for all } t \in [t_0, t_f] \quad (\text{IV.13})$$

Consequently, the above condition should be the stopping criterion for terminating the DCM algorithm. However, instead of using the above criterion, we have chosen the following stopping condition:

$$|Y^i(t_f) - 1| \leq 5\% \quad \text{for } i=2,3,4. \quad (\text{IV.14})$$

If this stopping condition is satisfied, the desired target set at final time has been hit by the conversion, the zeroth moment and the second moment within acceptable limits. It

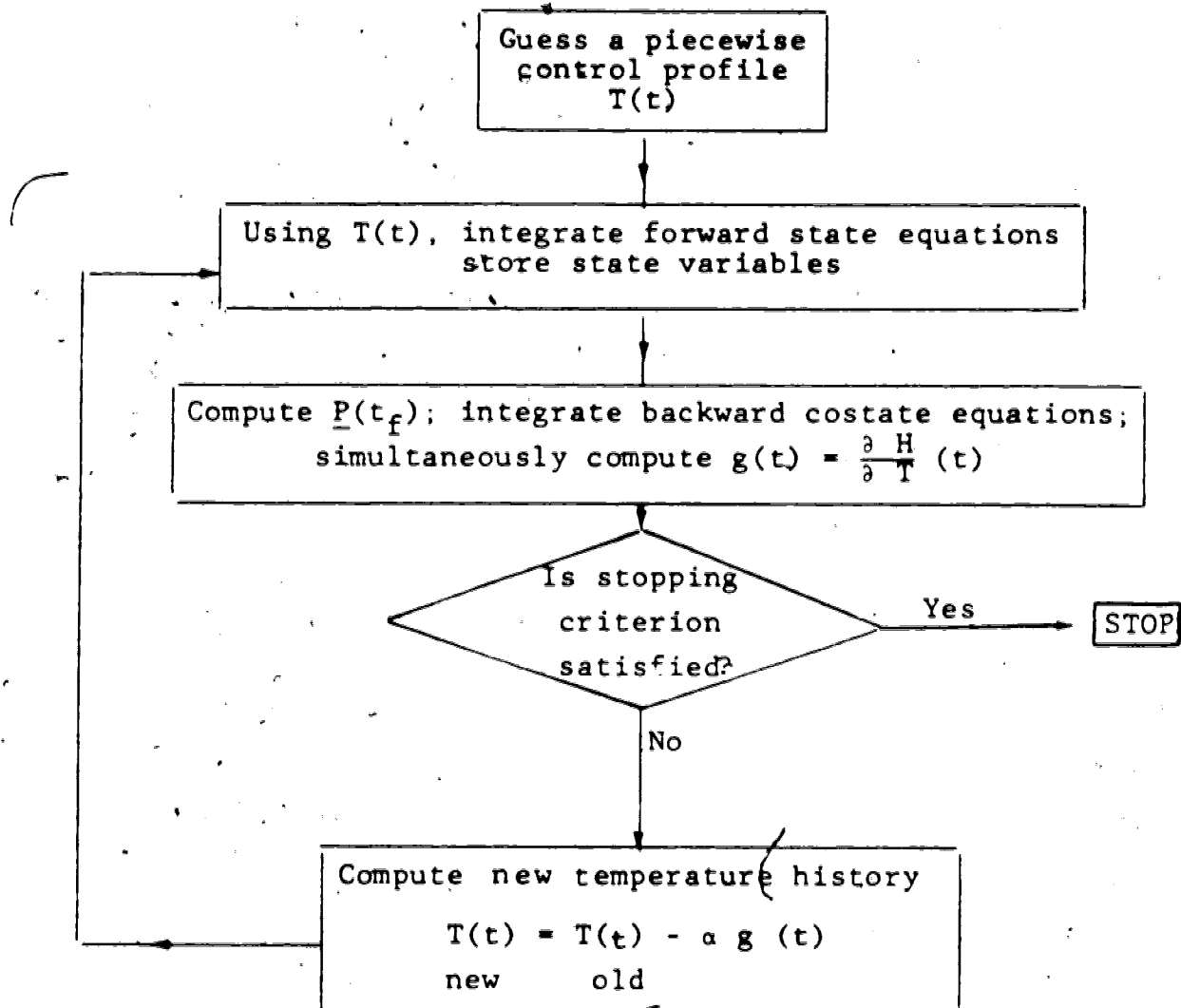


Figure IV.1: Discrete Control Method Algorithm

was found that when condition (IV.14) was satisfied, condition (IV.13) was also approximately satisfied. To verify that, the following norm for the gradient has been defined:

$$\| | g^i | | = \sum_{k=1}^N g^i(t_k)^2 \quad (\text{IV.15})$$

As the above norm decreases and approaches zero, the temperature profile computed by the DCM algorithm approaches the optimal temperature policy.

The integration of the differential equations (IV.1) and (IV.4) has been carried out using a Runge-Kunta routine of Shampine and Allen (1973). The routine estimates the local error and adjusts the integration step size dependently on the local error. The initial integration step size has been selected as 5 sec. Stiffness in the differential equations was not encountered, because of the use of dimensionless variables.

The gradient $g^i(t_k)$ can be calculated analytically in each subinterval $[t_{k-1}, t_k]$ from equation (III.16).

$$g^i(t_k) = -\frac{1}{T^2} \left[-\frac{E_d}{R} \frac{dY_1}{dt} P_1 + \frac{1}{2} \left(-\left(\frac{E_d+E_2}{R}\right) + A_1 Y_2^3 X_d^3 + B_1 Y_2^2 X_d^2 + C_1 \right) \frac{dY_2}{dt} P_2 \right. \\ \left. - \frac{E_d}{R} \frac{dY_3}{dt} P_3 + \left(-\frac{E_2}{R} + A_1 Y_2^3 X_d^3 + B_1 Y_2^2 X_d^2 + C_1 \right) \frac{dY_4}{dt} P_4 \right] \quad (\text{IV.16})$$

where E_d and E_2 are the activation energies corresponding to the rate constants k_d and K_2 , and R is the gas constant.

The following numerical values were used for E_d and E_2 (Balke, 1972):

$$E_d = 32387. \text{ cal. mole}^{-1}; E_2 = 5882. \text{ cal. mole}^{-1}$$

The choice of the length of the time subinterval $[t_{k-1}, t_k]$ is important. Figures IV.2 and IV.3 show the effect of the length of different subintervals on the optimal temperature profile. A longer time interval (25 min, 10 min) does not change the general shape of the optimal profile, but produces an obvious discontinuity in $T(t)$. Shorter time intervals (5s, 1 min, 2 min, 5 min) produce almost a continuous temperature profile, which clearly indicates that the calculated profile is independent of the length of the subinterval $[t_{k-1}, t_k]$. The smallest time interval entails the most accurate solution, and the most expensive run, speaking of computer money. It was found that convergence of the numerical solution was reasonably fast, accurate and inexpensive, when using a time subinterval of 1 min. Therefore, in all subsequent optimization runs with the DCM algorithm, a 1 min discretization interval was employed.

The initial guess of the temperature history $T^1(t)$ required to start the DCM algorithm was chosen to be an isothermal profile, for convenience reasons. A good initial guess is a matter of good knowledge of the physical behavior of the polymerization system. A

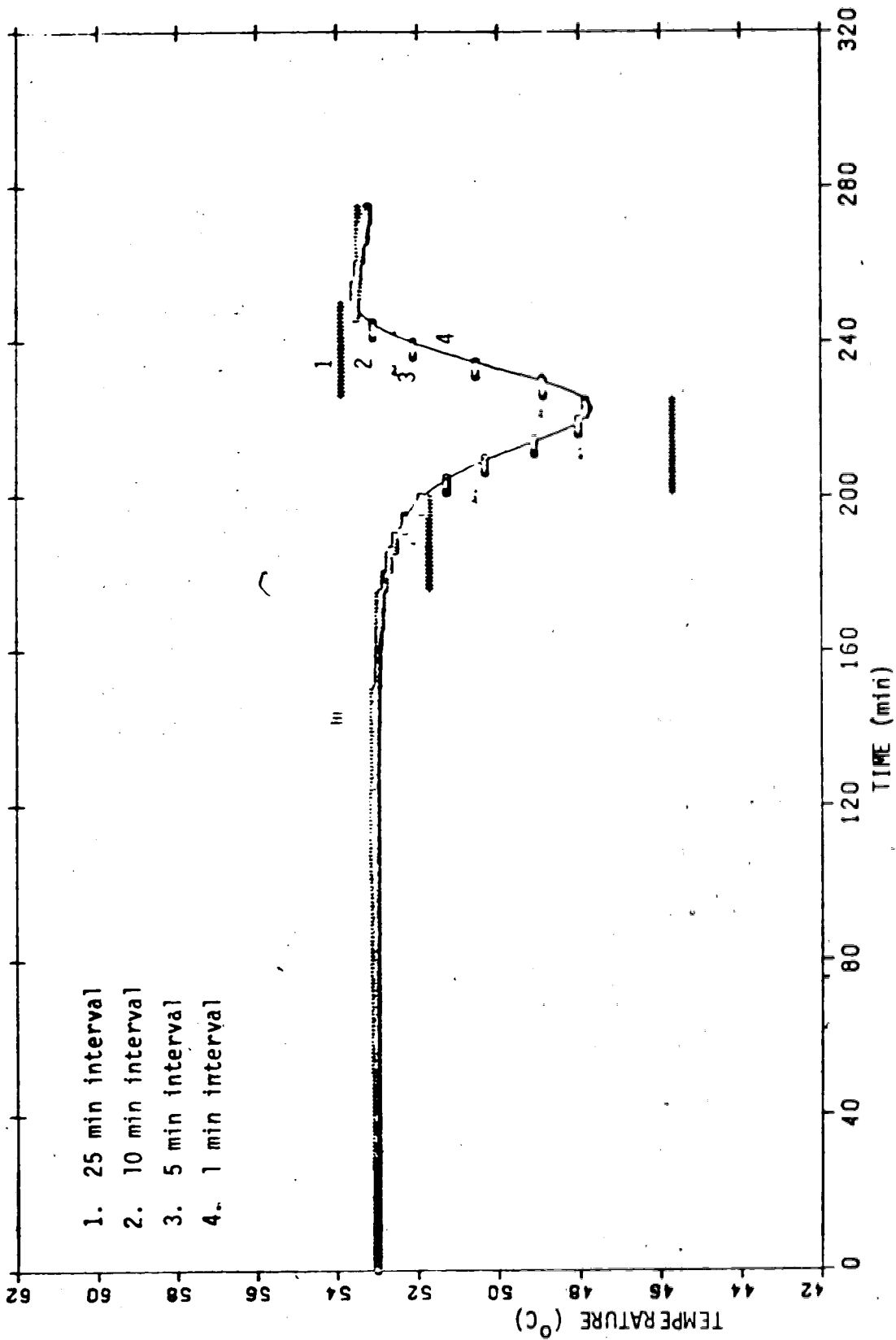


Figure IV.2: Effect of the Subinterval [t_{k-1}, t_k] Length on the Optimal Temperature Profile.
 ($I_0 = 0.01699 \text{ gmole.l}^{-1}$, $x_d = 0.9$, $\nu_{od} = 8.45 \times 10^{-4}$, $\mu_{2d} = 3.399 \times 10^5$)

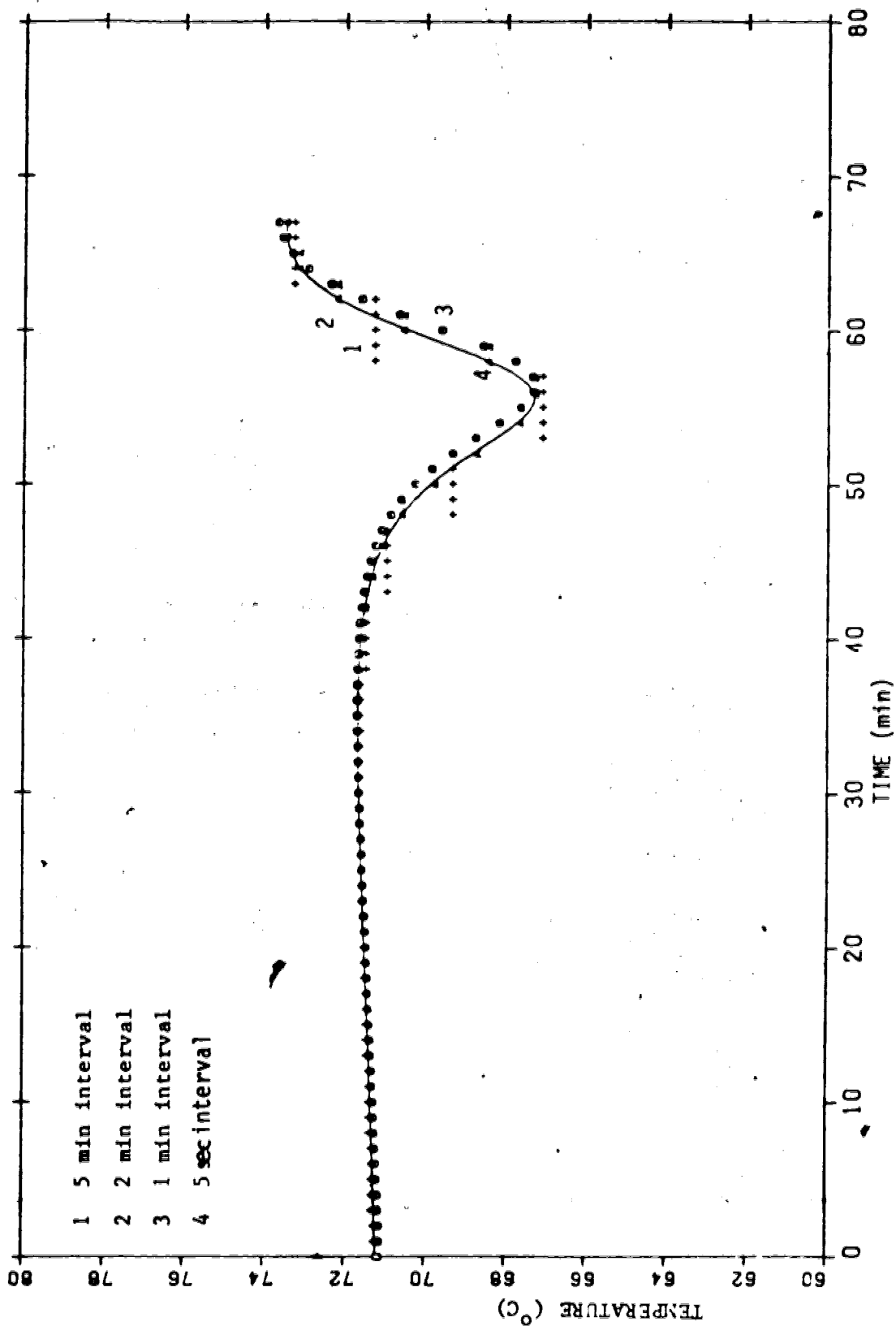


Figure IV.3: Effect of the Subinterval $[t_{k-1}, t_k]$ Length on the Optimal Temperature Profile.
 ($\lambda_0 = 0.01699 \text{ gmole.l}^{-1}$, $X_d = 2.88 \times 10^{-3}$, $\mu_{od} = 0.9$, $\mu_{2d} = 7.22 \times 10^4$).

perturbation of 3°C in the initially guessed isothermal profile could cause some serious convergence problems in the DCM algorithm.

The choice of the parameter α in equation (IV.12) is challenging, because a very large value of α produces an oscillatory or diverging numerical solution, while a very small value of α may increase considerably the number of iterations needed for convergence. The numerical value of α is directly related to the order of magnitude of $T^i(t_k)$ and $g^i(t_k)$ terms. T^i takes values in the range of 303°K to 373°K, and g^i varies from 10^{-6} to 10^{-9} . In this study, a value of $\alpha = 1 \times 10^{-5}$ has been proven to yield a satisfactory convergence rate. A value of α equal to $\alpha = 5 \times 10^{-5}$ leads to oscillations, while a value of $\alpha = 5 \times 10^{-4}$ increases the number of iterations needed for convergence from 18 to 41 iterations. The effect of different values of α on the optimal temperature profile is shown in Figure IV.4. It should be noted that a change in α changes only the number of iterations needed for convergence and not the optimal profile.

The reliability of the DCM algorithm and its convergence characteristics is again checked in Figure IV.5, where the effect of the number of iterations on the optimal temperature is investigated. In all cases, an isothermal temperature profile at 70°C is used as the initial guess. As the number of iterations increases, the profile gets steeper and finally converges to the optimal profile.

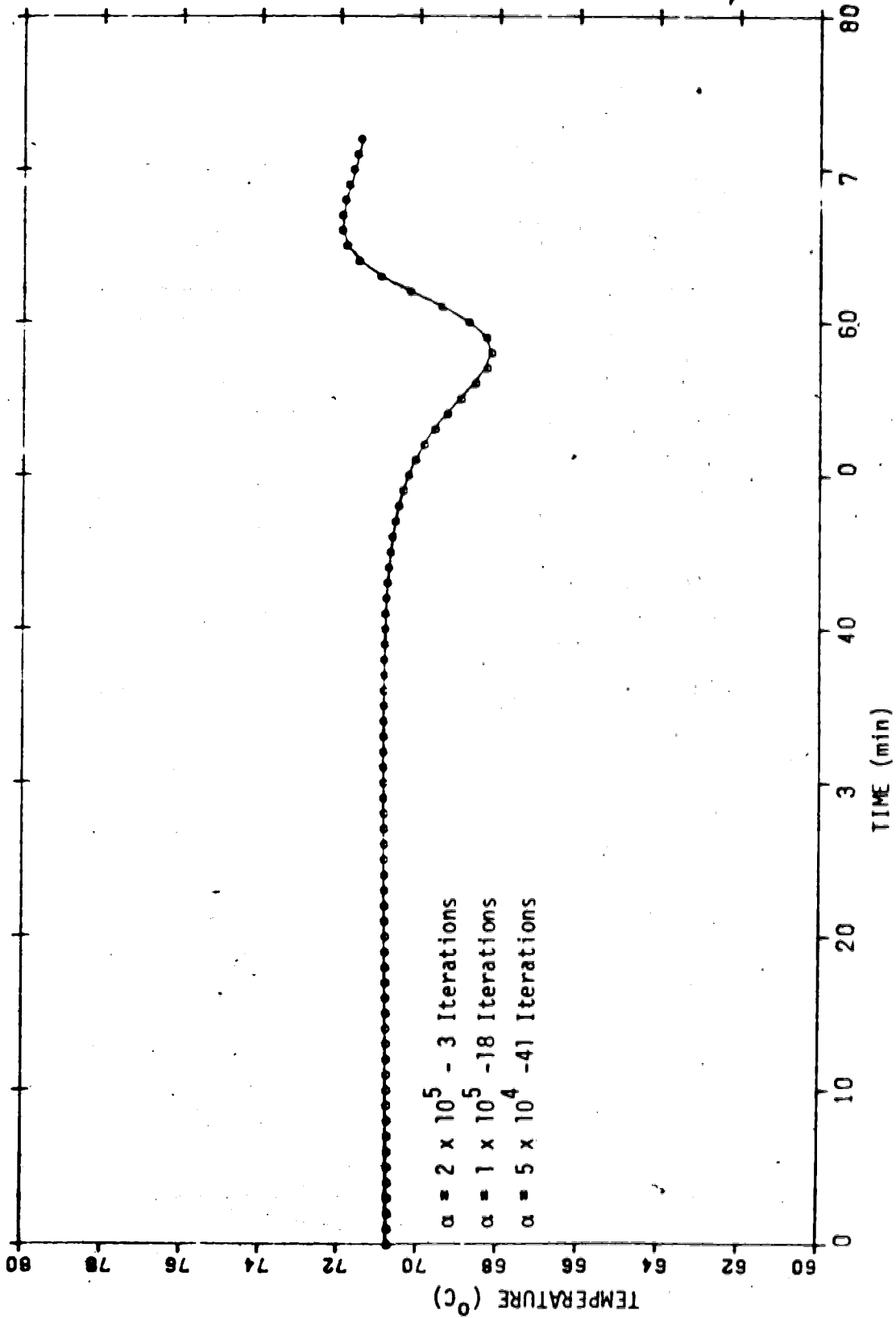


Figure IV.4: Effect of the Numerical Value of α on the Convergence of the DCM Algorithm
 ($I_0 = 0.01699 \text{ gmole.l}^{-1}$, $X_d = 0.9$, $\mu_{od} = 2.88 \times 10^{-3}$, $\mu_{2d} = 722 \times 10^4$)

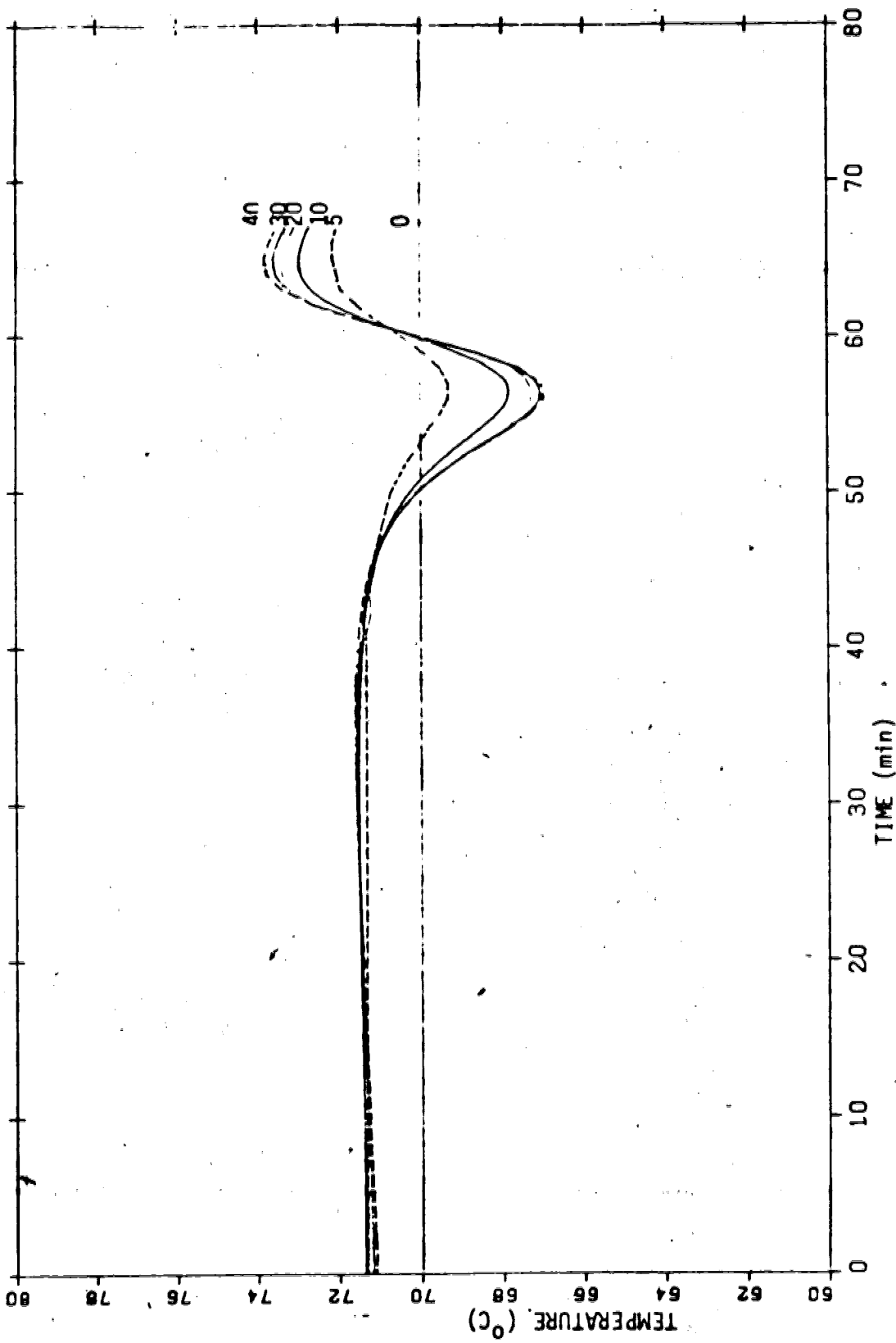


Figure IV.5: Effect of the Number of Iterations on the Optimal Temperature Profile.⁴
($\lambda_0 = 0.01699 \text{ gmole.l}^{-1}$, $X_d = 0.9$, $\mu_{od} = 2.88 \times 10^{-3}$, $\mu_{2d} = 7.22 \times 10^{-4}$).

IV.3 Shooting Method Algorithm

A slightly different formulation of the minimum time problem is used in this approach. The objective functional J' is defined as follows:

$$J' = \int_{t_0}^{t_f} w_t dt \quad (\text{IV.17})$$

Final conditions are imposed on $\underline{Y}(t_f)$, as each of the final state variables $Y_2(t_f)$, $Y_3(t_f)$, $Y_4(t_f)$ must be equal to one. In this case $G(\underline{Y}(t_f), t_f) = 0$. That means that the final condition (IV.5) for $\underline{P}(t_f)$ must change to the condition (IV.18):

$$\begin{aligned} P_1(t_f) &= 0, \\ P_2(t_f), P_3(t_f), P_4(t_f) &\text{ are free} \end{aligned} \quad (\text{IV.18})$$

The necessary condition on the Hamiltonian for optimality remains unchanged, that is:

$$\frac{\partial H}{\partial T} = 0. \quad (\text{IV.19})$$

If T is constrained, relationship (IV.19) breaks on the boundary and is replaced by the following relationship:

$$H(\underline{Y}^*, \underline{P}^*, T^*, t) \leq H(\underline{Y}^*, \underline{P}^*, T, t) \quad (\text{IV.20})$$

for all admissible temperatures T and all $t \in [t_0, t_f]$. As in the previous section of this chapter, we have to solve a two-point boundary value problem, which consists of eight differential equations (four state equations,

four costate equations) with four initial values ($\underline{Y}(0) = \underline{Y}_0$), and four final values ($P_1(t_f) = 0$; $Y_2(t_f) = Y_3(t_f) = Y_4(t_f) = 1$). The Hamiltonian must satisfy equation (IV.19) or equation (IV.20) along the optimal trajectory. A shooting method is used this time to solve the TPBV problem.

We shall now outline the steps involved in the shooting method algorithm.

Step 1: Guess an initial value $\underline{P}'(0)$ for the costate vector.

Step 2: Integrate forwards from t_0 to t_f together state and costate equations (IV.1) and (IV.4) with initial condition (IV.2) and the assumed initial value of $\underline{P}'(0)$. Simultaneously determine the temperature history by applying relations (IV.19) or (IV.20) along the state and costate trajectories.

Step 3: At final time (fixed in advance), compare $Y_2(t_f)$, $Y_3(t_f)$, $Y_4(t_f)$ and $P_1(t_f)$ with their respective desired values. If the stopping criterion described in equation (IV.14) is satisfied, then save the values of optimal control. If the stopping criterion is not satisfied, go to step 4.

Step 4: Compute new initial values for the costate variables, and return to step 2.

The SM algorithm is summarized in Figure IV.6. As in the previous algorithm, the final time is fixed. The minimum time is found by solving the TPBV problem for different

final times and selecting the smallest one for which convergence can be obtained.

Step 4 presents the greatest numerical difficulties because, during this step, four final values ($P_1(t_f)$, $Y_2(t_f)$, $Y_3(t_f)$, $Y_4(t_f)$) must be computed using the shooting method. In this step the roots of the vector function \underline{F} relatively to $\underline{P}(o)$ are determined. \underline{F} is defined in equation (IV.21).

$$\underline{F}(\underline{P}(o)) = \begin{bmatrix} F_1 \\ F_2 \\ F_3 \\ F_4 \end{bmatrix} = \begin{bmatrix} Y_2(t_f) - 1. \\ Y_3(t_f) - 1. \\ Y_4(t_f) - 1. \\ P_1(t_f) - 0. \end{bmatrix} \quad (\text{IV.21})$$

A Newton-Raphson method has been used to compute the new initial values of the costate vector.

$$\underline{P}(o)_{\text{new}} = \underline{P}(o)_{\text{old}} - \rho \underline{D}^{-1} \underline{F} \quad (\text{IV.22})$$

where ρ is a relaxation factor ($0 < \rho < 1$), and \underline{D} is the (4x4) Jacobian matrix of \underline{F} relative to $\underline{P}(o)$. The coefficients of \underline{D} are defined as:

$$D_{ij} = \frac{\partial F_i}{\partial P_j(o)} \quad \begin{array}{l} i=1,2,3,4 \\ j=1,2,3,4 \end{array} \quad (\text{IV.23})$$

\underline{F} is not an explicit function of $\underline{P}(o)$, therefore the Jacobian \underline{D} must be computed by a finite difference method. This involves four additional integrations of the state and costate equations and is carried out as follows:

(i) Perturb consecutively each component of the costate vector $\underline{P}(o)$, one at the time, while keeping constant the numerical values of the other components. Obtain four additional initial costate vectors $\underline{P}^2(o)$, $\underline{P}^3(o)$, $\underline{P}^4(o)$, $\underline{P}^5(o)$.

$$\underline{P}^i(o) = \underline{P}'(o) + \delta P_i(o) \cdot \underline{\epsilon}_i$$

$$\text{where } \underline{\epsilon}_i = (\delta_{i1}, \delta_{i2}, \delta_{i3}, \delta_{i4})^T, \quad i=1,2,3,4 \quad (\text{IV.24})$$

(ii) Integrate forwards the state and costate differential equations using initial condition (IV.2) for the state vector and the initial costate vector $\underline{P}^i(o)$ as calculated above. Optimize simultaneously the Hamiltonian along the state and costate trajectories. Four new function vectors \underline{F}^2 , \underline{F}^3 , \underline{F}^4 , \underline{F}^5 are thus obtained that correspond to the costate vectors $\underline{P}^2(o)$, $\underline{P}^3(o)$, $\underline{P}^4(o)$, $\underline{P}^5(o)$.

(iii) Calculate the partial derivatives in the Jacobian matrix \underline{D} using a finite difference approximation.

$$D_{ij} = \frac{\partial F_i}{\partial P_j(o)} = \frac{F_i^{j+1} - F_i^j}{\delta P_j(o)} \quad \begin{matrix} i=1,2,3,4 \\ j=1,2,3,4 \end{matrix} \quad (\text{IV.25})$$

The perturbation δP_i was taken as 10% of the corresponding value of the initial costate variable $P_i(o)$ during the first ten or twenty iterations. As the solution approached the optimal trajectory, δP_i was reduced to 5% of the corresponding value of $P_i(o)$.

The inversion of the Jacobian obtained numerically was performed with a very accurate algorithm proposed by

Moyer (1978). To avoid singularity of the Jacobian, the state variables have to be dimensionless and varying from 0 to 1.

The relaxation factor ρ was taken as 0.1 during the first ten or twenty iterations, then it was changed to 0.01 as the solution approached the optimal trajectory.

The same stopping criterion as the one used in the DCM algorithm was employed to terminate the algorithm, that is:

$$|Y_i(t_f) - 1| \leq 5\% \quad i = 2, 3, 4 \quad (\text{IV.26})$$

In addition to the above condition, $P_1(t_f)$ should be zero according to equation (IV.18). Indeed, it was found that $P_1(t_f)$ was approaching zero as the solution came nearer to the optimal temperature profile. We choose to impose final conditions on $\underline{Y}(t_f)$ instead of minimizing the cost functional J of equation (IV.3) as we did with DCM algorithm, because it was found that it was easier to satisfy these final state conditions than to satisfy the varying final conditions on $\underline{P}(t_f)$ imposed in equation (IV.5).

The integration of the differential equations (IV.1) and (IV.4) was performed by a Runge-Kunta routine, with an adjustable integration step size. The initial step size was five seconds. The differential system did not show any stiffness, due mainly to the use of dimensionless variables.

The optimal temperature profile was continuously calculated by calling the minimization routine at each integration point. Upper and lower bounds were imposed on the polymerization temperature (313°K and 373°K). The

temperature was computed by minimizing the Hamiltonian H . A half interval method was used to solve equation (IV.19) together with the analytical expression (IV.16) for $(\partial H/\partial T)$. If no solution for equation (IV.19) could be found in the interval $[313, 373]$, the optimal temperature was calculated from equation (IV.20),

$$\begin{aligned} T^* &= 373^\circ\text{K} & \text{if } \frac{\partial H}{\partial T} < 0 \\ T^* &= 313^\circ\text{K} & \text{if } \frac{\partial H}{\partial T} > 0 \end{aligned} \quad (\text{IV.27})$$

It was verified that the Hamiltonian was an unimodal function in the interval $[313, 373]$, meaning that the calculated optimal temperature policy was unique in that temperature range.

Convergence of the SM algorithm is highly dependent on the initial guess of the costate vector $\underline{P}^1(0)$. Since the costate variables have no physical meaning, it is rather difficult to know even their order of magnitude. To obtain reasonable initial values of the costate vector, we used the following method:

- (i) Pertube $Y_2(t_f)$, $Y_3(t_f)$, $Y_4(t_f)$ around their desired values. Set $P_1(t_f)$ to zero.
- (ii) Compute $P_2(t_f)$, $P_3(t_f)$, $P_4(t_f)$ from equation (IV.5). Assume a reasonable value for $Y_1(t_f)$.
- (iii) Integrate backwards state and costate differential equations (IV.1) and (IV.4) from t_f to t_0 . Compute simultaneously the polymerization temperature by using equations (IV.19) and (IV.20).

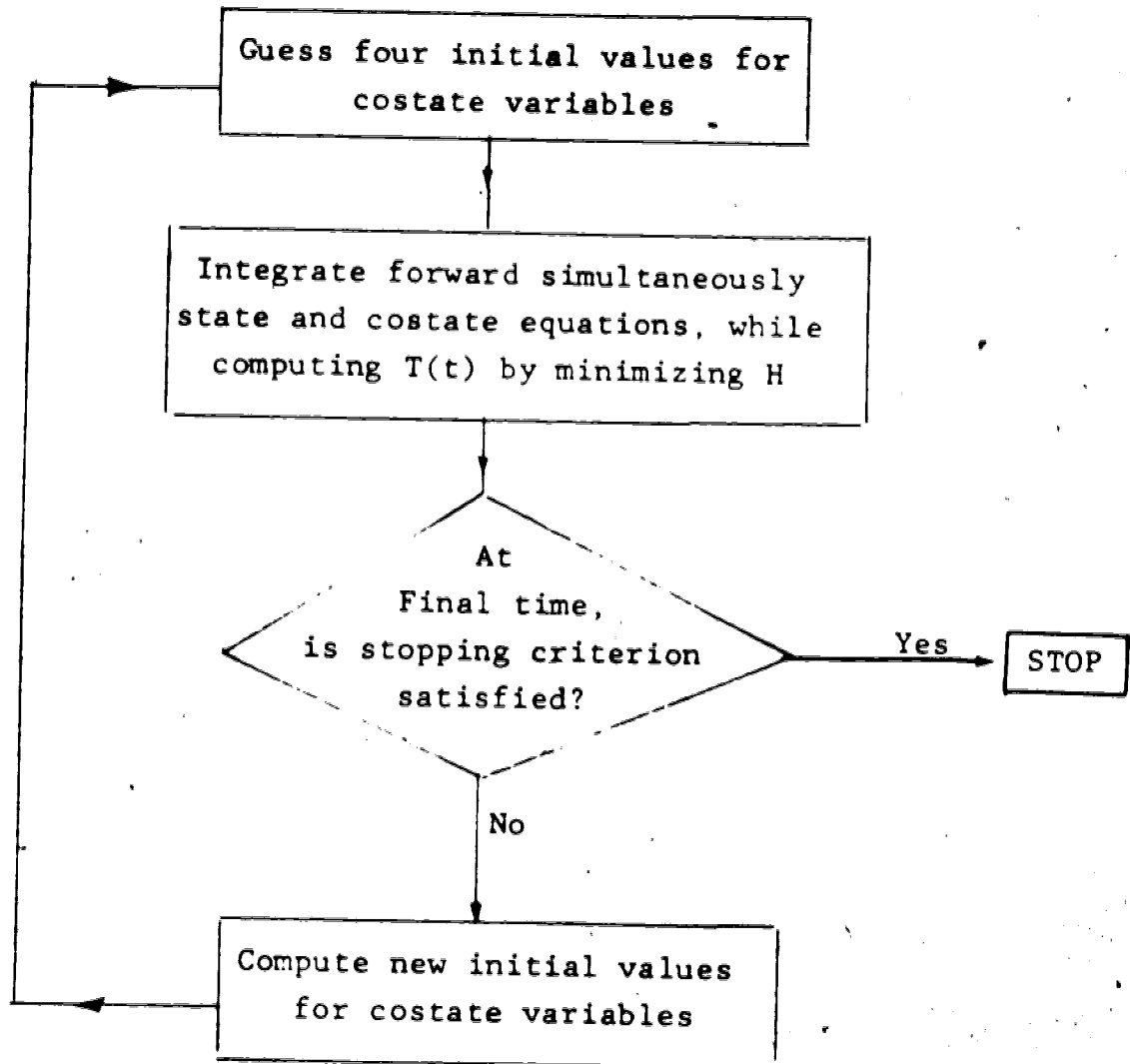


Figure IV.6: SM Algorithm

(iv) At $t_0 = 0$, check the initial conditions on \underline{Y} . If $Y_2(0)$ is zero, use the corresponding $\underline{P}(0)$ as the initial guess in Step 1 of the SM algorithm. If $Y_2(0)$ is not zero, restart from (i) with a different final time.

IV.4 Comparison of DCM and SM Algorithms

The two algorithms were tested by solving the same minimum time problem of obtaining a polymer with the desired MWD and final conversion as given in Table IV.1.

TABLE IV.1
Desired Properties

PD_d	X_d	μ_{0d}	μ_{2d}	M_n	M_w
2.5	0.9	8.45×10^{-4}	2.075×10^{-5}	990000	2480000

The results obtained by the two algorithms are presented in Table IV.2.

The difference between the final values obtained by the two algorithms can explain the small discrepancy between the two optimal temperature profiles plotted in Figure (IV.7). Furthermore, as it has been shown in Chapter II, the polymerization system is not very sensitive to temperature perturbations at the end of the polymerization. Thus the rise in temperature as computed by the SM algorithm does not result in a significant change of the MWD.

Let us now examine how both algorithms satisfy the necessary conditions for optimality. Both algorithms satisfy the differential equations (IV.1) and (IV.4) with

Table IV.2

Comparison of the Results of the two Algorithms

	DCM Algorithm	SM Algorithm
$Y_2(t_f) = X/X_d$	0.950	0.952
Conversion X	0.855	0.857
$Y_3(t_f) = \nu_0/\nu_{0d}$	0.998	0.996
0 th moment ν_0	8.43×10^{-4}	8.42×10^{-4}
$Y_4(t_f) = \nu_2/\nu_{2d}$	1.01	0.968
2 nd moment ν_2	2.09×10^5	2.01×10^5
Polydispersity	2.8	2.7
Minimum time	310min	300min

initial value (IV.2). In the DCM algorithm, $\underline{P}(t_f)$ is forced to satisfy the boundary condition (IV.5). The gradient of the Hamiltonian is continuously approaching to zero while the Hamiltonian remains constant along the state-costate trajectories, which is a strong indication that the computed temperature policy is close to the optimum temperature profile. In SM algorithm, $Y_2(t_f)$, $Y_3(t_f)$ and $Y_4(t_f)$ satisfy the conditions imposed on them within 5%. The gradient of the Hamiltonian is always zero, and the Hamiltonian is fairly constant, which indicates that the temperature policy computed

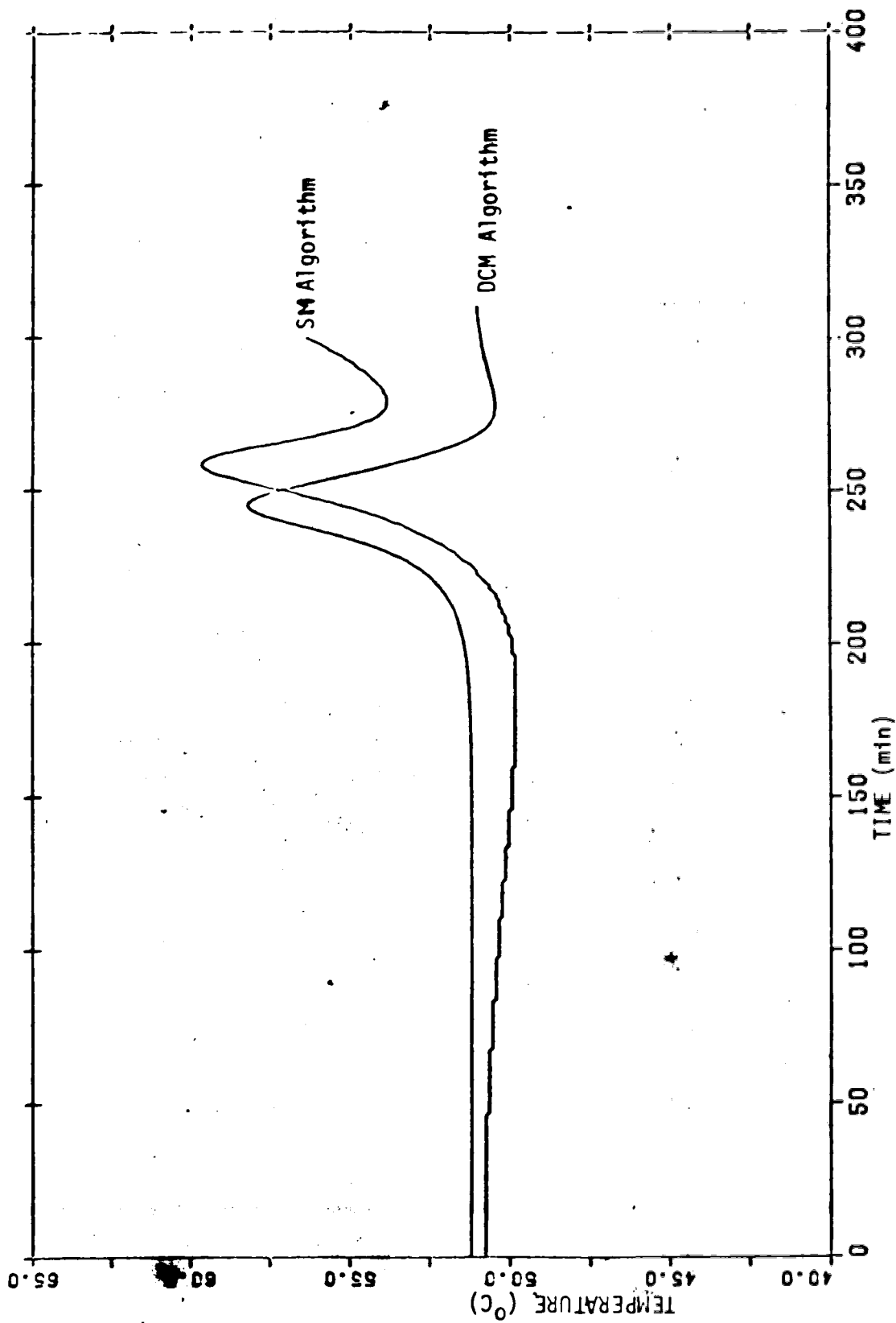


Figure IV.7: Comparison of DCM and SM Algorithms
 $(I_0 = 0.01699 \text{ gmole.l}^{-1}, X_d = 0.9, \mu_{od} = 8.45 \times 10^{-4},$
 $\mu_{2d} = 2.075 \times 10^5, PD_d = 2.5)$

by this algorithm is also very close to the optimal temperature policy.

For both algorithms, convergence is highly dependent on initial guesses. In the DCM algorithm, an initial temperature history has to be assumed over the polymerization interval $[t_0, t_f]$ before starting the algorithm. In the SM algorithm only the values of the costate vector $\underline{P}(0)$ must be known. However it was more difficult to guess the values for the four initial costate variables than to guess the whole temperature profile. This is due to the fact that temperature has a physical meaning and therefore good initial estimates can be easily found, especially if some knowledge about the behaviour of the system is available. Costate variables have no physical meaning, therefore it may be very difficult to find some reasonable values for $\underline{P}(0)$.

Twenty to forty iterations are usually needed to obtain convergence with both algorithms, depending on the accuracy of the initial guesses, and on the relaxation factors α and ρ . For the DCM algorithm, one iteration involves the integration of two systems of four differential equations. For the SM algorithm, one iteration involves the integration of five times eight differential equations, and the solution of the equation $(\partial H/\partial T) = 0$ at all integration points (usually 10,000 points). For comparison reasons, both algorithms were implemented on a very slow computer (HP 1000). Ten to twelve hours were needed to get convergence with the DCM algorithm, against three or four days for the SM algo-

rithm. The same test performed on the Amdahl 470/V computer at the University of Alberta gives a CPU time for the DCM algorithm of approximately one hundred seconds.

The fact that both algorithms predict the same optimal temperature profile using two different numerical methods, that the gradient of the Hamiltonian relative to the temperature is close to zero, and that the Hamiltonian is almost constant during the time of the reaction, strongly indicates that the solution obtained by these algorithms is close to the true optimal profile. However, it is difficult to show in a mathematically rigorous manner that the computed solution is the true optimal.

The DCM algorithm has two main advantages over the SM algorithm: (a) it has faster convergence rate, (b) it is more efficient. Therefore, for computational reasons, all optimal temperature profiles subsequently presented are computed by the discrete control method algorithm.

CHAPTER V

OPTIMAL TEMPERATURE POLICIES

V.1 Reduction of the Batch Polymerization Time.

The isothermal polymerization of MMA at 50°C requires a reaction time of 425 min to attain a conversion of 90%. The M_n and M_w of the polymer product at the end of the isothermal run are given in Table V.1.

Table V.1

Final MWD for the Isothermal Polymerization
of MMA at 50°C

X	M_n	M_w	PD	μ_0	μ_2
0.9	0.991×10^6	0.406×10^7	4.1	8.45×10^{-4}	3.399×10^5

Using the DCM algorithm to calculate the optimal temperature policy, we were able to obtain a polymer product with the specifications of Table V.1 only in 275 min. That is, we get a 23.5% decrease in the total polymerization time compared to the isothermal run at 50°C. The calculated optimal temperature profile is shown in Figure V.1.

The isothermal polymerization of MMA at 70°C requires a reaction time of 81 min to reach a conversion of 90%. The corresponding MWD obtained at the end of this run is presented in Table V.2.

Table V.2
Final MWD for the Isothermal Polymerization
of MMA at 70°C

X	M_n	M_w	PD	ν_0	ν_2
0.9	2.91×10^5	8.63×10^5	3.0	2.88×10^{-3}	7.22×10^4

Using the DCM algorithm to solve the minimum time problem, we obtain a polymer product with the specifications of Table V.2 in only 67 min. The batch time is therefore reduced by 19%. The optimal temperature profile is shown in Figure V.2.

Both optimal profiles (Figures V.1 and V.2) have the same shape. Up to about 70% conversion, the temperature remains almost constant, then it sharply decreases and finally, at about 90% conversion, the temperature increases to a final value slightly above the corresponding isothermal temperature. Under isothermal polymerization conditions, the rate of polymerization would sharply increase as a result of the gel effect (Chapter II). This in turn would cause a large increase in ν_2 due to the decrease of the termination rate constant. It should be noted that the gel effect is more important at low polymerization temperatures than at higher ones. Thus if we wish to increase the polydispersity (M_w/M_n) of the final product, a decrease in the temperature profile at the onset of the gel effect phenomenon would cause a dramatic increase in ν_2 and a subsequent increase in the

polydispersity of the product. On the other hand, if we wish to obtain a product of low polydispersity, the temperature profile should increase to suppress an increase in ν_2 due to the onset of the gel effect. In Figures IV.3 to IV.6, the monomer conversion and the rate of polymerization are plotted as a function of reaction time. It can be seen that in this case, the optimal temperature policy has a tendency to flatten the rate of polymerization profile.

V.2 Quality Improvement of the Polymer Product

The minimum time problem has been solved to produce polymers with different molecular weight distributions. The corresponding physical properties of a product obtained under these optimal temperature policies cannot be gotten by any isothermal run.

By fixing the number average molecular weight M_n to a value equal to that obtained at the end of the 50°C - isothermal run ($M_n = 991,000$), and by varying the weight average molecular weight M_w , different desired polydispersities have been obtained using the DCM algorithm. The desired MWDs and the corresponding computed optimal values are presented in Table V.3. Figure V.7 shows the computed optimal profiles for products with different polydispersities. The corresponding profiles for the rate of polymerization, M_n , M_w and polydispersity are displayed as a function of time in Figures V.8, V.9, V.10.

By fixing the weight average molecular weight M_w to a

Table V.3

Desired and Attained ~~MWD~~: Fixed M_n , Varying M_w

	Conversion X	Polydispersity PD	M_n	M_w	0th moment μ_0	2nd moment μ_2	Minimum Time
Desired	0.9	2.5	9.91×10^5	2.48×10^6	8.45×10^{-4}	2.08×10^5	
Attained	0.866	2.8	9.44×10^5	2.70×10^6	8.53×10^{-4}	2.18×10^5	310 min
Desired	0.9	3.0	9.91×10^5	2.97×10^6	8.45×10^{-4}	2.49×10^5	
Attained	0.855	3.4	9.43×10^5	3.18×10^6	8.43×10^{-4}	2.48×10^5	280 min
Desired	0.9	4.1	9.91×10^5	4.06×10^6	8.45×10^{-4}	3.40×10^5	
Attained	0.855	4.4	9.44×10^5	4.12×10^6	8.42×10^{-4}	3.28×10^5	275 min
Desired	0.9	5.0	9.91×10^5	4.95×10^6	8.45×10^{-4}	4.15×10^5	
Attained	0.855	5.4	9.41×10^5	5.15×10^6	8.44×10^{-4}	4.09×10^5	270 min
Desired	0.9	6.0	9.91×10^5	5.94×10^6	8.45×10^{-4}	4.97×10^5	
Attained	0.855	6.4	9.40×10^5	6.02×10^6	8.42×10^{-4}	4.97×10^5	275 min

Table V.4
Desired and Attained MWD - Varying M_n , Fixed M_w

	Conversion X	Polydispersity PD ζ	M_n	M_w	0 th moment μ_0	2 nd moment μ_2	Minimum Time
Desired	0.9	3.0	1.35×10^6	4.06×10^6	6.12×10^{-4}	3.40×10^5	
Attained	0.855	3.4	1.26×10^6	4.45×10^6	6.24×10^{-4}	3.54×10^5	400 min
Desired	0.9	4.1	9.91×10^5	4.06×10^6	8.45×10^{-4}	3.40×10^5	
Attained	0.855	4.4	9.44×10^5	4.12×10^6	8.42×10^{-4}	3.43×10^5	275 min
Desired	0.9	5.0	8.13×10^5	4.06×10^6	1.03×10^{-3}	3.28×10^5	
Attained	0.859	5.3	7.76×10^5	4.09×10^6	1.02×10^{-3}	3.15×10^5	225 min
Desired	0.9	6.0	6.75×10^5	4.06×10^6	1.24×10^{-3}	3.40×10^5	
Attained	0.871	6.1	6.56×10^5	4.02×10^6	1.23×10^{-3}	3.26×10^5	200 min

value equal to that obtained at the end of the 50°C - isothermal run ($M_w = 4.06 \times 10^6$) and by varying M_n , another set of optimal profiles has been obtained. The different desired MWDs and the corresponding computed optimal values are given in Table V.4. The corresponding optimal temperature profiles are presented in Figure V.11. The rate of polymerization, M_n , M_w and the polydispersity associated with these optimal profiles are shown in Figures V.12, V.13 and V.14.

When the minimum time problem is solved to obtain narrow molecular weight distributions (polydispersity $\approx 2.5, 3.0$) the optimal temperature profile shows a pike-shaped increase in temperature around 70 - 90% conversion. For the case of broader MWDs (PD $\approx 4.1, 5.0, 6.0$), the computed optimal temperature profiles show a pike-shaped decrease in temperature around the same conversion range. When a polymer product of high polydispersity (PD $\approx 5.0, 6.0$) is desired, the rate of polymerization shows strong variations and even a bimodal form. As shown in Figures V.10 and V.14, the polydispersity always goes through a maximum at around 60 - 80% conversion. This is due to the acceleration in the rate of change of ν_2 , due to the gel effect. After an 80% conversion, the polydispersity of the polymer drops dramatically as a result of the decrease in $(K_2 = k_p^2/k_t)$ which involves a limiting ν_2 and a limiting conversion.

By comparing the two sets of optimal profiles shown in Figures V.7 and V.11, it can be seen that shorter minimum batch times are obtained in the second set (where M_n is fixed

and M_w is varying). From Tables V.3 and V.4, it can be seen that in fact the shortest minimum time is always obtained for the smallest desired M_w .

From the above results, it is expected that any sensible molecular weight distribution can be obtained by computing the optimal temperature policy using the discrete control algorithm.

As shown in Chapter II, the system responses are sensitive to variations in kinetic parameters. Therefore it may be anticipated that perturbations in the kinetic parameters will result in some changes in the minimum batch time and in the optimal temperature profile. To find out if any perturbation in the kinetic parameters affects the shape of the calculated optimal temperature profile, the minimum time problem was solved several times, each time perturbing one kinetic parameter from its nominal value. Results of this analysis are summarized in Table V.5 and in Figure V.15.

Table V.5
Effect of Parameter Perturbations on the Minimum
Time Problem

Parameter	I_0	k_d	K_{20}	A_1	A_2	B_1	B_2	C_1	C_2
Perturbation	+1%	+1%	+1%	+0.1%	+0.1%	+0.1%	-0.1%	-0.1%	-1%
Computed Minimum Time	67mn	67mn	67mn	65mn	65mn	65mn	69mn	67mn	67mn

The kinetic parameters A_1 , A_2 , B_1 , B_2 have a significant effect on the optimal temperature policy and on the computed minimum time. This is understandable since the conversion and the second moment are exponentially dependent on A_1 , A_2 , B_1 , B_2 parameters. Again, it can be seen that much care is recommended when estimating these parameters.

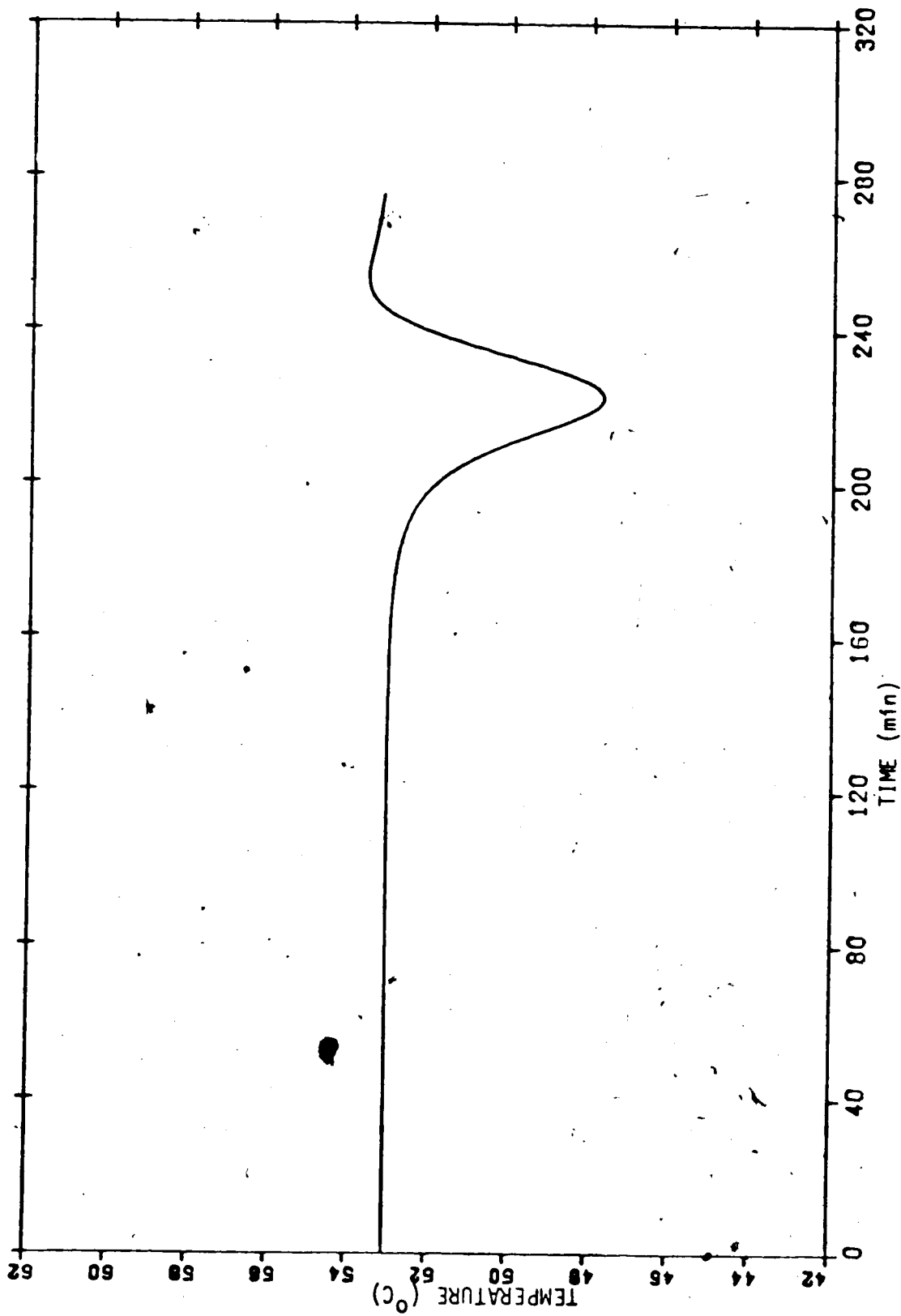


Figure V.1: Optimal Temperature Profile - ($I_0 = 0.01699 \text{ gmole } \ell^{-1}$,
 $X_d = 0.9$; $\nu_{od} = 8.45 \times 10^{-4} \text{ moles, } \ell^{-1}$; $\nu_{2d} = 3.399 \times 10^5 \text{ mole} \cdot \ell^{-1}$, $PD_d = 4.1$)

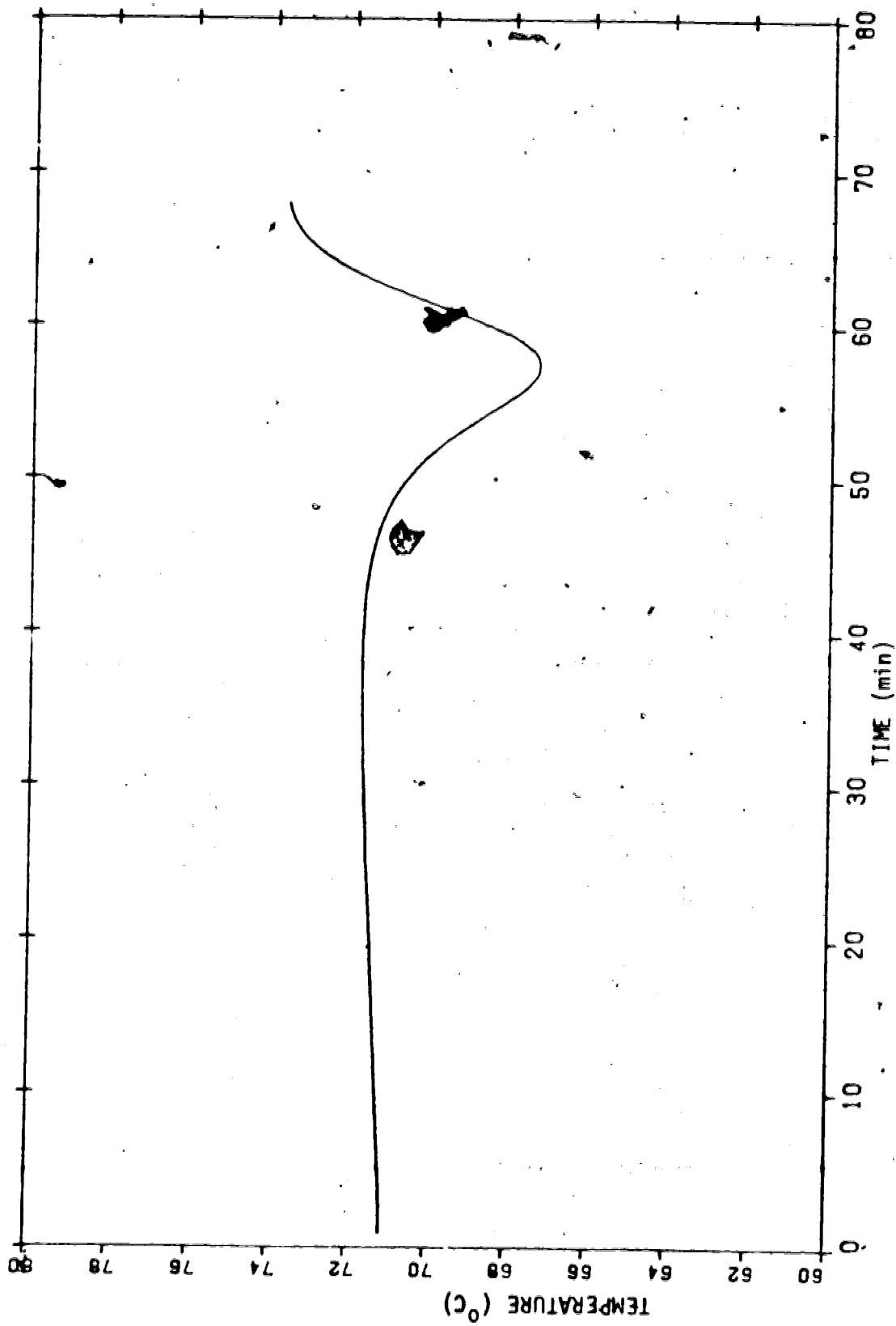


Figure V.2: Optimal Temperature Profile ($\lambda_0 = 0.01699 \text{ mole.l}^{-1}$;
 $X_d = 0.9$; $\mu_{cd} = 2.88 \times 10^{-3} \text{ mole.l}^{-1}$; $\mu_{2d} = 7.22 \times 10^4 \text{ mole.l}^{-1}$, $PD_d = 3.0$).

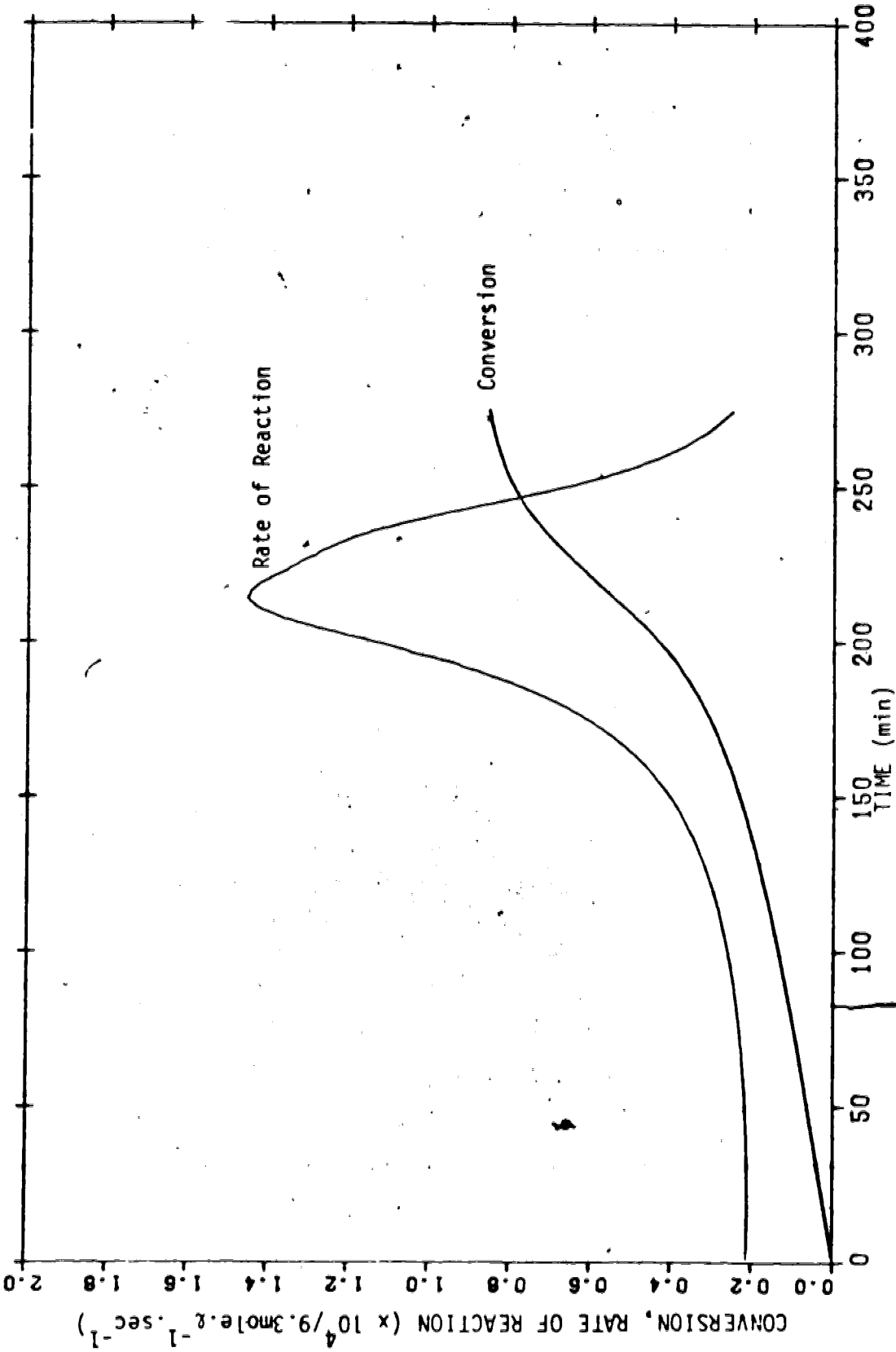


Figure V.3: Conversion and Rate of Polymerization, for the Optimal Pup ($I_0 = 0.01699 \text{ mole} \cdot \text{L}^{-1}$;
 $X_d = 0.9$; $\nu_{od} = 8.45 \times 10^{-4} \text{ mole} \cdot \text{L}^{-1}$; $\nu_{2d} = 3.399 \times 10^{-4} \text{ mole} \cdot \text{L}^{-1}$)

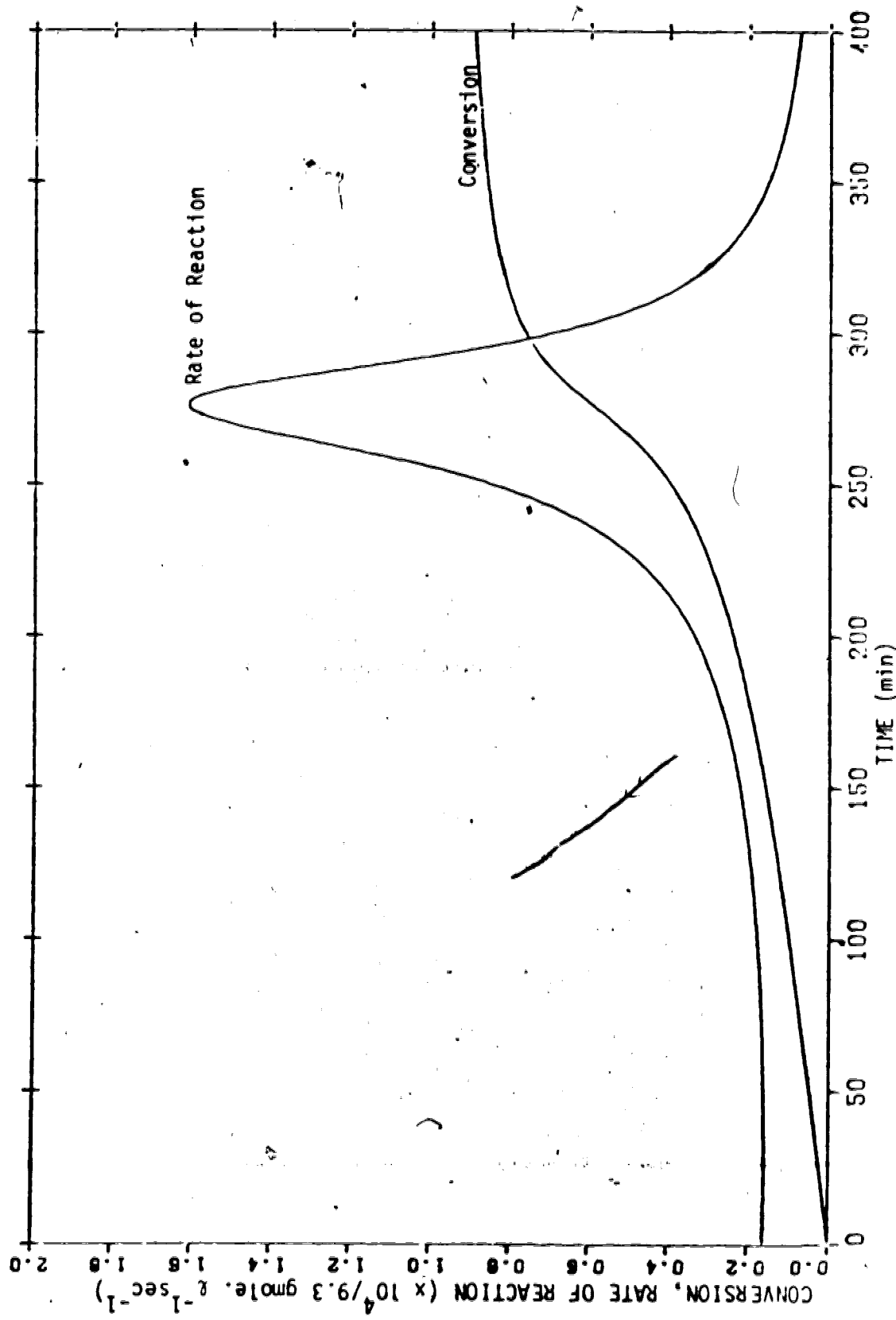


Figure 7.4: Conversion and Rate of Polymerization for Isothermal Run at 50°C
 (I₀ = 0.01699 gmole.l⁻¹).

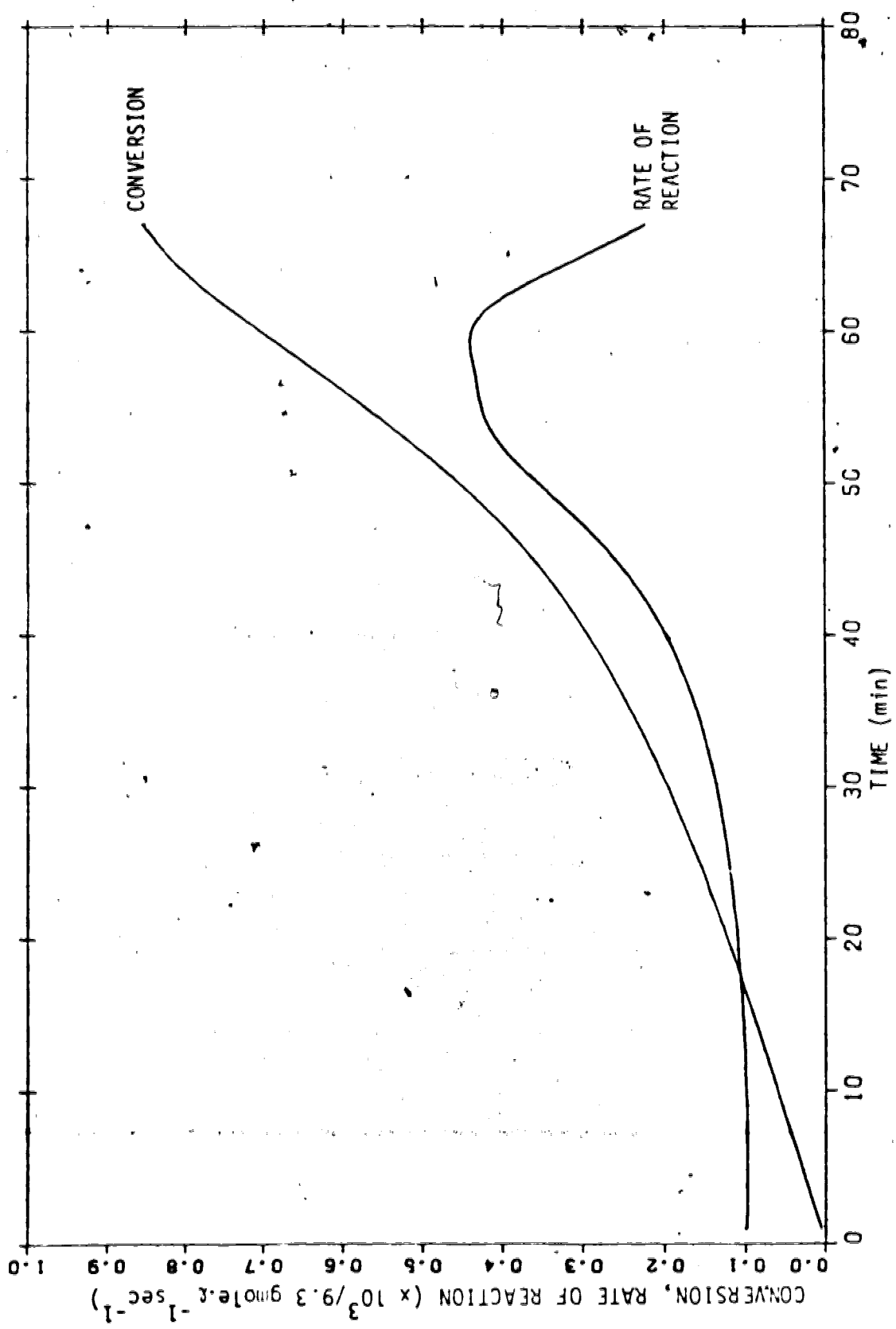


Figure V.5: Conversion and Rate of Polymerization for the Optimal Run.
 ($I_0 = 0.01699 \text{ gmole l}^{-1}$; $X_d = 0.9$; $\nu_{1d} = -2.88 \times 10^{-3}$; $\nu_{2d} = 7.22 \times 10^{-4}$)

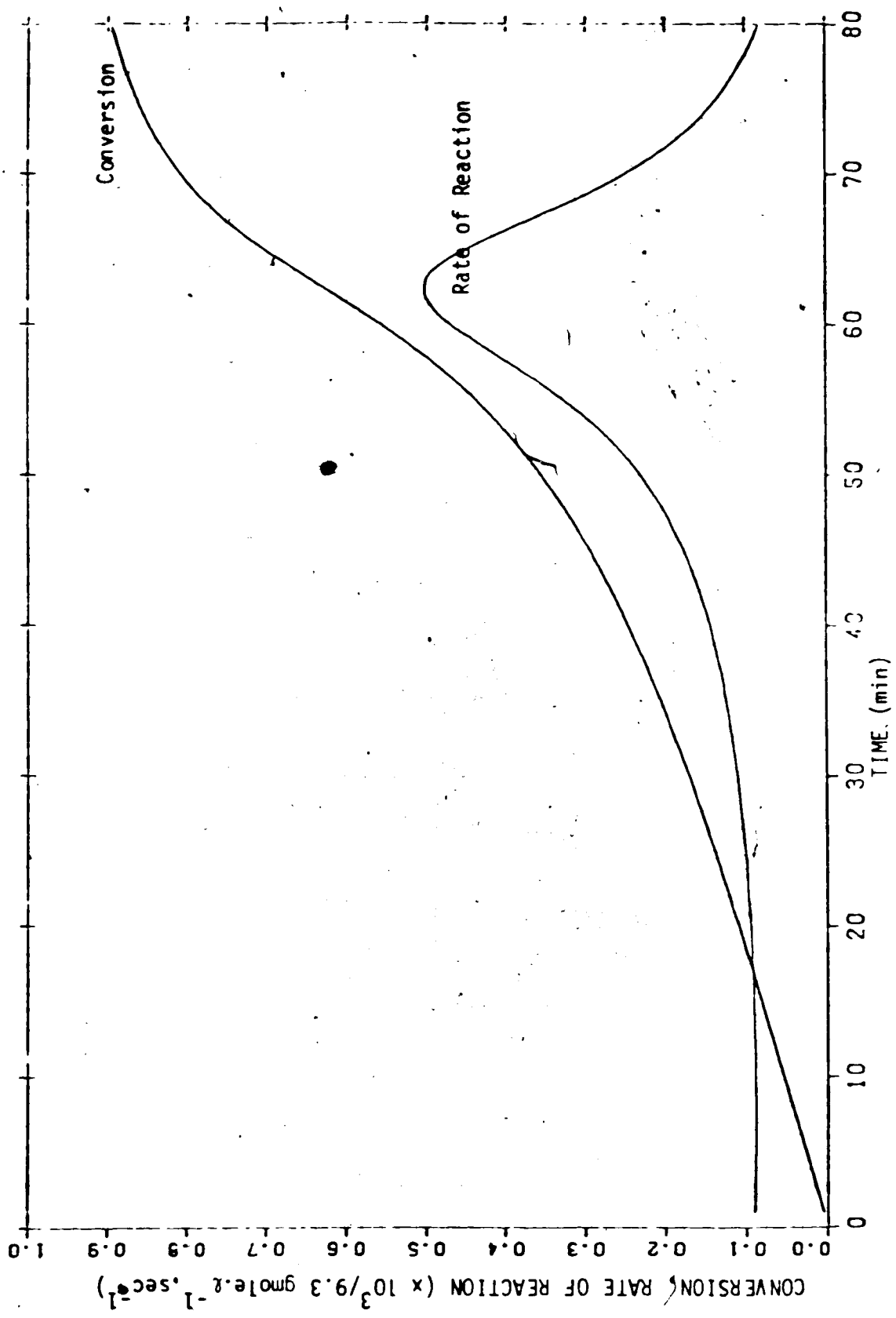


Figure V.6. Conversion and Rate of Polymerization for Tetrafunctional Run at 70°C (I₀ = 0.01699 gmole. l⁻¹).

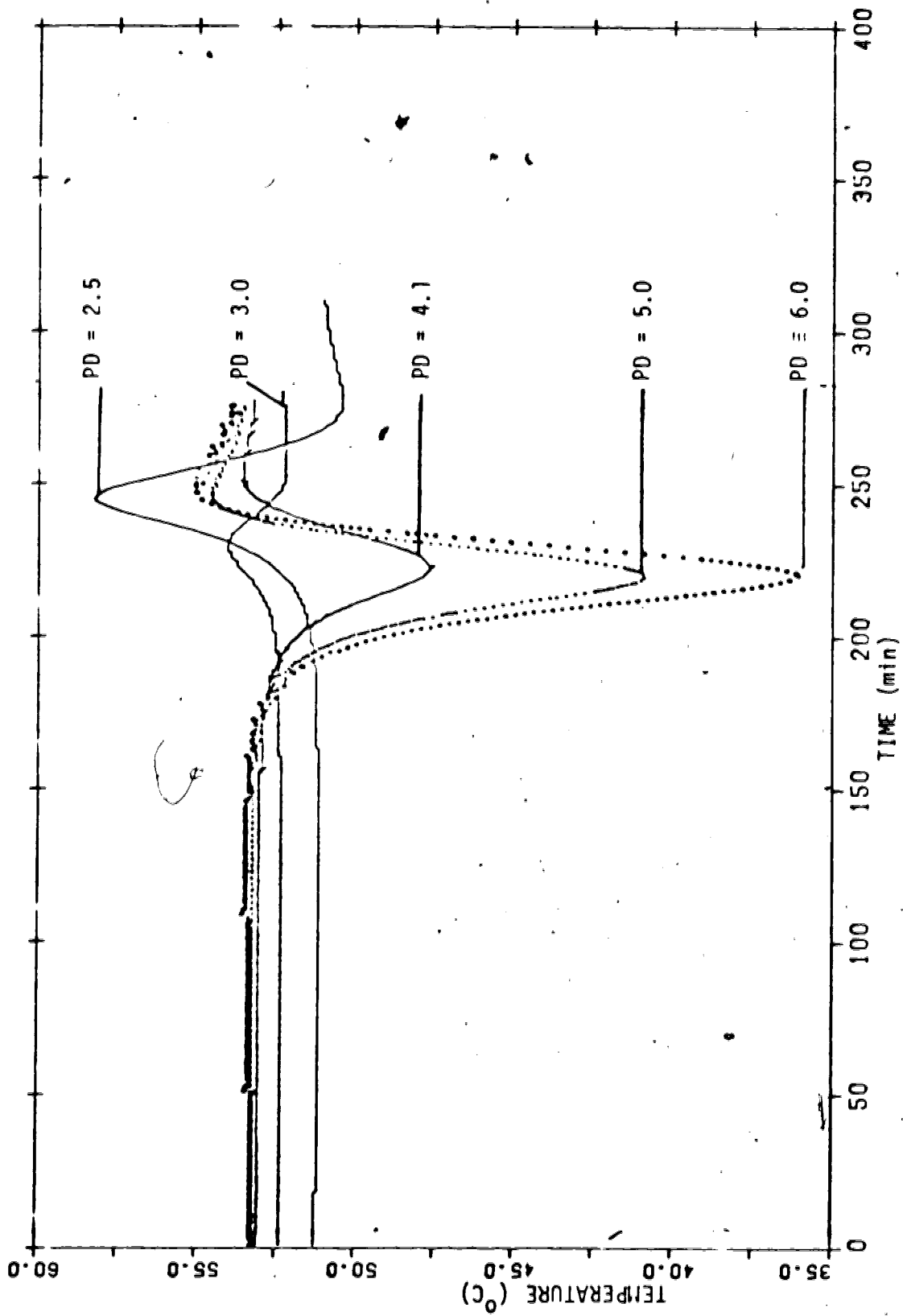


Figure V.7: Optimal Temperature Profiles. (Desired MWD's are given in Table V.3; $I_0 = 0.01699 \text{ gmole.l}^{-1}$).

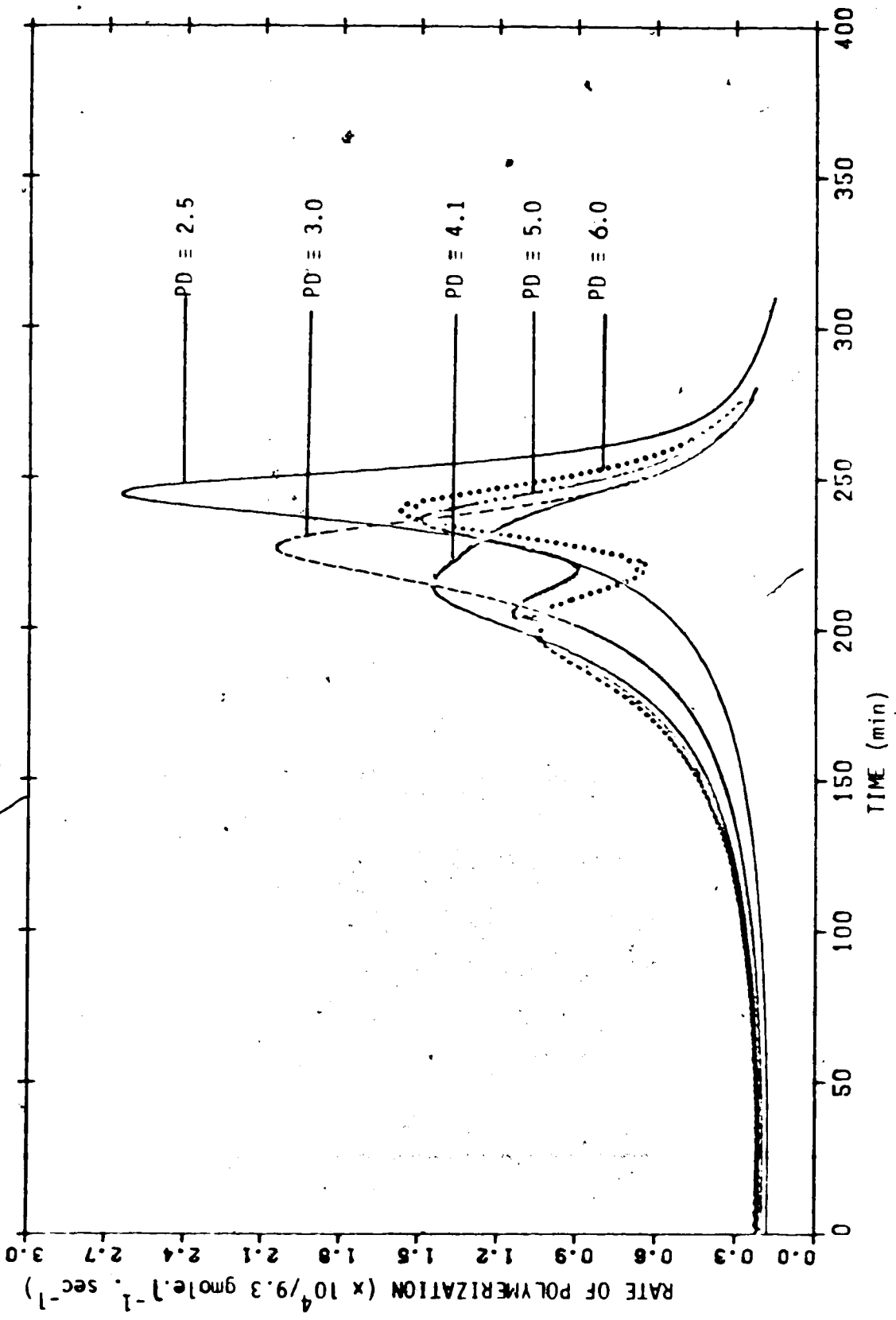


Figure V.8: Rates of Polymerization for the Optimal Runs. (Desired MWD's are given in Table V.3; $I_0 = 0.01699 \text{ mole.l}^{-1}$)

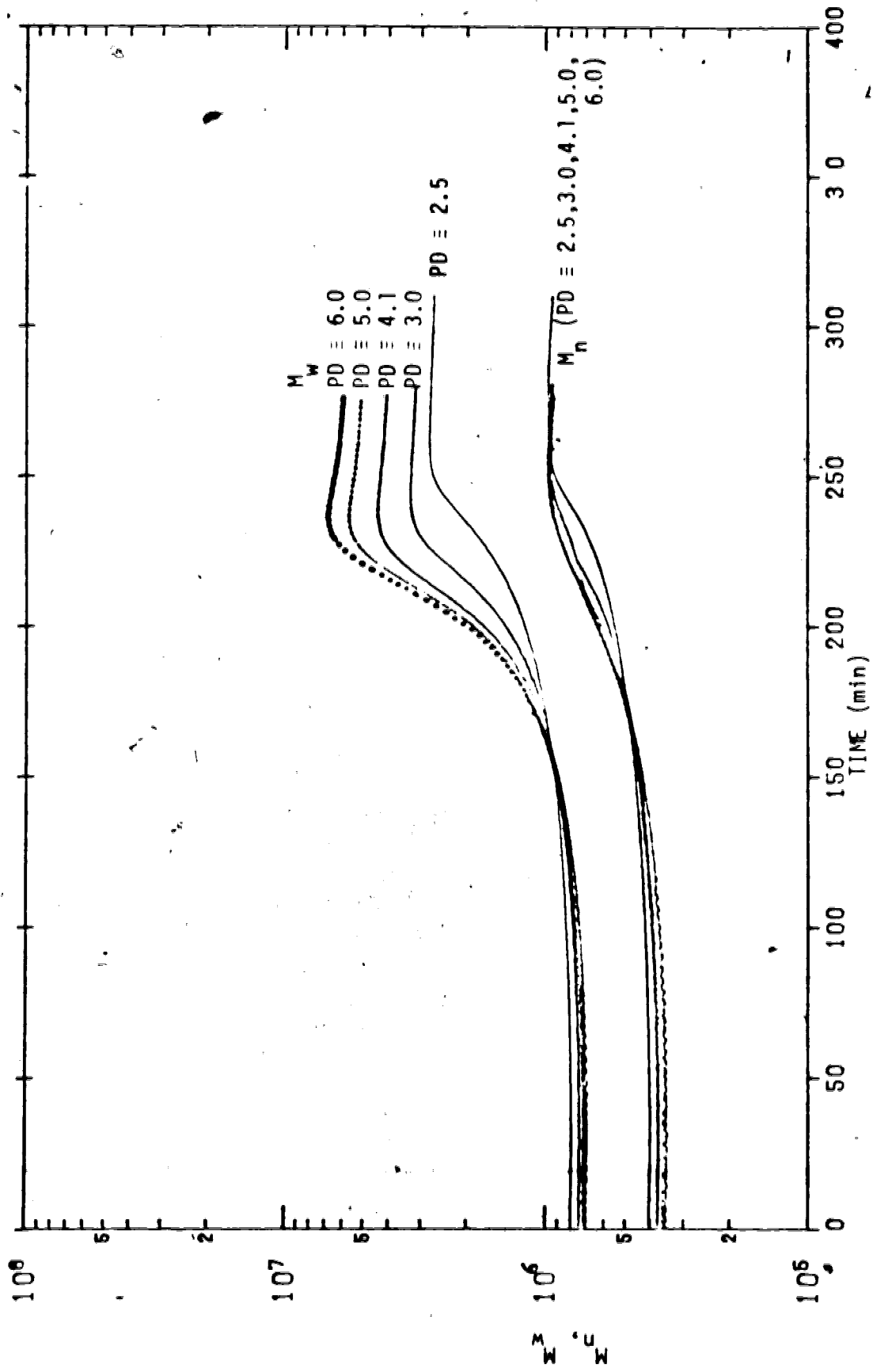


Figure V.9: Number and Weight Average Molecular Weights for Optimal Runs. $\tau_0 = 0.01599$ gmole. l^{-1} (Desired PD's are given in Table V.3)

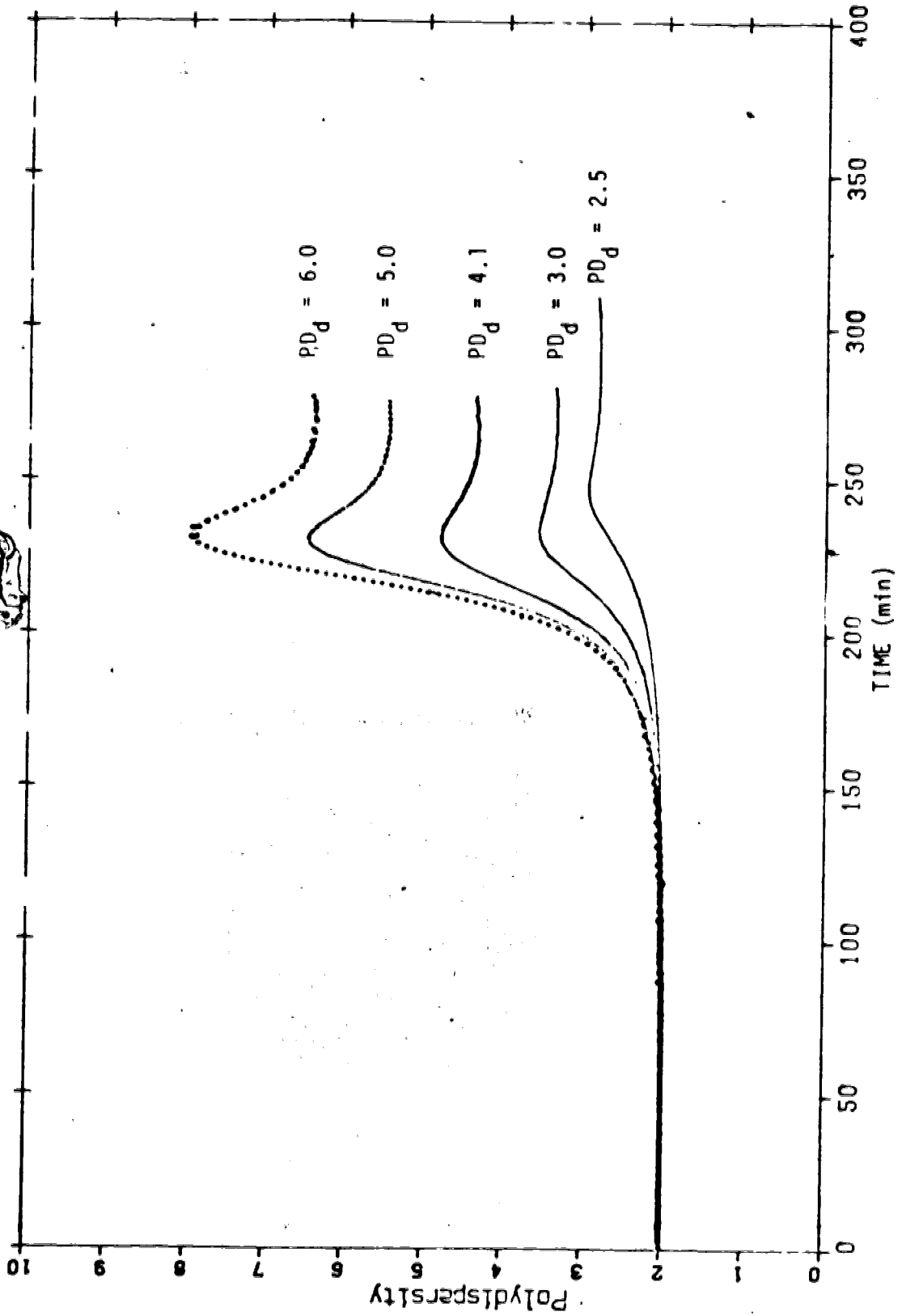


Figure V.10: Polydispersities for Optimal Runs. (Desired M_w/D 's are given in Table V.3; $I_0 = 0.01699 \text{ gmole.l}^{-1}$).

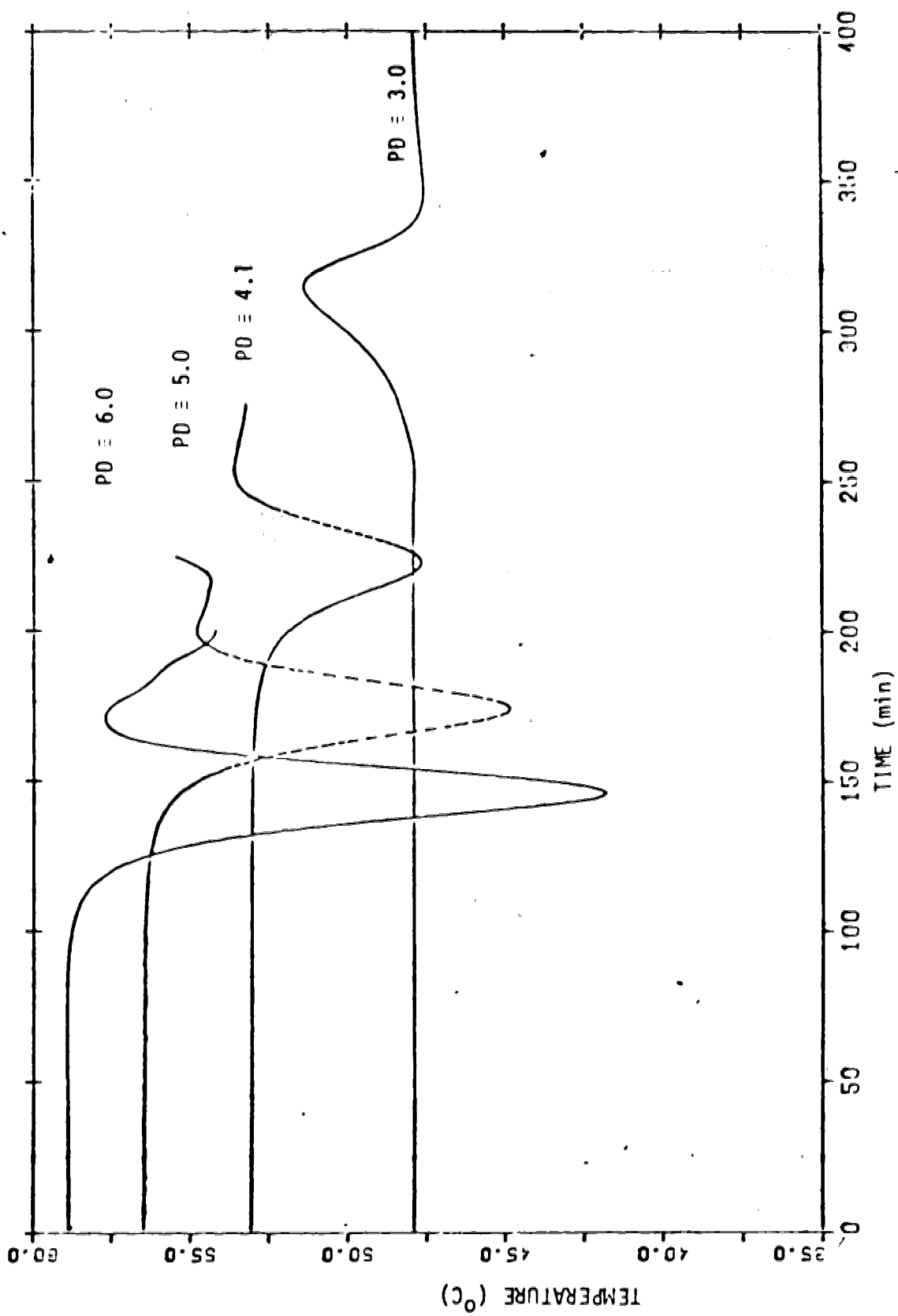


Figure V.11: Optimal Temperature Profiles (The desired MID's are given in Table V.4; $I_0 = 0.01699 \text{ gmole. l}^{-1}$)

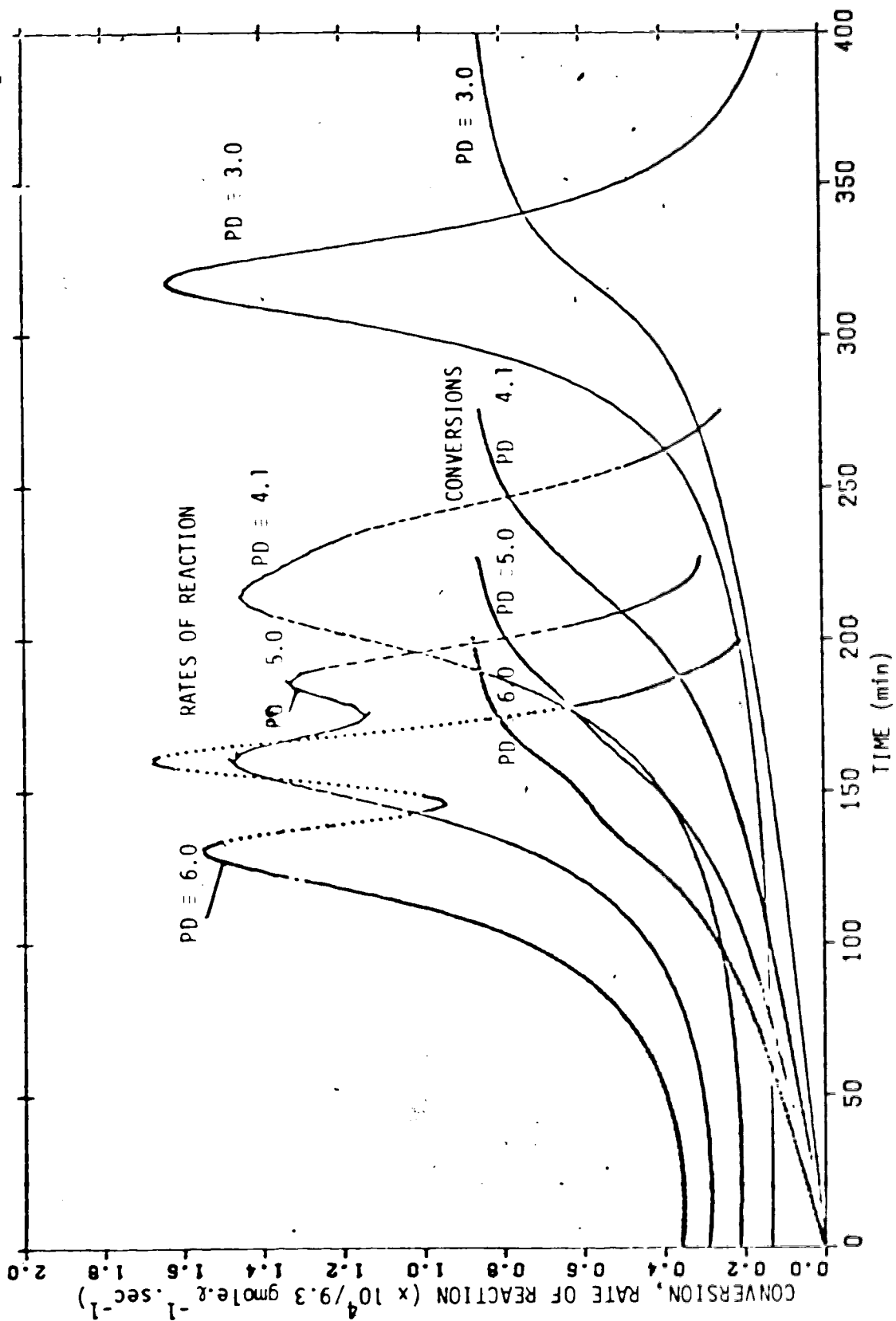


Figure V.12: Conversion and Rate of Polymerization for Optimal Runs. (The desired MWD's are given in Table V.4; $I_0 = 0.01699 \text{ gmole.l}^{-1}$)

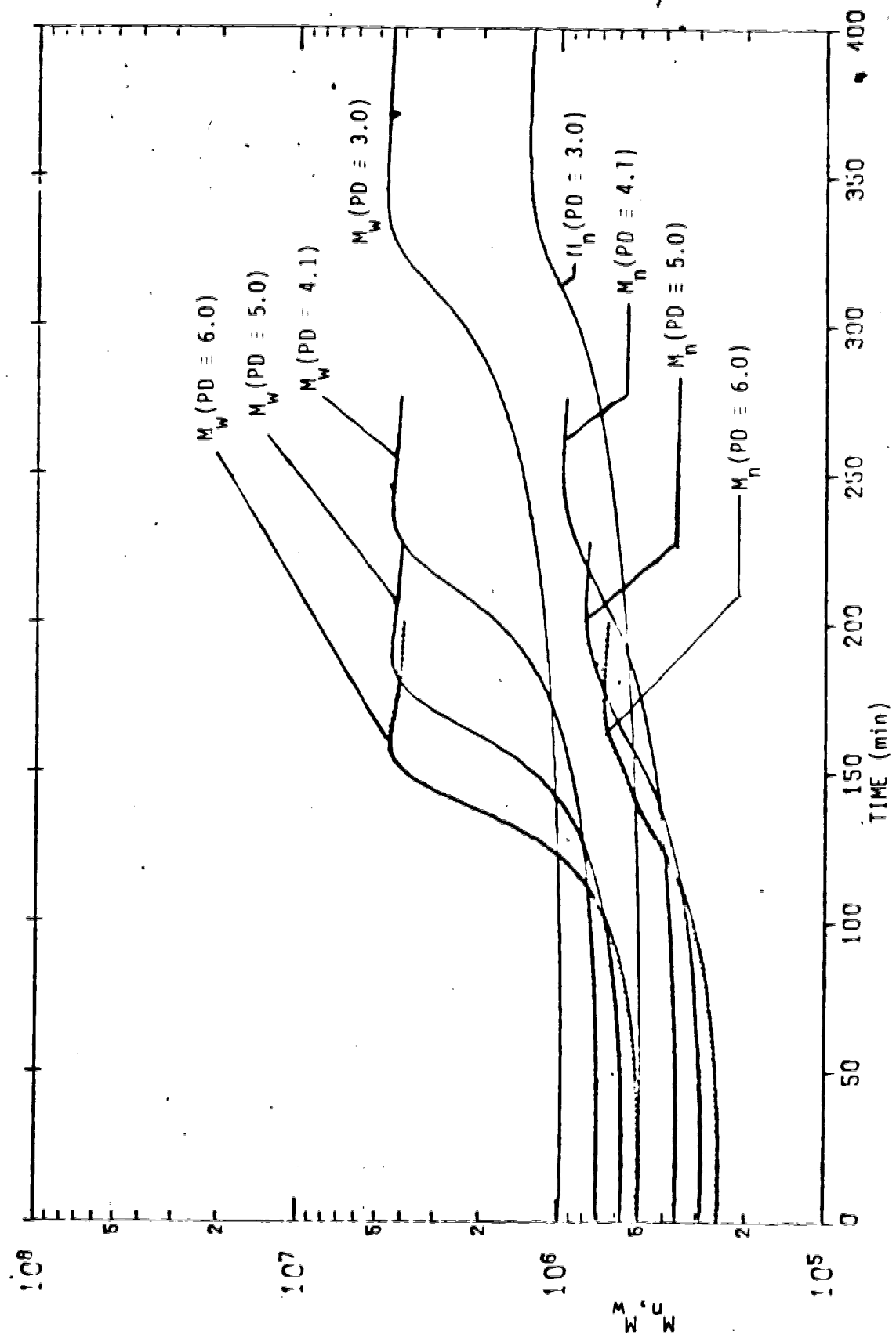


Figure V.13: Number and Weight Average Molecular Weights for the Optimal Runs (The desired MWD 's are given in Table V.13 as 0.01699 $gmole.l^{-1}$).

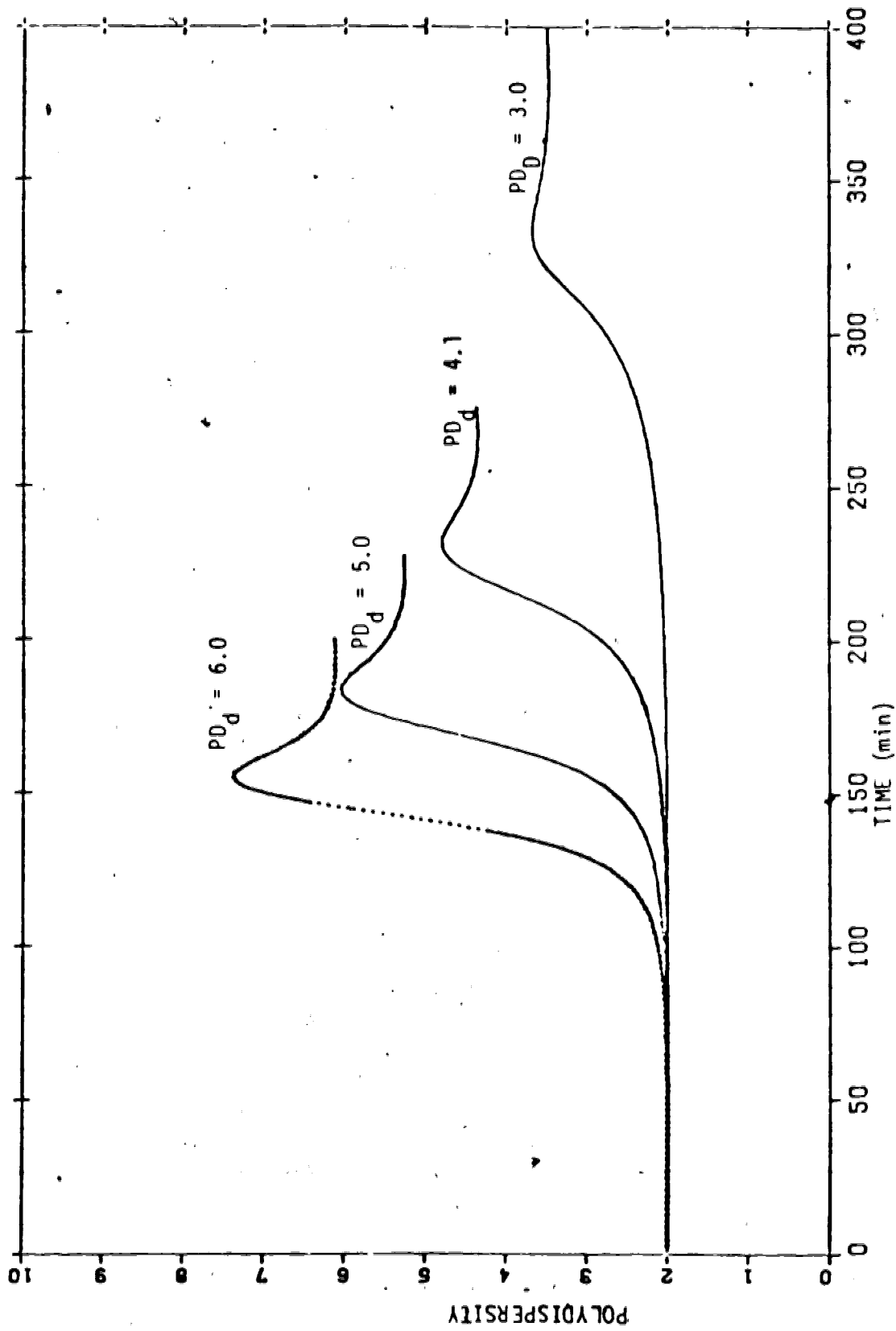


Figure V.14: Polydispersities for Optimal Runs. (The desired MMD's are given in Table V.4; $I_0 = 0.01699 \text{ mole.l}^{-1}$)

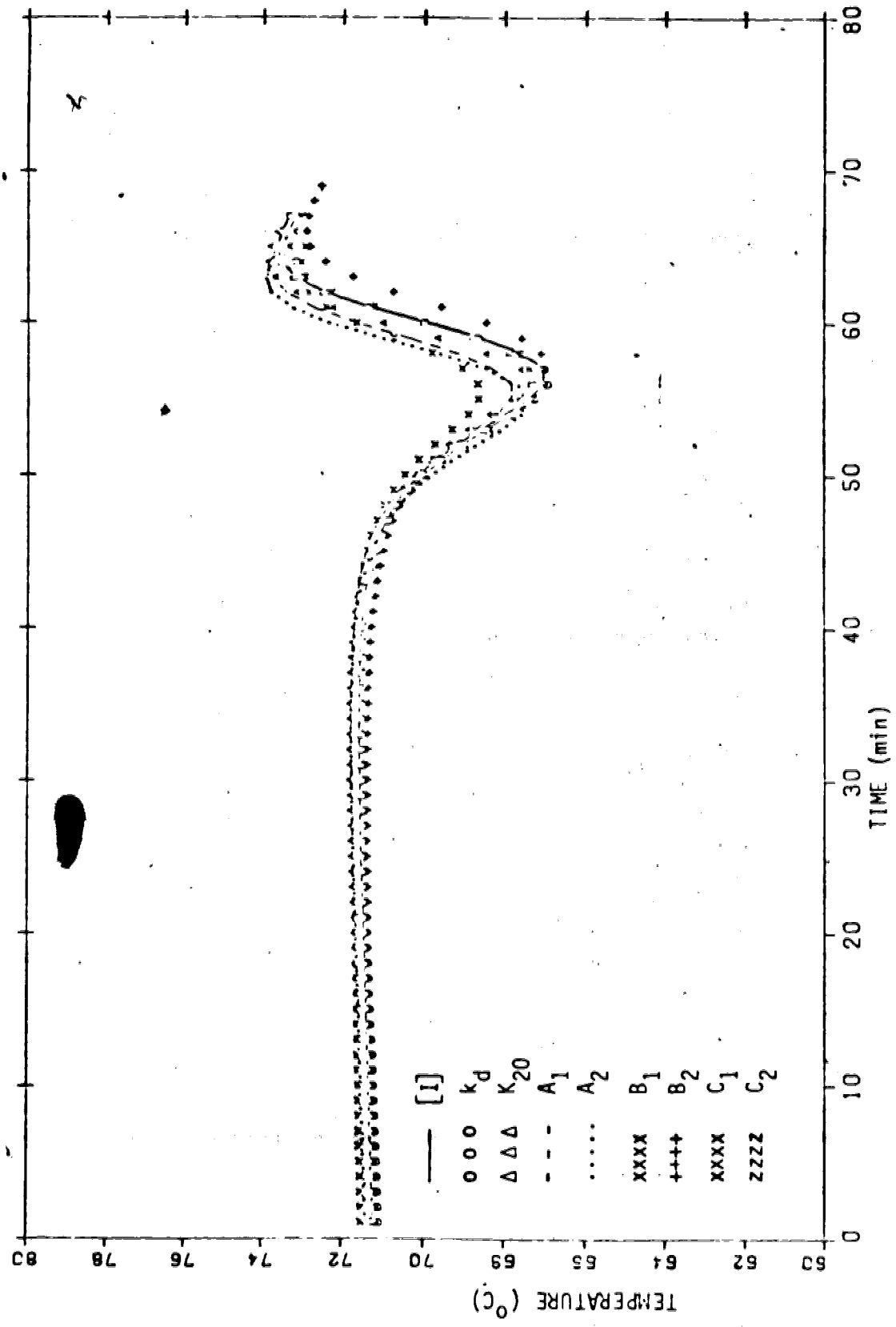


Figure V.15: The Effect of Perturbations in the Kinetic Parameters on the Optimal Temperature Profile. ($I_0 = 0.01699$ mole. l^{-1} ; $X_d = 0.9$; $\mu_{od} = 2.88 \times 10^{-3}$; $\mu_{2d} = 7.22 \times 10^{-4}$).

CHAPTER VI
OPTIMAL CATALYST FEED RATE POLICIES

Up to this point, the only control variable considered was the polymerization temperature. In this chapter, the minimum time problem is solved by optimizing both temperature and catalyst feed rate.

VI.1 Problem Formulation

Let F_c be the catalyst feed rate. The polymerization of MMA in a batch reactor is described by the set of differential equations III.11 derived in Chapter III.

$$\frac{dY}{dt} = \underline{f}(Y, F_c, T, t) \quad (\text{VI.1})$$

The Hamiltonian of the system can be expressed as follows (eq. III.16)

$$H = \left(-k_d Y_1 + \frac{F_c}{V[I_0]} \right) P_1 + \left(2 f k_d [I_0] Y_1 K_2 \frac{(1 - Y_2 X_d)}{X_d} \right) P_2 + \frac{2 f k_d [I_0] Y_1}{\nu_{od}} P_3 + \frac{2 K_2 M_o^2 (1 - Y_2 X_d)^2}{\nu_{2d}} P_4 \quad (\text{VI.2})$$

F_c appears linearly in the Hamiltonian, thus the necessary condition for optimality ($dH/dF_c = 0$) does not allow us to calculate the optimal policy for F_c . Therefore the Pontryagin Minimum Principle has to be applied to calculate the optimal feed rate F_c^* :

$$H(\underline{Y}^*, \underline{P}^*, T^*, F_c^*, t) \leq H(\underline{Y}^*, P^*, T^*, F_c, t) \quad (\text{VI.3})$$

for all admissible F_c and all $t \in [t_0, t_f]$.

Design reasons require that F_c be constrained between a lower and upper F_c value,

$$0 \leq F_c \leq F_c \text{ max} \quad (\text{VI.4})$$

Taking into account the constraints on F_c , equation VI.3 can provide the solution to the optimal catalyst feed rate policy. This policy will be of the on-off type given as:

$$\begin{aligned} \text{If } P_1 > 0 & \quad F_c = 0 \\ \text{If } P_1 < 0 & \quad F_c = F_c \text{ max} \end{aligned} \quad (\text{VI.5})$$

If $P_1 = 0$, F_c is undetermined and can take any value between 0 and $F_c \text{ max}$. Such an optimal policy is called bang-bang control. An attempt to solve the minimum time problem by applying this bang-bang policy to our numerical model did not produce any meaningful results due mainly to convergence reasons. This may be due to the fact that for a too small or too large $F_c \text{ max}$ value, a solution to the minimum time problem might not exist. In order to find the optimal policy, $[I_0]$ and $F_c \text{ max}$ should be optimized simultaneously with the computation of the optimal catalyst feed rate policy. An alternative is to consider $[I]$, the initiator

concentration, as the control variable, instead of F_c .

$[I]$ can be manipulated by controlling the catalyst or inhibitor addition rate into the reactor. Once the optimal profile for catalyst concentration is known, the catalyst and inhibitor feed rates can be calculated from the mass balances on catalyst and inhibitor species:

$$\frac{d[I]}{dt} = k_d[I] - k_N[I][N] + \frac{F_c}{V} \quad (\text{VI.6})$$

$$\frac{d[N]}{dt} = -k_N[I][N] + \frac{F_N}{V} \quad (\text{VI.7})$$

where $[N]$ is the inhibitor concentration in the reactor, F_N is the inhibitor feed rate, and k_N is the rate constant for consumption of initiator radicals by the inhibitor. It is assumed that there is no change in the volume of the reacting mixture due to catalyst and inhibitor addition.

The polymerization can be described by three state variables (dimensionless conversion, dimensionless zeroth moment, dimensionless second moment) and two control variables (polymerization temperature, initiator concentration).

$$\frac{d Y_1'}{dt} = \sqrt{2 f k_d K_2 [I]} \frac{1 - Y_1' X_d}{X_d}$$

$$\frac{d Y_2'}{dt} = \frac{2 f k_d [I]}{\nu_{od}} \quad (\text{VI.8})$$

$$\frac{d Y_3'}{dt} = \frac{2 K_2 [M_o]^2 (1 - Y_1' X_d)^2}{\nu_{2d}}$$

$$\underline{Y}'(o) = (0., 0., 0.)^T \quad (\text{VI.9})$$

$$\text{where } \underline{Y}' = \left(\frac{X}{\nu_d}, \frac{\nu_o}{\nu_{od}}, \frac{\nu_2}{\nu_{2d}} \right)^T \quad (\text{VI.10})$$

The objective function in terms of the Y' variables is rewritten as:

$$J' = w_t t_f + \sum_{i=1}^3 (Y_i'(t_f) - 1)^2 \quad (\text{VI.11})$$

The Hamiltonian H' for the above system can be expressed as:

$$H = \sqrt{2 f k_d K_2 [I]} \frac{(1 - Y_1' X_d)}{X_d} P_1' + \frac{2 f k_d [I]}{\nu_{od}} P_2' + \frac{2 K_2 M_o^2 (1 - Y_1' X_d)^2}{\nu_{2d}} P_3' \quad (\text{VI.12})$$

and the costate vector P' is governed by the following differential equation:

$$\frac{d P_1}{dt} = \left[+1 - \frac{1}{2}(3 A Y_1'^2 X_d^3 + 2 B Y_1' X_d^2) \frac{(1 - Y_1' X_d)}{X_d} \right] \sqrt{2 f k_d K_2 [I]'} P_1' + \left[4 X_d - 2(3 A Y_1'^2 X_d^3 + 2 B Y_1' X_d^2) (1 - Y_1' X_d) \right] \frac{K_2 M_o^2 (1 - Y_1' X_d)}{v_{2d}}$$

$$\frac{d P_2'}{dt} = 0$$

(VI.13)

$$\frac{d P_3'}{dt} = 0$$

$$P_i'(t_f) = 2(Y_i'(t_f) - 1) \quad i = 1, 2, 3 \quad (\text{IV.14})$$

VI.2 The Optimal Initiator Policy

In this case, we consider the initiator concentration $[I]$ in the reactor as the only control variable. The temperature T is arbitrarily fixed to a constant value. The algorithm used to solve this problem is similar to the algorithm used in Chapter V to calculate the optimal temperature profile. The initiator concentration is updated in each interval $[t_{k-1}, t_k]$ by applying a first order gradient method:

$$[I]t_{k,\text{new}} = [I]t_{k,\text{old}} - \alpha_2 \frac{\partial H}{\partial [I]} \Big|_{t_k} \quad (\text{VI.15})$$

α_2 has been chosen such that $\alpha_2 \frac{\partial H}{\partial [I]}$ has the same order of

Table VI.1

Desired and Attained MWDs - Optimization of [I] only

X_d	Attained Conversion	μ_{od}	Attained 0 th moment	μ_{2d}	Attained 2 nd moment	PD ₂	Attained Polydispersity	Minimum Time
0.9	0.855	8.45×10^{-4}	8.87×10^{-4}	2.075×10^5	1.996×10^5	2.5	2.8	290 min
0.9	0.855	8.45×10^{-4}	8.62×10^{-4}	3.399×10^5	3.287×10^5	4.1	4.5	285 min

Table VI.2

Desired and Attained MWDs - Simultaneous Optimization of [I] and T

X_d	Attained Conversion	μ_{od}	Attained 0 th moment	μ_{2d}	Attained 2 nd moment	PD ₂	Attained Polydispersity	Minimum Time
0.9	0.857	8.45×10^{-4}	8.70×10^{-4}	2.075×10^5	2.069×10^5	2.5	2.8	290 min
0.9	0.855	8.45×10^{-4}	8.45×10^{-4}	3.394×10^5	3.392×10^5	4.1	4.5	280 min

magnitude as the term $[I]$. A value of $\alpha = 2$ was proven to yield a good convergence. The gradient of the Hamiltonian relative to the initiator concentration can be calculated from the following analytical expression:

$$\frac{\partial H}{\partial [I]} = \sqrt{\frac{f k_d K_2}{2[I]}} \frac{(1 - Y_1' X_d)}{X_d} P_1' + \frac{2 f k_d}{\nu_{od}} P_2' \quad (\text{VI.15})$$

The numerical solution starts by assuming a constant profile for $[I]_t$ throughout the polymerization time from t_0 to t_f . Again the discretization time interval was chosen as 1 min.

The minimum time problem has been solved for two desired molecular weight distributions, given in Table VI.1. The corresponding optimal profiles are shown in Figures VI.1 and VI.2. For the same desired MWD, the shape of the optimal catalyst concentration profile is similar to the shape of the optimal temperature profile. This is understandable, since an increase in initiator concentration and an increase in polymerization temperature have a similar effect on the state variables, as shown on Figures II.12 and II.13, where temperature and $[I_0]$ sensitivity coefficients were presented.

VI.3 The Optimal Temperature and Initiator Policies

In this section, both the polymerization temperature T and the catalyst concentration $[I]$, are considered as control variables. The DCM algorithm is used to solve the minimum time problem. The two control variables are updated

using the following equation:

$$T(t_k)_{\text{new}} = T(t_k)_{\text{old}} - \alpha_1 \left. \frac{\partial H}{\partial T} \right|_{t_k} \quad (\text{VI.17})$$

$$[I](t_k)_{\text{new}} = [I](t_k)_{\text{old}} - \alpha_2 \left. \frac{\partial H}{\partial [I]} \right|_{t_k}$$

The numerical values of α_1 and α_2 were chosen as 1×10^5 and 2, respectively. For these values, reasonably fast convergence was obtained. The initial guesses for $T(t)$ and $[I](t)$ were respectively an isothermal profile (50°C) and a constant initiator concentration (0.02 mole.l^{-1}).

The optimal temperature and initiator policies that minimize the batch time were calculated for two desired MWDs described in Table VI.2. The optimal initiator concentration policies are shown in Figures VI.1 and VI.2 and compared with the optimal initiator concentration policies computed by considering only $[I]$ as a control variable. The optimal temperature policies are shown in Figures VI.3 and VI.4 and compared with the optimal temperature policies computed by considering only T as a control variable. The shape of the optimal temperature profiles and of the optimal initiator profiles are alike for the same desired MWD, but the simultaneous optimization of $[I]$ and T has a smoothing effect on the profiles.

VI.4 Controllability of the System

The system of differential equations which describe the polymerization of methyl methacrylate is non-linear, therefore it is difficult to show or to demonstrate if the system is "controllable" in the technical sense, i.e. if it is possible to transfer an arbitrary initial state to an arbitrary final state in a finite time. In this work, convergence is always obtained because the final desired output values are allowed to lie anywhere within a $\pm 5\%$ band, which is satisfactory from a practical engineering point of view. If a smaller tolerance were imposed on the final desired output, it may have been more difficult and, in some cases, impossible to obtain a true optimal control policy. This observation is supported by the following results:

For two computer runs, the desired final conversion, 0th and 2nd moments of the molecular weight distribution were specified as:

$$\begin{aligned}x_d &= 0.9 \\ \mu_{0d} &= 8.45 \times 10^{-4} \\ \mu_{2d} &= 2.075 \times 10^5\end{aligned}$$

For the first run, a tolerance of $\pm 5\%$ was imposed on the final desired outputs. As shown in Table VI.3, convergence was obtained in a reaction time of 290 minutes. For the second run, a tolerance of $\pm 1\%$ was imposed on the desired final output. Even by increasing the reaction time to 335 minutes, the difference between desired output

and the actual output was reduced only to 3%.

Table VI.3

Effect of Tolerance Limits on the Convergence

	Final Time	Error in Conversion	Error in M_n	Error in M_w
Run I	290 mins	-4.8%	+3%	0%
Run II	335 mins	-3%	+1%	2%

As it was shown in Chapter II, at the end of the reaction, the conversion and second moments are not very sensitive to temperature and initiator concentration (the two control variables). This means that it is difficult to get the desired final value for conversion and second moment once we have passed a critical point after which the sensitivity coefficients for conversion and second moment get opposite signs.

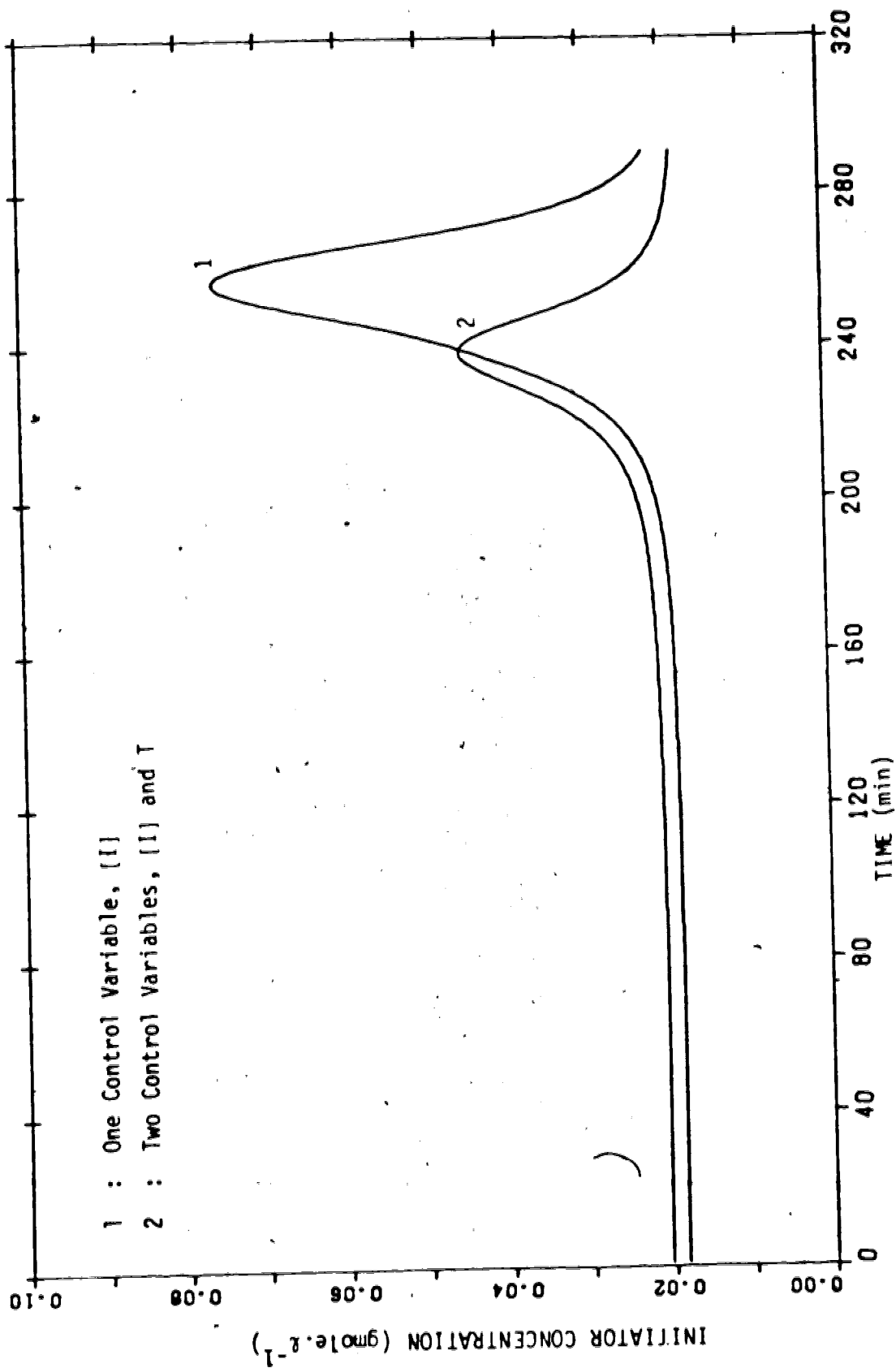


Figure VI.1: Initiator Concentration Profiles for Optimal Ryms.
 $(X_d = 0.9; \mu_{od} = 8.45 \times 10^{-4}; \tau_{2d} = 2.075 \times 10^{-5}; P0_d = 2.5)$

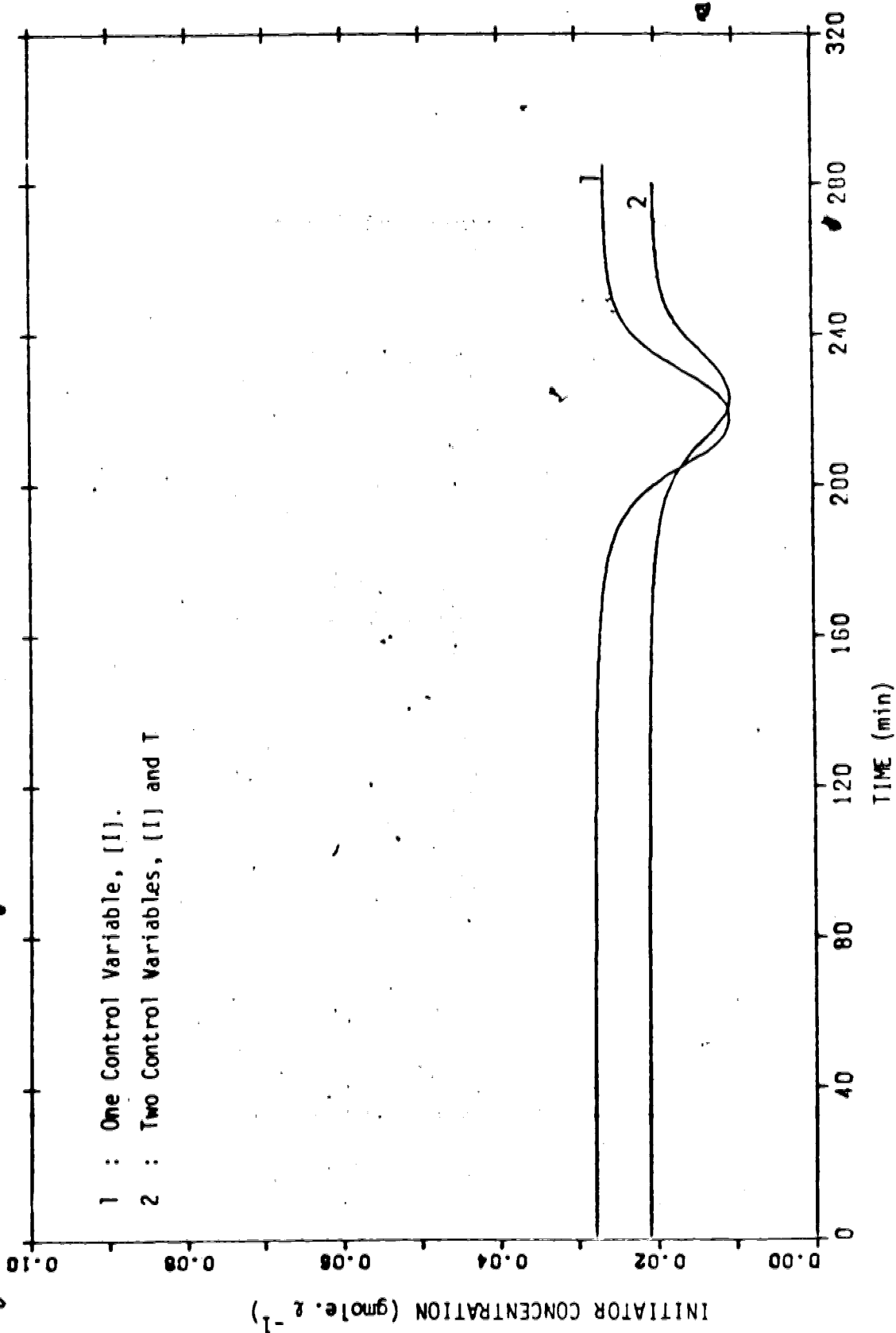


Figure VI.2: Initiator Concentration Profiles for Optimal Runs.
($X_d = 0.9$; $\mu_{od} = 8.45 \times 10^{-4}$; $\mu_{2d} = 3.399 \times 10^{-5}$; $PD_d = 4.1$)

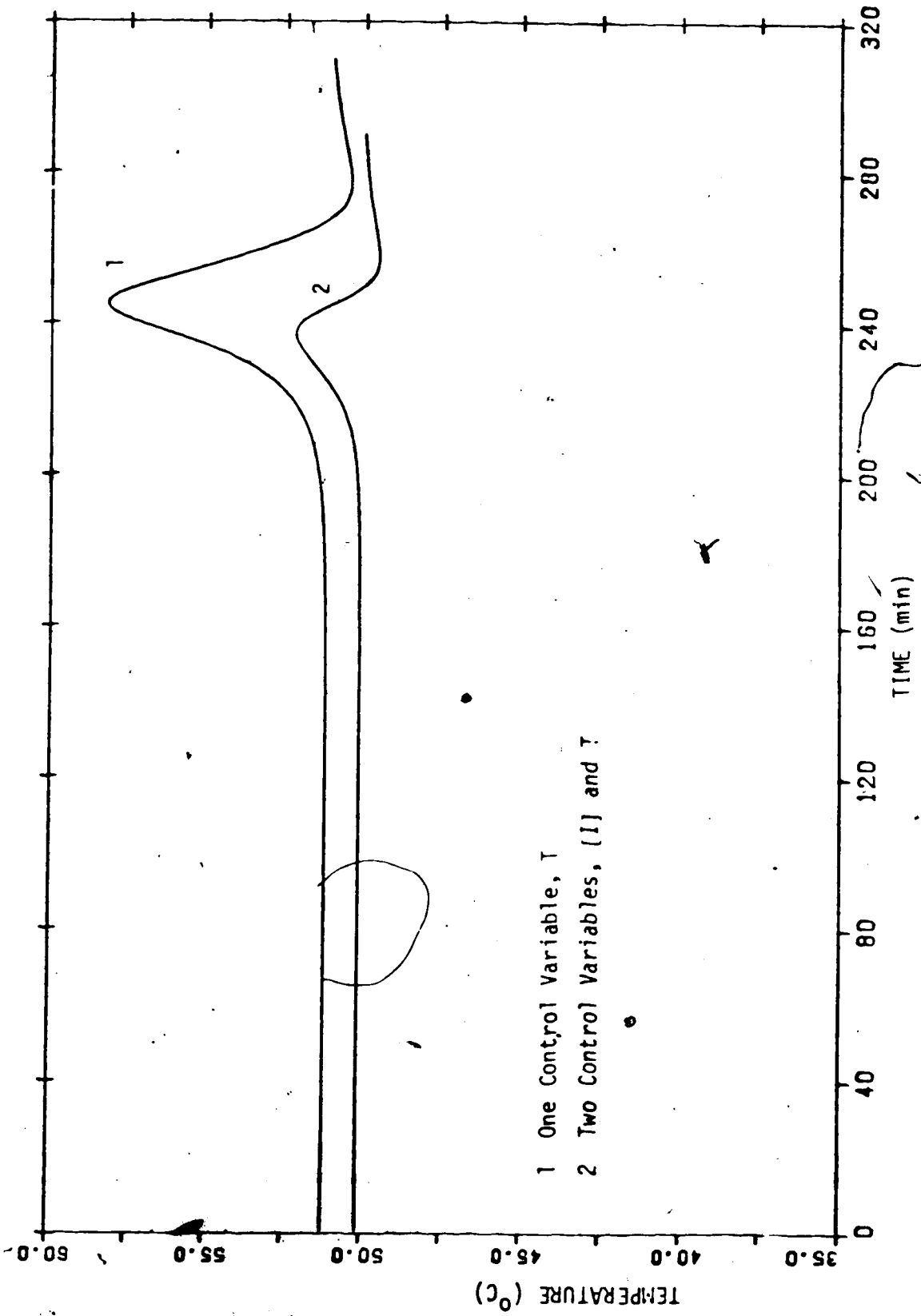


Figure VI.3: Temperature Profiles for Optimal Runs.
($x_D = 0.9$; $\mu_{od} = 8.45 \times 10^{-4}$; $\mu_{2d} = 2.075 \times 10^5$; $PD_D = 2.5$)

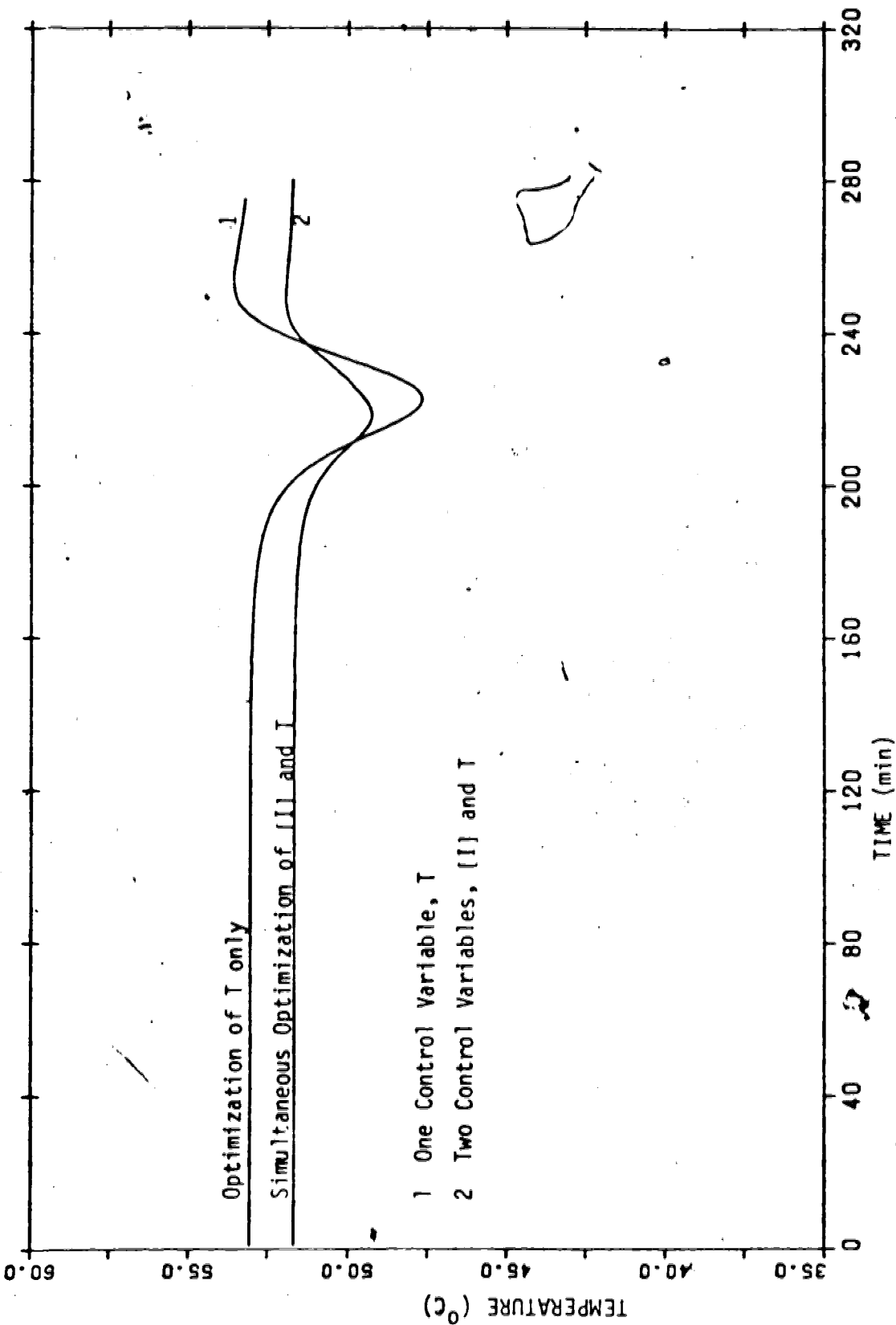


Figure VI.4: Temperature Profiles for Optimal Runs.
 $(X_d = 0.9; \nu_{od} = 8.45 \times 10^{-4}; \nu_{2d} = 3.399 \times 10^5; PD_d = 4.1)$

CHAPTER VII

CONCLUSION

A mathematical model has been developed for the free radical bulk polymerization of methyl methacrylate initiated by AIBN. The dynamics of the polymerization system are described in terms of monomer conversion, zeroth and second moments of the molecular weight distribution. The kinetic parameters of the model have been estimated by fitting the experimental data of Balke (1972). The sensitivity coefficients of the system outputs relative to the kinetic parameters have been calculated. It is shown that the second moment of the molecular weight distribution and the monomer conversion are very sensitive to the polymerization temperature, and to the kinetic parameters A_1 , B_1 , A_2 , B_2 describing the autoacceleration of the reaction due to the gel effect. Therefore much care is recommended in the estimation of the above parameters.

Our main objective of applying the optimal control theory to a polymerization system has been accomplished. The minimum batch time problem for the bulk polymerization of MMA has been solved by considering the polymerization temperature and/or initiator concentration as control variables. Using the calculated optimal policies we were able to reduce the batch time of the corresponding isothermal batch time by 25% while keeping the same polymer quality. Furthermore, we show that a desired MWD can be obtained

by applying the computed optimal temperature and initiator concentration policies to the polymerization reactor. Two algorithms (DCM and SM) are developed in this work to solve the two-point boundary value problem generated by the application of the Pontryagin Minimum Principle to the mathematical model of the polymerization of MMA. Although both algorithms give comparable results in terms of minimum batch time and optimal temperature profiles, the discrete control algorithm has proven to be the fastest and most reliable.

As a result of this investigation, the following future projects are suggested:

(i) Experimental verification of the optimal policies.

Optimal policies and particularly the optimal temperature policy can be implemented easily on a pilot polymerization reactor. Such a pilot plant system has been built, and is at this time ready for implementing time optimal control algorithms.

(ii) Extension of this work to other chemical reactions.

The algorithms developed in this thesis are very general and can be used for the optimization of a large number of chemical reactors. Reactor productivity could therefore be greatly improved.

(iii) Reduction of energy consumption.

Other objective functionals than minimum batch time should be considered. The expenditure of

energy to control the reactor temperature should be taken into account. Still the same algorithms could be used by deriving an other expression for the Hamiltonian.

REFERENCES

- Athans, M. and Falb, P.L., Optimal Control, McGraw-Hill, (1966).
- Atherton, R.W., Shainker, R.B. and Ducot, E.R., AICHE J., 21, No.3, pp. 441-448 (1975).
- Balke S. T., The Free Radical Polymerization of Methyl Methacrylate to High Conversions, Ph.D. Thesis, McMaster University, Ontario (1972).
- Bamford, C.H., Barb, W.G., Jenkins, A.D. and Onyon, P.F., The Kinetics of Vinyl Polymerization by Radical Mechanisms, Butterworths, London (1958).
- Beck, J.V. and Arnold, K.J., Parameter Estimation in Engineering and Science, John Wiley & Sons, (1977).
- Boltyanskii, V.G., Doklady Akad. Nauk SSSR, 119, No. 6 (1958).
- Brandrup, J. and Immergut, E.H., Polymer Handbook, Interscience, New York (1966).
- Bryson, A.E. and Ho, Y.C., Applied Optimal Control, Blaisdell Pub. Co. (1969).
- Chen, S.A. and Lin, K.F., J. of the Chinese Institute of Engineers, Taiwan, 1, No. 2, pp. 23-27 (1978).
- Chen, S.A. and Jeng, W.F., Chem. Eng. Sci., 33, pp. 735-743 (1978).
- Chen, S.A. and Lin, K.F., Chem. Eng. Sci., 35, pp. 2325-2335 (1980).
- Clough, D.E., Masterson, P.M. and Payne, S.R., Computer Simulation Conference, July, AFIPS pp. 279-280 (1978).
- Crescitelli, S. and Nicoletti, B., Chem. Eng. Sci., 28, pp. 463-471 (1973).
- Fan, L.T., The Continuous Maximum Principle, John Wiley, New York (1966).
- Fan, L.T. and Wang, C.S., The Discrete Maximum Principle, John Wiley, New York (1966).
- Ferington, T.E. and Tobolsky, A.V., J. of Colloid Science, 12, pp. 325-326 (1957).

- Flory, P.J., J. of Am. Chem. Soc., 59, p. 241 (1937).
- Friis, N. and Hamielec, A.E., Gel Effect in Emulsion Polymerization of Vinyl Monomers, preprints of A.C.S. meeting, Am. Chem. Soc., Division of Pol. Chem. (1975).
- Gabasov, R. and Kirillova, F., The Qualitative Theory of Optimal Processes, Marcel Dekker Inc., New York (1976).
- Gourishankar, V., Optimal Control, Course notes, University of Alberta (1980).
- Hamielec, A.E. and Friis, N., Polymer Reaction Engineering, Course notes, McMaster University, Ontario, (1976).
- Hayden, P. and Melville, H., J. of Pol. Sci., 43, pp. 201-214 (1960)
- Hicks, J., Mohan, A. and Ray, W.H., Can. J. of Chem. Eng., 47, pp. 590-597 (1969).
- Hoffman, R.F., Schreiber, S. and Rosen, G., Ind. Eng. Chem., 56, p. 51 (1964).
- IMSL Library, routine ZXSSQ, MTS, University of Alberta.
- Ito, K., J. of Pol. Sci., A1, 7, p. 827 (1969).
- Mahabadi, H.K. and Meyerhoff, G., European Pol. J., 15, pp. 607-613 (1979).
- Masterson, P.M., The Time-Optimal Control of a Batch Polymerization System, M.Sc. Thesis, University of Colorado, Colorado (1977).
- Matheson, M.S., Auer, E.E., Bevilacqua, E.B. and Hart, E.J., J. of Am. Chem. Soc., 71, pp. 497-504 (1949).
- Moyer, A.L., JACC, Proc. Vol. IV, pp. 191-199, Philadelphia Oct. 15-20 (1978).
- Nandi, U.S., J. of Colloid Sci., 12, pp. 321-324 (1957).
- Odian, G., Principles of Polymerization, McGraw-Hill, New York (1970).
- O'Driscoll, K.F. and Dickson, J.R., J. Macromol. Sci. Chem. A2, pp. 449 (1968).

- Osakada, K. and Fan, L.T., *J. of Applied Pol. Sci.*, 14, pp. 3065-3082 (1970).
- Paul, D.R., Fowler, D.W. and Houston, J.T., *J. of Applied Pol. Sci.*, 17, pp.2771-2782 (1973).
- Pavlinets, I. and Lazar, M., *Vyzokomol. soyed*, A15, 8, pp. 1767-1769 (1973).
- Pontryagin, L.S., *Am. Math. Soc. Trans., Ser. 2*, 18, pp. 321-329 (1961).
- Pontryagin, L.S., Boltyanskii, V.G., Gamkrelidze, R.F. and Mishchenko, E.F., *The Mathematical Theory of Optimal Processes*, Interscience, New York (1962).
- Rabinowitch, E., Wood, W.C., *Trans. Faraday Soc.*, 32, 1381 (1936).
- Ray, W.H., *Can. J. of Chem. Eng.*, 45, pp. 356-360 (1967).
- Sacks, M.E., Lee, S.I. and Biesenberger, J.A., *Chem. Eng. Sci.*, 27, pp. 2281-2289 (1972).
- Shatkan, F.A. and Gilman, I.M., *Pol. Sci. USSR*, 8, No. 3, pp. 548 (1966).
- Sawada, H., *J. of Pol. Sci.*, B1, p. 305 (1963).
- Shampine, L.F. and Allen, R.C., *An Introduction to Numerical Computing*, Saunders, Philadelphia (1973).
- Schulz, G.V. and Blaschke, F., *Z. Physik. Chem.* B51, 75 (1942).
- Schulz, G.V. and Harborth, G., *Angew. Chem.* 59A, 90 (1947).
- Tonoyan, A.O. et al., *Vyzokomol. soyed*, A15, No. 8, pp. 1847-1851 (1973).
- Wu, G.Z.A., Denton, L.A. and Laurence, R.L., *Annual Meeting of the Am. Inst. of Chem. Eng.*, Chicago (1980).
- Yokota, K., Kani, M. and Ishii, Y., *J. of Pol. Sci.*, A1, 6, pp. 1325-1339 (1968).

APPENDIX A

DERIVATION OF KINETIC EQUATIONS

The mechanism of the bulk free radical polymerization of MMA initiated by a free radical catalyst is described as follows:

Catalyst decomposition



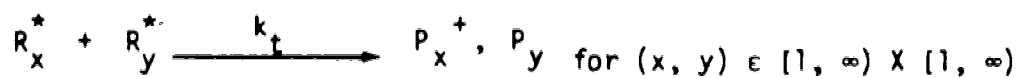
Initiation



Propagation



Termination by disproportionation



Where I represents the initiator molecules, R_0 the initiator radicals and R_0^* the activated initiator radicals. M denotes the MMA monomer. R_x^* is the live radicals of chain length x . P_x is the dead polymer of chain length x . f is the initiator efficiency factor. k_d , k_i , k_p , k_t are the rate constants for initiator dissociation, initiator, propagation and termination reactions. It is assumed that rate constants are independent of chain lengths.

According to the above kinetic scheme, the mass balance equations for the different species in the reactor are derived.

Catalyst

The mass balance for the catalyst can be expressed as:

$$d \frac{[I]}{dt} = -k_d [I] \quad (A.1)$$

Where $[I]$ is the catalyst concentration in the reactor, and t is the time. If catalyst is added during the reaction, it is assumed that the quantity of catalyst added will be small, so there is no change in the volume of the reacting mixture. In this case, the mass balance equation for catalyst is written:

$$d \frac{[I]}{dt} = -k_d [I] + \frac{F_c}{V} \quad (A.2)$$

Where F_c is the catalyst feed rate, and V the volume of the reactor.

Monomer

Monomer is consumed through propagation and initiation reactions. Generation of monomer results from termination reaction between a free radical of chain length one, and any other radical.

$$d \frac{[M]}{dt} = -k_i [M] [R_0^*] - k_p [M] \sum_{x=1}^{\infty} [R_x^*] + k_t [R_1^*] \sum_{x=1}^{\infty} [R_x^*] \quad (A.3)$$

where $[M]$ is the monomer concentration, $[R_x^*]$ is the concentration of live radicals of chain length x , $[R_0^*]$ is the concentration of catalyst activated radicals.

Activated radicals of catalyst

$$\frac{d[R_0^*]}{dt} = 2f k_d [I] - k_i [M][R_0^*] \quad (\text{A.4})$$

Activated radicals of chain length one

$$\frac{d[R_1^*]}{dt} = k_i [M][R_0^*] - k_p [M][R_1^*] - k_t [R_1^*] \sum_{x=1}^{\infty} [R_x^*] \quad (\text{A.5})$$

Activated radicals of chain length greater than one

$$\frac{d[R_x^*]}{dt} = -k_p [R_x^*][M] + k_p [R_{x-1}^*][M] - k_t [R_x^*] \sum_{y=1}^{\infty} [R_y^*] \quad (\text{A.6})$$

Dead polymer of chain length x (x > 1)

$$\frac{d[P_x]}{dt} = k_t [R_x^*] \cdot \sum_{y=1}^{\infty} [R_y^*] \quad (\text{A.7})$$

Where $[P_x]$ is the concentration of dead polymer of chain length x.

The moments of the MWD are defined as follows:

k^{th} moment of live radicals distribution:

$$\lambda_k = \sum_{x=1}^{\infty} x^k [R_x^*] \quad (\text{A.8})$$

k^{th} moment of dead polymer distribution:

$$\mu_k = \sum_{x=2}^{\infty} x^k [P_x] \quad (\text{A.9})$$

The rate of change for the moments of the MWD can be obtained by differentiating equations (A.8) and (A.9).

$$\frac{d \lambda_k}{dt} = \sum_{x=1}^{\infty} x^k \frac{d [R_x^*]}{dt} \quad (\text{A.10})$$

$$\frac{d \lambda_k}{dt} = \sum_{x=2}^{\infty} x^k \frac{d [P_x]}{dt} \quad (\text{A.11})$$

Substituting equations (A.5) and (A.6) into equation (A.10), a differential equation for the k^{th} amount of live radicals can be defined:

$$\begin{aligned} \frac{d \lambda_k}{dt} = & k_i [M] [R_0^*] - k_p [M] [R_1^*] - k_t [R_1^*] \sum_{x=1}^{\infty} [R_x^*] \\ & + \sum_{x=2}^{\infty} x^k (-k_p [M] [R_x^*] + k_p [R_x^2] [M] - k_t [R_x^*] \sum_{y=1}^{\infty} [R_y^*]) \end{aligned} \quad (\text{A.12})$$

Using the definition of the k^{th} moment of the live radical distribution (eg (A.8)), equation (A.12) can be rewritten as:

$$\frac{d \lambda_k}{dt} = k_i [M] [R_0^*] + k_p [M] \sum_{x=1}^{\infty} [(x+1)^k - x^k] [R_x^*] - k_t \lambda_0 \lambda_k \quad (\text{A.13})$$

Therefore:

$$\frac{d \lambda_0}{dt} = k_i [M] [R_0^*] - k_t \lambda_0^2 \quad (\text{A.14})$$

$$\frac{d\lambda_1}{dt} = k_i [M] [R_0^*] - k_t \lambda_0 \lambda_1 + k_p [M] \lambda_0 \quad (\text{A.15})$$

$$\frac{d\lambda_2}{dt} = k_i [M] [R_0^*] - k_t \lambda_0 \lambda_2 + 2 k_p [M] \lambda_1 + k_p [M] \lambda_0 \quad (\text{A.16})$$

In order to simplify the above equations, the quasi steady state (QSS) approximation for the live radicals is employed, which means, that the derivatives in equations (A.4), (A.5), (A.6) can be set to zero. Similarly the derivatives in equations (A.14), (A.15) and (A.16) can also be set to zero. Thus equations (A.4) and (A.14) can be rewritten as:

$$2f k_d [I] = k_i [M] [R_0^*] \quad (\text{A.17})$$

$$\lambda_0^2 = \frac{k_i [M] [R_0^*]}{k_t} \quad (\text{A.18})$$

Combining equations, (A.17) and (A.18), an algebraic expression for λ_0 can be obtained.

$$\lambda_0 = \sqrt{\frac{2f k_d [I]}{k_t}} \quad (\text{A.19})$$

Using the QSS approximation, equation (A.15) can be recast into equation (A.20)

$$\lambda_1 = \frac{k_i [M] [R_0^*] + k_p [M] \lambda_0}{k_t \lambda_0} \quad (\text{A.20})$$

or

$$\lambda_1 = \frac{2f k_d [I] + k_p [M] \lambda_0}{k_t \lambda_0} \quad (\text{A.21})$$

Since the term $(2f k_d [I])$ is negligible compared to $(k_p [M] \lambda_0)$, the following expression for λ_1 is obtained:

$$\lambda_1 = \frac{k_p [M]}{k_t} \quad (\text{A.22})$$

Justification for these approximations is given at the end of this appendix.

Similarly, equation (A.16) can be rewritten as:

$$\lambda_2 = \frac{2f k_d [I] + 2 k_p [M] \lambda_1 + k_p [M] \lambda_0}{k_t \lambda_0} \quad (\text{A.23})$$

Since (λ_0) is negligible compared to (λ_1) , and $(2f k_d [I])$ is negligible compared to $(k_p [M] \lambda_0)$, a simple expression for λ_2 may be derived from equation (A.23):

$$\lambda_2 = \frac{2 k_p [M] \lambda_1}{k_t \lambda_0} \quad (\text{A.24})$$

Substituting equation (A.7) into equation (A.11), differential equations describing the rate of change of the zeroth, first and second moments of the dead polymer distribution may be derived:

$$\frac{d\mu_0}{dt} = k_t \lambda_0^2 \quad (\text{A.25})$$

$$\frac{d\mu_1}{dt} = k_t \lambda_0 \lambda_1 \quad (\text{A.26})$$

$$\frac{d\mu_2}{dt} = k_t \lambda_0 \lambda_2 \quad (\text{A.27})$$

Substituting equations (A.19), (A.22) and (A.24) into equations (A.25), (A.26), (A.27), we obtain:

$$\frac{d\mu_0}{dt} = 2 f k_d [I] \quad (\text{A.28})$$

$$\frac{d\mu_1}{dt} = k_p [M] \sqrt{\frac{2f k_d [I]}{k_t}} \quad (\text{A.29})$$

$$\frac{d\mu_2}{dt} = 2 \frac{k_p^2}{k_t} [M]^2 \quad (\text{A.30})$$

The monomer conversion X is defined by the following equation:

$$X = \frac{[M_0] - [M]}{[M_0]} \quad (\text{A.31})$$

Where $[M_0]$ is the concentration of monomer at time $t=0$. By differentiating equation (A.31), the rate of change of conversion is obtained:

$$\frac{dX}{dt} = \frac{1}{[M_0]} \frac{d[M]}{dt} \quad (\text{A.32})$$

Substituting equation (A.3) into equation (A.32), we get:

$$\frac{dX}{dt} = \frac{-1}{[M_0]} (-2f k_d [I] + k_p [M] \lambda_0 + k_t [R_1^*] \lambda_0) \quad (\text{A.33})$$

Since $(2f k_d [I] + k_t [R_1^*] \lambda_0)$ is negligible compared to $(k_p [M] \lambda_0)$, equation (A.33) can be simplified.

$$\frac{dX}{dt} = \frac{k_p [M] \lambda_0}{[M_0]} \quad (\text{A.34})$$

Substituting equations (A.19) and (A.31) into equations (A.34), the following differential equation for the conversion is derived:

$$\frac{dX}{dt} = \sqrt{\frac{2f k_d [I]}{k_t}} k_p (1-X) \quad (\text{A.35})$$

By noting that the sum of the first moments of the dead and live polymer distributions is equal to the monomer consumed:

$$\mu_1 + \lambda_1 = [M_0] - [M] \quad (\text{A.36})$$

Neglecting the contribution of λ_1 in equation (A.36), we obtain:

$$\mu_1 = [M_0] X \quad (\text{A.37})$$

Differentiating the last equation, we get:

$$\frac{d\mu_1}{dt} = [M_0] \frac{dX}{dt}$$

This last result can be verified by combining equations (A.29) and (A.35).

Thus, the polymerization of MMA in a batch reactor can be completely described by the set of equations (A.2), (A.35), (A.28) and (A.30).

Justification of the Approximations in Equations (A.21), (A.23), (A.33).

This section intends to justify the approximations made in deriving equations (A.22), (A.24) and (A.34). Table A.1 shows the numerical values of the different terms which appear in the kinetic equations. The following numerical values for the kinetic parameters have been taken after Sacks et al. (1972):

$$k_d = 1.58 \times 10^{15} \times \text{EXP} (-30800/RT) \text{ s}^{-1}$$

$$k_p = 5.1 \times 10^6 \times \text{EXP} (-6300/RT) \text{ l. mole}^{-1} \text{ s}^{-1}$$

$$k_t = 7.8 \times 10^8 \text{ EXP} (-2800/RT) \text{ l. mole}^{-1} \text{ s}^{-1}$$

$$f = 0.6$$

$$[I] = 1 \times 10^{-2} \text{ mole/l}$$

$$[M] = 5 \text{ mole/l}$$

From the numerical results of Table 2.1, it can be seen that $\lambda_0 \ll \lambda_1$.

$$2 f k_d [I] \ll k_p [M] \quad \text{and} \quad k_t [R_1^*] \ll k_p [M]$$

TABLE A.1

JUSTIFICATION OF APPROXIMATIONS

Temp	k_d	k_p	k_t	$2f k_d$	λ_0	$k_p [M] \lambda_0$	$[R_1^*]$	λ_1	$k_t [R_1^*] \lambda_0$
30°C	1.33×10^{-7}	155.82	7.68×10^6	1.59×10^{-9}	1.44×10^{-8}	1.12×10^{-5}	2.04×10^{-12}	10^{-4}	2.28×10^{-13}
60°C	1.30×10^{-5}	397.53	11.64×10^6	1.56×10^{-7}	1.16×10^{-7}	2.3×10^{-4}	7.85×10^{-11}	1.7×10^{-4}	1.1×10^{-10}
90°C	6×10^{-4}	869	16.5×10^6	7.2×10^{-6}	6.6×10^{-7}	2.8×10^{-3}	1.6×10^{-9}	2.6×10^{-4}	1.78×10^{-8}

APPENDIX B

DERIVATION OF THE SENSITIVITY EQUATIONS

The bulk polymerization of MMA in a batch reactor is described by a set of four differential equations (A.2), (A.35), (A.28), (A.30):

$$\frac{dZ}{dt} = F(Z, p, t) \quad (B.1)$$

and a set of four initial conditions:

$$Z|_{t=0} = Z_0 \quad (B.2)$$

where Z is the output vector and p the parameter vector.

$$Z = ([I], X, u_0, u_2)^T \quad (B.3)$$

$$p = (k_d, f, K_{20}, A_1, A_2, B_1, B_2, C_1, C_2, T, [I_0]) \quad (B.4)$$

These parameters have been identified by fitting the experimental data of Balke (1972) with our own mathematical model. The purpose of this appendix is to describe the steps required to calculate the sensitivity coefficients that show the effect of perturbations in the parameters on the output of the system.

The sensitivity coefficient for the parameter p_j and the output Z_i is defined as the first partial derivative of Z_i with respect to p_j :

$$\phi_{ij} = \frac{\partial Z_i}{\partial p_j} \quad \begin{matrix} i = 1, 2, 3, 4 \\ j = 1, 2, \dots, 11 \end{matrix} \quad (B.5)$$

The sensitivity matrix is the matrix of the sensitivity coefficients:

$$\phi_{ij} = \frac{\partial Z_i}{\partial p_j} = \frac{\partial Z}{\partial p} \quad (B.6)$$

The information provided by the model must be used to determine $\frac{\partial Z}{\partial p}$. However, since equation (B.1) cannot be integrated analytically, the sensitivity analysis cannot be calculated analytically from equation (B.6). By using the sensitivity analysis method (Atherton et al. (1975), Beck and Arnold (1977)), a differential equation for the sensitivity matrix may be derived. To do so, we interchange the order of differentiation in the expression below and use equation (B.1) to obtain:

$$\frac{d}{dt} \left(\frac{\partial Z}{\partial p} \right) = \frac{\partial}{\partial t} \left(\frac{dZ}{dt} \right) = \frac{\partial}{\partial p} f(Z, p, t) \quad (B.7)$$

Since Z is a function of p , the right hand expression is expanded to give:

$$\frac{d}{dt} \left(\frac{\partial Z}{\partial p} \right) = \frac{\partial f}{\partial Z} \frac{\partial Z}{\partial p} + \frac{\partial f}{\partial p} \quad (B.8)$$

The matrix of derivatives are defined in the usual manner as in equation (B.6). By introducing the sensitivity coefficient ϕ_{ij} defined as in equation (B.5), equation (B.8) may be written in the following form:

$$\frac{d\phi_{ij}}{dt} = \sum_{l=1}^{l=4} \frac{\partial f_{il}}{\partial Z_l} \phi_{lj} + \frac{\partial f_{ij}}{\partial p_j} \quad \begin{array}{l} i = 1, 2, \dots, 4 \\ j = 1, 2, \dots, 11 \end{array} \quad (B.9)$$

To determine the initial conditions for equation (B.8), we note that at $t = 0$:

$$\begin{aligned} \frac{\partial Z_i(0)}{\partial p_j} &= \delta_{ij} \text{ if } p_j \text{ is an initial condition (as } p_{11} = [1_0] \text{)} \\ \frac{\partial Z_i(0)}{\partial p_j} &= 0 \text{ if } p_j \text{ is not an initial condition} \end{aligned} \quad (B.10)$$

These conditions are summarized as:

$$\phi_{ij}(0) = \begin{cases} 0 & \text{if } p_j \text{ is not an initial condition} \\ \delta_{ij} & \text{if } p_j \text{ is an initial condition} \end{cases} \quad (\text{B.11})$$

Equations (B.9) and (B.11) give a set of differential equations whose solution determines the numerical value of the sensitivity matrix as a function of time. The number of equations is equal to the number of state variables times the number of parameters (i.e. $4 \times 11 = 44$). It can be seen that each sensitivity equation is linear in the ϕ_{ij} 's and has variable coefficients which are determined by the state \underline{Z} .

The equation (B.1) describing the polymerization system has been derived in appendix A (eg. (A.2), (A.35), (A.28), (A.30)). It is as follows:

$$\frac{dZ_1}{dt} = -k_d [Z] + \frac{F_c}{V}$$

$$\frac{dZ_2}{dt} = \sqrt{2 f k_d Z_1 K_2} (1 - Z_2)$$

(B.12)

$$\frac{dZ_3}{dt} = 2 f k_d Z_1$$

$$\frac{dZ_4}{dt} = 2K_2 M_0^2 (1 - Z_2)^2$$

Where $K_2 = K_{20} \text{ EXP } (AZ_2^3 + \frac{BZ_2^2}{C} + C)$

Application of sensitivity equations (B.9) and (B.11) to the system (B.12) yields the following differential equations for the sensitivity coefficients:

For the dissociation rate constant k_d :

$$\frac{d \zeta_{11}}{dt} = S_1 \zeta_{11} - Z_1$$

$$\frac{d \zeta_{21}}{dt} = S_2 \zeta_{11} + S_3 \zeta_{21} + \sqrt{\frac{fk_2 Z_1}{2k_d}} (1-Z_2) \quad (\text{B.13})$$

$$\frac{d \zeta_{31}}{dt} = S_4 \zeta_{11} + 2fZ_1$$

$$\frac{d \zeta_{41}}{dt} = S_5 \zeta_{21}$$

$$\zeta_{11}(0) = 0; \zeta_{21}(0) = 0; \zeta_{31}(0) = 0; \zeta_{41}(0) = 0 \quad (\text{B.14})$$

Where S_1, S_2, S_3, S_4, S_5 are defined as:

$$S_1 = -k_d$$

$$S_2 = \sqrt{\frac{fk_d k_2}{2Z_1}} \times (1 - Z_2)$$

$$S_3 = \left[\frac{1}{2} (3A Z_2^2 + 2B Z_2)(1 - Z_2) - 1 \right] \sqrt{2fk_d Z_1 k_2} \quad (\text{B.15})$$

$$S_4 = 2 f k_d$$

$$S_5 = 2[-2 + (3 A Z_2^2 + 2 B Z_2) \cdot (1 - Z_2)] [K_2 M_0^2 (1 - Z_2)]$$

For the initiator efficiency f

$$\frac{d \phi_{12}}{dt} = S_1 \phi_{12}$$

$$\frac{d \phi_{22}}{dt} = S_2 \phi_{12} + S_3 \phi_{22} + \sqrt{\frac{k_d k_2 Z_1}{2f}} (1 - Z_2) \quad (B.16)$$

$$\frac{d \phi_{32}}{dt} = S_4 \phi_{12} + 2 k_d Z_1$$

$$\frac{d \phi_{42}}{dt} = S_5 \phi_{22}$$

$$\phi_{12}(0) = 0; \quad \phi_{22}(0) = 0; \quad \phi_{32}(0) = 0; \quad \phi_{42}(0) = 0. \quad (B.17)$$

For K_{20} ($K_{20} = k_p^2/k_t$ at $X = 0$)

$$\frac{d \phi_{13}}{dt} = S_1 \phi_{13}$$

$$\frac{d \phi_{23}}{dt} = S_2 \phi_{13} + S_3 \phi_{23} + \sqrt{\frac{k_d f Z_1 \cdot e^{(A Z_2^3 + B Z_2^2 + C)}}{2 K_{20}}} (1 - Z_2)$$

$$\frac{d \phi_{33}}{dt} = S_4 \phi_{13}$$

(B.18)

$$\frac{d\phi_{43}}{dt} = S_5 \phi_{23} + 2 \left(e^{AZ_2^3} + BZ_2^2 + C \right) M_0^2 (1 - Z_2)^2$$

$$\phi_{13}(0) = 0; \quad \phi_{23}(0) = 0; \quad \phi_{33}(p) = 0; \quad \phi_{43}(0) = 0. \quad (\text{B.19})$$

For parameter A₁

$$\frac{d\phi_{14}}{dt} = S_1 \phi_{14}$$

$$\frac{d\phi_{24}}{dt} = S_2 \phi_{14} + S_3 \phi_{24} + \frac{Z_2^3}{2T} \sqrt{2 f k_d Z_1 K_2} (1 - Z_2)$$

(B.20)

$$\frac{d\phi_{34}}{dt} = S_4 \phi_{14}$$

$$\frac{d\phi_{44}}{dt} = S_5 \phi_{24} + 2 \frac{Z_2^3}{T} K_2 M_0^2 (1 - Z_2)^2$$

$$\phi_{14}(0) = 0; \quad \phi_{24}(0) = 0; \quad \phi_{34}(0) = 0; \quad \phi_{44}(0) = 0; \quad (\text{B.21})$$

For parameter A₂

$$\frac{d\phi_{15}}{dt} = S_1 \phi_{15}$$

$$\frac{d\phi_{25}}{dt} = S_2 \phi_{15} + S_3 \phi_{25} + \frac{Z_2^3}{2} \sqrt{2 f k_d Z_1 K_2} (1 - Z_2) \quad (\text{B.22})$$

$$\frac{d\phi_{35}}{dt} = S_4 \phi_{15}$$

$$\frac{d \phi_{45}}{dt} = S_5 \phi_{25} + 2Z_2^3 K_2 M_0^2 (1-Z_2)^2$$

$$\phi_{15}(0) = 0; \phi_{25}(0) = 0; \phi_{35}(0) = 0; \phi_{45}(0) = 0 \quad (\text{B.23})$$

For parameter B₁

$$\frac{d \phi_{16}}{dt} = S_1 \phi_{16}$$

$$\frac{d \phi_{26}}{dt} = S_2 \phi_{16} + S_3 \phi_{26} + \frac{Z_2^2}{2T} \sqrt{2f k_d Z_1 K_2} (1-Z_2) \quad (\text{B.24})$$

$$\frac{d \phi_{36}}{dt} = S_4 \phi_{16}$$

$$\frac{d \phi_{46}}{dt} = S_5 \phi_{26} + 2 \frac{Z_2^2}{T} M_0^2 K_2 (1-Z_2)^2$$

$$\phi_{16}(0) = 0; \phi_{26}(0) = 0; \phi_{36}(0) = 0; \phi_{46}(0) = 0; \quad (\text{B.25})$$

For parameter B₂

$$\frac{d \phi_{17}}{dt} = S_1 \phi_{17}$$

$$\frac{d \phi_{27}}{dt} = S_2 \phi_{17} + S_3 \phi_{27} + \frac{Z_2^2}{2} \sqrt{2f k_d Z_1 K_2} (1-Z_2) \quad (\text{B.26})$$

$$\frac{d \phi_{37}}{dt} = S_4 \phi_{17}$$

$$\frac{d \phi_{47}}{dt} = S_5 \phi_{27} + 2Z_2^2 K_2 M_0^2 (1-Z_2)^2$$

$$\phi_{17}(0) = 0; \quad \phi_{27}(0) = 0; \quad \phi_{37}(0) = 0; \quad \phi_{47}(0) = 0; \quad (\text{B.27})$$

For parameter C₁

$$\frac{d \phi_{18}}{dt} = S_1 \phi_{18}$$

$$\frac{d \phi_{28}}{dt} = S_2 \phi_{18} + S_3 \phi_{28} + \frac{1}{2T} \sqrt{2f k_d Z_1 K_2} (1-Z_2) \quad (\text{B.28})$$

$$\frac{d \phi_{38}}{dt} = S_4 \phi_{18}$$

$$\frac{d \phi_{48}}{dt} = S_5 \phi_{28} + \frac{2}{T} K_2 M_0^2 (1-Z_2)^2$$

$$\phi_{18}(0) = 0; \quad \phi_{28}(0) = 0; \quad \phi_{38}(0) = 0; \quad \phi_{48}(0) = 0; \quad (\text{B.29})$$

For parameter C₂

$$\frac{d \phi_{19}}{dt} = S_1 \phi_{19}$$

$$\frac{d \phi_{19}}{dt} = S_2 \phi_{19} + S_3 \phi_{29} + \frac{1}{2} \sqrt{2f k_d Z_1 K_2} (1-Z_2) \quad (\text{B.30})$$

$$\frac{d\phi_{39}}{dt} = S_4 \phi_{19}$$

$$\frac{d\phi_{49}}{dt} = S_5 \phi_{29} + 2 K_2 M_0^2 (1-Z_2)^2$$

$$\phi_{19}(0) = 0; \quad \phi_{29}(0) = 0; \quad \phi_{39}(0) = 0; \quad \phi_{49}(0) = 0; \quad (\text{B.31})$$

For Temperature T

$$\frac{d\phi_{110}}{dt} = S_1 \phi_{110} - \frac{E_d}{R} k_d Z_1 / T^2$$

$$\frac{d\phi_{210}}{dt} = S_2 \phi_{110} + S_3 \phi_{210} - \frac{1}{2} \left(-\frac{E_d}{R} - \frac{E_2}{R} + A_1 Z_2^3 + B_1 Z_2^2 + C_1 \right)$$

$$\sqrt{2f k_d Z_1 K_2 (1-Z_2)} / T^2$$

$$\frac{d\phi_{310}}{dt} = S_4 \phi_{110} + 2 \frac{E_d}{R} f k_d Z_1 / T^2 \quad (\text{B.32})$$

$$\frac{d\phi_{410}}{dt} = S_5 \phi_{210} - 2 \left[-\frac{E_2}{R} + A_1 Z_2^3 + B_1 Z_2^2 + C_1 \right] K_2 M_0^2 (1-Z_2)^2 / T^2$$

$$\phi_{110}(0) = 0; \quad \phi_{210}(0) = 0; \quad \phi_{310}(0) = 0; \quad \phi_{410}(0) = 0; \quad (\text{B.33})$$

For initial initiator concentration $[I_0]$

$$\frac{d\phi_{111}}{dt} = S_1 \phi_{111}$$

$$\frac{d\phi_{211}}{dt} = S_2 \phi_{111} + S_3 \phi_{211}$$

$$\frac{d\phi_{311}}{dt} = S_4 \phi_{111}$$

(B.34)

$$\frac{d\phi_{411}}{dt} = S_5 \phi_{211}$$

$$\phi_{111}(0) = 1; \phi_{211}(0) = 0; \phi_{311}(0) = 0; \phi_{411}(0) = 0; \quad (\text{B.35})$$

The numerical integration of the sensitivity equations has been performed along with the numerical integration of the state equations, using a fourth order Runge-Kunta with variable step size integration routine.

Alternatively a finite difference method could be used to compute the sensitivity coefficients. The finite difference approximation for the i^{th} output variable and the parameter p_j is defined as:

$$\frac{\partial z_i}{\partial p_j} = \phi_{ij} = \frac{z_i(p_1, p_2, \dots, p_j + \delta p_j, \dots, p_{11}) - z_i(p_1, p_2, \dots, p_j, \dots, p_{11})}{\delta p_j}$$

Following the recommendations of Beck and Arnold (1977), δp_j has been chosen as:

$$\delta p_j = 0.0001 \cdot p_j$$

This method was used to verify the correct integration of the sensitivity differential equations. Sensitivity coefficients calculated by the two different methods, did not vary significantly.

In order to show the relative influence of the parameters on the output variables, a normalized sensitivity coefficient was used in place of the true sensitivity coefficient. It was defined as follows:

$$\psi_{ij} = \phi_{ij} \cdot \frac{p_j}{Z_i}$$

These normalized coefficients are plotted in Figures II.8 to II.11.

APPENDIX C

DERIVATION OF NECESSARY CONDITIONS FOR OPTIMALITY

This appendix presents a heuristic proof of the necessary conditions for optimality derived from the classical calculus of variations.

A detailed proof of the necessary conditions for optimality and of the Minimum Principle can be found in the work of Pontryagin et al. (1962).

The process to be optimized is described by a set of differential equations for the state variables together with initial values:

$$\frac{d\underline{y}}{dt} = f(\underline{y}, \underline{u}, t); \quad \underline{y}(t_0) = \underline{y}_0 \quad (C.1)$$

where \underline{y} is an n-dimensional state vector and \underline{u} is an m-dimensional control vector. Suppose that we wish to minimize the functional J,

$$J = G(\underline{y}(t_f), t_f) + \int_{t_0}^{t_f} L(\underline{y}(t), \underline{u}(t), t) dt. \quad (C.2)$$

Where G and L are two scalar functions.

Introduce the n-dimensional costate vector $\underline{p}(t)$ and rewrite the functional J as follows:

$$J = G(\underline{y}(t_f), t_f) + \int_{t_0}^{t_f} \left\{ L + \underline{p}^T (f - \dot{\underline{y}}) \right\} dt \quad (C.3)$$

Where the superscript T indicates transpose of a matrix.

In order to minimize J, we must make $\delta J = 0$.

Let $\delta \underline{u}$, $\delta \underline{Y}$, $\delta \underline{P}^T$ be the first variations of \underline{u} , \underline{Y} , \underline{P}^T . We obtain the perturbed value \tilde{J} of the objective function by replacing \underline{Y} by $\underline{Y} + \delta \underline{Y}$, \underline{u} by $\underline{u} + \delta \underline{u}$, \underline{P}^T by $\underline{P}^T + \delta \underline{P}^T$ in equation (C.3).

$$\tilde{J} = G(\underline{Y} + \delta \underline{Y}, t) \Big|_{t_0}^{t_f} + \int_{t_0}^{t_f} \left\{ L(\underline{Y} + \delta \underline{Y}, \underline{u} + \delta \underline{u}, t) + (\underline{P}^T + \delta \underline{P}^T) \left[\underline{f}(\underline{Y} + \delta \underline{Y}, \underline{u} + \delta \underline{u}, t) - (\dot{\underline{Y}} + \delta \dot{\underline{Y}}) \right] \right\} dt \quad (C.4)$$

Expanding the terms in equation (C.4) to the first order,

$$G(\underline{Y} + \delta \underline{Y}, t) \Big|_{t_f} = G(\underline{Y}(t_f), t_f) + \left(\frac{\partial G^T}{\partial \underline{Y}} \right) \cdot \delta \underline{Y} \Big|_{t_f} \quad (C.5)$$

$$L(\underline{Y} + \delta \underline{Y}, \underline{u} + \delta \underline{u}, t) = L(\underline{Y}, \underline{u}, t) + \frac{\partial L^T}{\partial \underline{Y}} \cdot \delta \underline{Y} + \frac{\partial L^T}{\partial \underline{u}} \cdot \delta \underline{u} \quad (C.6)$$

$$\underline{f}(\underline{Y} + \delta \underline{Y}, \underline{u} + \delta \underline{u}, t) = \underline{f}(\underline{Y}, \underline{u}, t) + \frac{\partial \underline{f}}{\partial \underline{Y}} \cdot \delta \underline{Y} + \frac{\partial \underline{f}}{\partial \underline{u}} \cdot \delta \underline{u} \quad (C.7)$$

$$\delta J = \tilde{J} - J \quad (C.8)$$

Substituting equations (C.5), (C.6) and (C.7) into equation (C.4), and using equation (C.8) to calculate the first order variation δJ , we obtain:

$$\delta J = \left(\frac{\partial G}{\partial \underline{Y}} \right)^T \delta \underline{Y} \Big|_{t_f} + \int_{t_0}^{t_f} \left\{ \left(\frac{\partial L}{\partial \underline{Y}} \right)^T \delta \underline{Y} + \left(\frac{\partial L}{\partial \underline{u}} \right)^T \delta \underline{u} + \delta \underline{P}^T (\underline{f} - \dot{\underline{Y}}) \right. \\ \left. + \underline{P}^T \left[\frac{\partial f}{\partial \underline{Y}} \delta \underline{Y} + \frac{\partial f}{\partial \underline{u}} \delta \underline{u} - \delta \dot{\underline{Y}} \right] \right\} dt \quad (C.9)$$

Since $(\underline{f} - \dot{\underline{Y}} = 0)$, the coefficient of $\delta \underline{P}^T$ vanishes.

Integrating by parts the integral $\int_{t_0}^{t_f} \underline{P}^T \delta \dot{\underline{Y}} dt$ we obtain

$$\int_{t_0}^{t_f} \underline{P}^T \delta \dot{\underline{Y}} dt = \left[\underline{P}^T \cdot \delta \underline{Y} \right]_{t_0}^{t_f} - \int_{t_0}^{t_f} \dot{\underline{P}} \delta \underline{Y} dt \quad (C.10)$$

Since initial conditions for $\underline{Y}(t_0)$ are fixed,

$$\delta \underline{Y} \Big|_{t_0} = \underline{0}. \quad (C.11)$$

Substituting equation (C.10) into equation (C.9) and rearranging, we get,

$$\delta \bar{J} = \left(\frac{\partial \bar{G}}{\partial \underline{Y}} - \underline{P}^T \right) \Big|_{t_f} \delta \underline{Y}(t_f) +$$

$$\int_{t_0}^{t_f} \left\{ \left[\frac{\partial L}{\partial \underline{Y}} + \underline{P}^T \frac{\partial f}{\partial \underline{Y}} + \dot{\underline{P}}^T \right] \delta \underline{Y} + \left[\frac{\partial L}{\partial \underline{u}} + \underline{P}^T \frac{\partial f}{\partial \underline{u}} \right] \delta \underline{u} \right\} dt \quad (C.12)$$

$\delta \underline{Y}$ and $\delta \underline{u}$ are arbitrary variations, therefore necessary conditions for δJ to be zero are that the coefficient of $\delta \underline{Y}$ and $\delta \underline{u}$ are zero:

$$\frac{\partial L}{\partial \underline{Y}} + \underline{P}^T \frac{\partial f}{\partial \underline{Y}} + \dot{\underline{P}}^T = \underline{0} \quad (C.13)$$

$$\frac{\partial L}{\partial \underline{u}} + \underline{P}^T \frac{\partial f}{\partial \underline{u}} = \underline{0} \quad (C.14)$$

Define the Hamiltonian H of the system as follows:

$$H(\underline{Y}, \underline{P}, \underline{u}, t) = k(\underline{Y}, \underline{u}, t) + \underline{P}^T \underline{f} \quad (C.15)$$

Equations (C.13) and (C.14) can be rewritten in terms of the Hamiltonian:

$$\dot{\underline{P}}^T = - \frac{\partial H}{\partial \underline{Y}} \quad (C.16)$$

$$\frac{\partial H}{\partial \underline{u}} = 0 \quad (C.17)$$

Suppose that $Y_i(t_f)$ is fixed for $i = 1, 2, \dots, r$

and $Y_j(t_f)$ is free for $j = r + 1, r + 2, \dots, n$

then $\delta Y_i(t_f) = 0$ for $i = 1, 2, \dots, r$

and $\delta Y_j(t_f)$ is an arbitrary variation for $j = r + 1, \dots, n$

The following final conditions for $\underline{P}(t_f)$ can be then derived from equation (C.12) by forcing δJ to become zero:

$$P_j(t_f) = \left. \frac{\partial G}{\partial Y_j} \right|_{t_f} \quad \text{for } j = r + 1, r + 2, \dots, n$$

$$P_i(t_f) \text{ is free} \quad \text{for } i = 1, 2, \dots, r \quad (C.18)$$

It should be noted that in the minimum time problem, H is not an explicit function of t , thus $(\partial H / \partial t) = 0$.

Differentiating H with respect to time:

$$\frac{dH}{dt} = \frac{\partial H}{\partial t} + \frac{\partial H}{\partial \underline{u}} \frac{d\underline{u}}{dt} + \frac{\partial H}{\partial \underline{P}} \frac{d\underline{P}}{dt} + \frac{\partial H}{\partial \underline{Y}} \frac{d\underline{Y}}{dt} \quad (C.19)$$

However, along the optimal trajectory, the necessary conditions for optimality will be:

$$\frac{d\underline{P}}{dt} = - \frac{\partial H}{\partial \underline{Y}} ; \frac{d\underline{Y}}{dt} = \frac{\partial H}{\partial \underline{P}} ; \frac{\partial H}{\partial \underline{u}} = 0. \quad (C.20)$$

Therefore, H is constant along the optimal trajectory,

$$(dH/dt) = 0. \quad (C.21)$$

APPENDIX D

DCM and SM Algorithms Computer Programs


```

121 C
122 C START ITERATIONS BY NEWTON-RAPHSON METHOD
123 C
124 DC 10 I12 8
125 DC 10 J12 8
126 GUESS 1 1 GUESS 2 1
127 GUESS 3 1 GUESS 3 2 +DELTA 1
128 GUESS 4 3 GUESS 4 2 +DELTA 2
129 GUESS 5 4 GUESS 5 3 +DELTA 3
130 GUESS 6 4 GUESS 6 4 +DELTA 4
131 C
132 DC 11 I12 8
133 R=0
134 Y 1 0
135 Y 2 0
136 Y 3 0
137 Y 4 0
138 Y 5 GUESS 1 1
139 Y 6 GUESS 1 2
140 Y 7 GUESS 1 3
141 Y 8 GUESS 1 4
142 DC 12 I11 MPIN
143 DC 14 L11 12
144 SAHS
145 HWS
146 HWS
147 RELE=0
148 ABSER=0
149 CALL R00TH Y H0RY T0PT SH0RY L12
150 TEMPT=0
151 HAM=0
152 DHAM=DERH TEMP
153 CALL R00TH Y NDIM FCT DA HN HWS ABSER RELE IFLAG
154 CONTINUE
155 CONTINUE
156 CALL OUTP R Y IFLAG L11
157 WRITE LUT 15 3 1 1 1 1 1 1 1 1 1 1
158 FORMAT 15 F7.0 3E 3 1 1
159 F 1 2 0 1 3
160 F 1 3 0 1 4
161 F 1 4 0 1 5
162 CONTINUE
163 C
164 C COMPUTE THE JACOBIAN
165 DC 16 I11 4
166 DC 16 J11 4
167 JAC 1 1 1 1 1 1 1 1 1 1 1 1 1 1 1 1 DELTA 1
168 WRITE LUT 16 3 1 1 1 1 1 1 1 1 1 1 1 1 1 1
169 FORMAT 16 3E 3 1 1 1 1 1 1 1 1 1 1 1 1 1 1
170 CONTINUE
171 C INVERSE THE JACOBIAN
172 DC 17 I11 4
173 DC 17 J11 4
174 H11=J11
175 AMAT=H11
176 H11=0
177 EPS=1E-03
178 CALL IN12 AMAT NROW NCOL A R R EPS IER
179 I1=0
180 WRITE LUT 17 1E0
181 FORMAT 17 3E0 CODE OUTPUT OF INVD 1E 18
182 WRITE LUT 18 3E 3 1 1 1 1 1 1 1 1 1 1 1 1 1 1
183 FORMAT 18 3E 3 1 1 1 1 1 1 1 1 1 1 1 1 1 1
184 C NEWTON-RAPHSON ITERATION
185 FAC=1.0
186 C FAC IS THE RELAXATION FACTOR
187 DC 19 I11 4
188 DC 19 J11 4
189 H11=0
190 CALL MULTI A NROW NCOL B0 NCOL NROW FAC CE NCOL NROW IER
191 WRITE LUT 19 1E0
192 FORMAT 19 3E0 CODE OUTPUT OF MULTI 1E 18
193 DC 19 I11 4
194 CONTINUE
195 H11=H11+H11*FAC
196 WRITE LUT 20 3E 3 1 1 1 1 1 1 1 1 1 1 1 1 1 1
197 FORMAT 20 3E 3 1 1 1 1 1 1 1 1 1 1 1 1 1 1
198 DC 20 I11 4
199 GUESS 1 1 GUESS 1 1 -CE
200 C
201 C TEST THE NEW GUESS
202 Y 1 0
203 Y 2 0
204 Y 3 0
205 Y 4 0
206 Y 5 GUESS 1 1
207 Y 6 GUESS 1 2
208 Y 7 GUESS 1 3
209 Y 8 GUESS 1 4
210 C
211 WRITE LUT 30 ICOUNT 1 1 1 1 1 1 1 1 1 1 1 1 1 1 1 1
212 FORMAT 30 I12 ITERATION NUMBER 1E 18 THE NEW GUESS IS 1E 18
213 I12=10 1E 18 1E 18 1E 18 1E 18 1E 18 1E 18 1E 18 1E 18 1E 18 1E 18 1E 18 1E 18 1E 18 1E 18 1E 18
214 C
215 ICOUNT=ICOUNT+1
216 R=0
217 L11
218 DC 123 I11 MPIN
219 DC 124 L11 12
220 SAHS
221 HWS
222 HWS
223 RELE=0
224 ABSER=0
225 CALL R00TH Y H0RY T0PT SH0RY L12
226 TEMPT=0
227 HAM=0
228 DHAM=DERH TEMP
229 CALL R00TH Y NDIM FCT DA HN HWS ABSER RELE IFLAG
230 CONTINUE
231 HWS
232 L11
233 CALL OUTP R Y IFLAG L11
234 CONTINUE
235 WRITE LUT 125 3 1 1 1 1 1 1 1 1 1 1 1 1 1 1 1
236 FORMAT 125 3E 3 1 1 1 1 1 1 1 1 1 1 1 1 1 1
237 I12 9 3E 3 1 1 1 1 1 1 1 1 1 1 1 1 1 1
238 C
239 F 1 1 0 1 2
240 F 1 2 0 1 3

```



```

481 7 TOP*Y2
482 80 TO 80
483 8 TOP*Y1
484 80 TO 80
485 2 IF P1 S A 1
486 8 TOP*Y1
487 80 TO 80
488 8 TOP*Y2
489 80 TO 80
490 1 CONTINUE
491
492
493 200 T2= T1-T2 / 2
494 C *EST* THE MAGNITUDE OF THE INTERVAL T1 T2
495 80000000 T2 T1
496 IF 80000000 0 000 SC TO 100
497 TOP*Y3
498 80 TO 80
499 C *OC* P3=0000 T3 1
500 P2=0000 T3 1
501 P1 P3 P2
502 IF P1 T2 T3
503 IF P3 T2 T3
504 TOP*Y3
505 80 TO 80
506 TOP*Y3
507 80 TO 80
508 T1 T2
509 T2 T3
510 80 TO 200
511 T1 T2
512 T2 T3
513 80 TO 200
514
515 C
516 31 80000000 TOP*Y1
517 80000000 TOP*Y2
518 C
519 31 80000000 31 TOP*Y1 80000000 Y2
520 C
521 31 80000000 31 31 31 810 3
522 40 RETURN
523 END

```

END OF FILE

1964-1965

APPENDIX E
EXPERIMENTAL EQUIPMENT

Experimental equipment was built in the polymer laboratory of the Department of Chemical Engineering at the University of Alberta, in order to verify the optimal temperature policies for a polymerization reaction, and particularly for the polymerization of methyl-methacrylate, as part of another project. The experimental apparatus is described in Figure E.1.

I. Measurements. In order to verify the validity of the mathematical model and the optimal temperature policies, conversion and molecular weight distribution must be measured continuously during the reaction. Samples are therefore taken in a continuous manner from the bottom of the reactor by means of displacement pumps then directed through a density meter and a gel permeation chromatograph (GPC), which are interfaced to a HP 1000 computer. Measurements of conversion and molecular weight distribution are recorded on charts and in a data file of the HP 1000.

II. Temperature Control of the Reactor. Since polymerization is highly sensitive to variations of temperature in the reactor, it is important that there be good control of the temperature in the polymerization reactor. In this experimental system, the temperature is controlled by a PID temperature controller. The manipulated variable of the temperature loop is the cold water flowrate entering the cooling coil in the reactor. The set point of the PID controller can be activated manually or by means of a supervisory control program on the HP 1000 computer to follow the optimal temperature policy. The high temperature

necessary to start the polymerization is obtained by means of a steady flow of hot water in the outside jacket of the reactor. Regulation of the reactor temperature is good within $\pm 0.5^{\circ}\text{C}$, and has proven satisfactory.

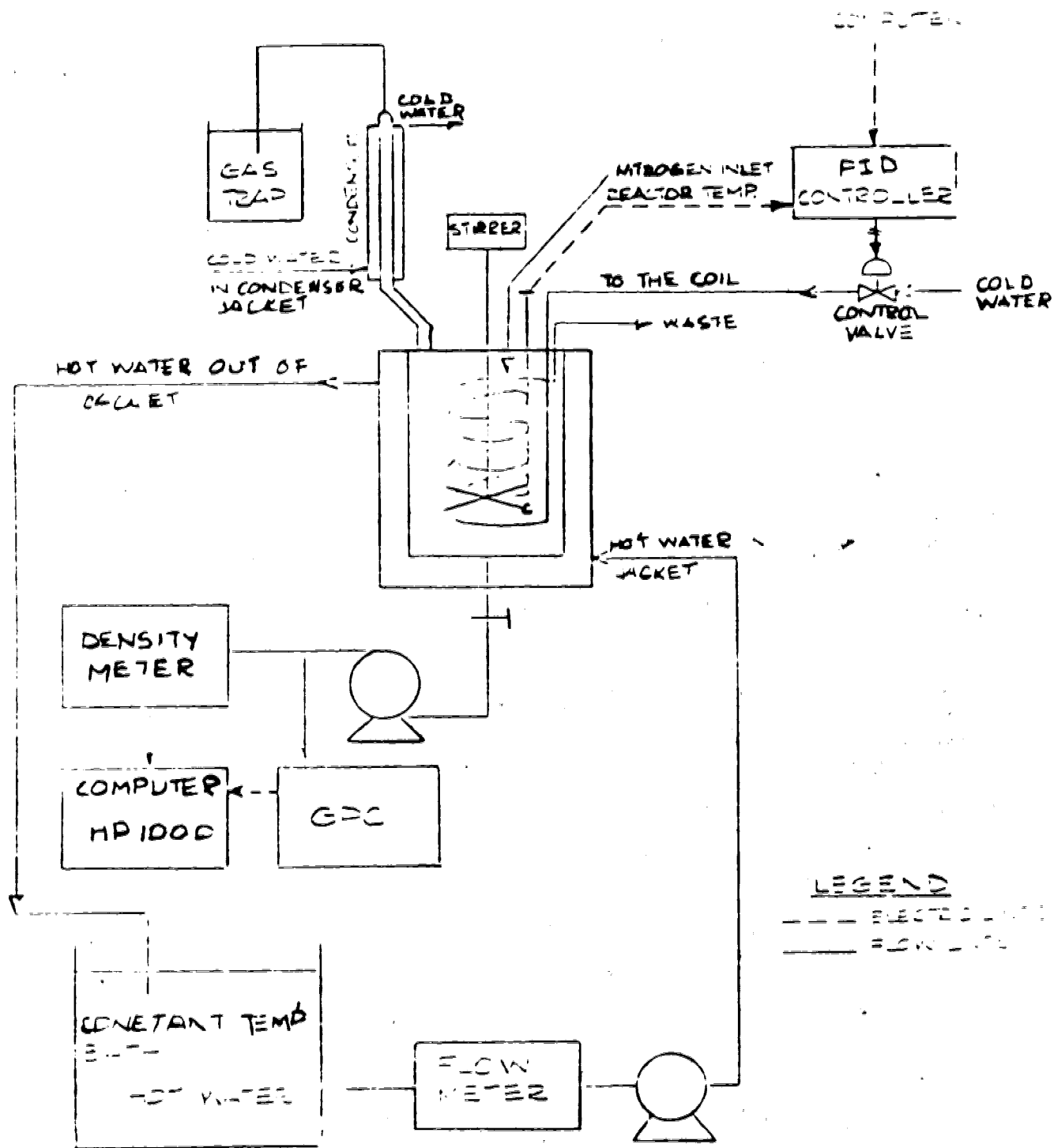


FIG. 1 EXPERIMENTAL APPARATUS